Aus der
Abteilung für Klinische Pharmakologie
Klinikum der Ludwig-Maximilians-Universität

Interleukin-1-Beta-Differentiated Th9 CD4+ T Cells as a Novel Effector Cell Subset for Chimeric Antigen Receptor T Cell Therapy

Dissertation
zum Erwerb des Doktorgrades der Medizin
an der Medizinischen Fakultät der
Ludwig-Maximilians-Universität München

vorgelegt von
Anna-Kristina Klüver

aus
München

Jahr
2025

Mit Genehmigung der Medizinischen Fakultät der
Ludwig-Maximilians-Universität zu München

Erstes Gutachten:	Prof. Dr. med. Sebastian Kobold
Zweites Gutachten:	Prof. Dr. Sebastian Theurich
Drittes Gutachten:	Prof. Dr. Andreas Humpe
Mitbetreuung durch den promovierten Mitarbeiter:	Mohamed-Reda Benmebarek, Ph.D.
Dekan:	Prof. Dr. med. Thomas Gudermann
Tag der mündlichen Prüfung:	23.07.2025

Table of contents

List of abbreviations

Abbreviation	Definition
4-1BB	CD137, TNF receptor superfamily member 9
AKT	Protein kinase B
ALL	Acute lymphoblastic leukemia
ANOVA	Analysis of variance
APC	Antigen presenting cell
apeglm	Approximate posterior estimation for the general linear model
BATF	Basic leucine zipper transcription factor ATF-like
BCL-6	B cell lymphoma 6 protein
BSA	Bovine serum albumin
CAR	Chimeric antigen receptor
CD	Cluster of differentiation
CLL	Chronic lymphocytic leukemia
DMEM	Dulbecco's modified Eagle medium
DMSO	Dimethyl sulfoxide
DNA	Deoxyribonucleic acid
EDTA	Ethylenediaminetetraacetic acid
ELISA	Enzyme-linked immunosorbent assay
EMA	European Medicines Agency
FACS	Fluorescence-activated cell sorting
Fas	Fas receptor (CD95)
FBS	Fetal bovine serum
FDA	Food and Drug Administration
GALV	Gibbon ape leukemia virus
GATA-3	Trans-acting T cell-specific transcription factor GATA-3
GSEA	Gene set enrichment analysis
h	Hours
ICD	Intracellular domain
ICOS	Inducible T cell costimulator (CD278)
IFN	Interferon
IL	Interleukin
IRF	Interferon regulatory factor
ISR	Integrated stress response
LCMV	Lymphocytic choriomeningitis virus
MACS	Magnetic-activated cell sorting
MCPIP-1	Monocyte chemotactic protein-induced protein 1

MHC	Major histocompatibility complex
MSLN	Mesothelin
NES	Normalized enrichment score
NF-κB	Nuclear factor κ-light-chain-enhancer of activated B cells
NFAT	Nuclear factor of activated T cells
NHL	Non-Hodgkin lymphoma
OVA	Ovalbumin
PBMC	Peripheral blood mononuclear cell
PBS	Polybutylene succinate
PD-1	Programmed cell death protein 1
PI3K	Phosphoinositide 3-kinase
RNA	Ribonucleic acid
ROS	Reactive oxygen species
RPMI	Roswell Park Memorial Institute
RTCA	Real-time cell analysis
SASP	Senescence-associated secretory phenotype
scFv	Single-chain variable fragment
SEM	Standard error of the mean
SMAD	Mothers against decapentaplegic homolog
STAT	Signal transducer and activator of transcription
T-bet	T-box transcription factor TBX21
Tcm	Central memory T cell
TCR	T cell receptor
Teff	Effector T cell
Tem	Effector memory T cell
TGF	Transforming growth factor
Th	T helper
TIL	Tumor-infiltrating lymphocyte
TLR	Toll-like receptor
TNF	Tumor necrosis factor
TNFR	Tumor necrosis factor receptor
TRAF	TNF receptor associated factor

Introduction

Cancer is a leading cause of death worldwide, accounting for an estimated ten million deaths in 2020 (Sung et al., 2021). The leading causes were lung, liver and colorectal cancer in men and breast, lung and colorectal cancer in women (Sung et al., 2021). The global burden of cancer is projected to increase considerably with an estimated 28.4 million new cancer cases predicted for 2040, representing a 50 % increase compared to 2020 (Sung et al., 2021). Cancer therapy classically relies on three pillars of treatment: surgery, radiotherapy and chemotherapy (Hunter, 2017). In the last two decades, a fourth treatment pillar - immunotherapy - has emerged, harnessing the immune system's ability to detect and eradicate anomalous cells (Hunter, 2017). Immunotherapies include monoclonal antibodies, immune checkpoint inhibitors as well as cellular therapies such as tumor-infiltrating leukocyte (TIL) and chimeric antigen receptor (CAR) T cell therapy (Hunter, 2017, Weber et al., 2020). TIL therapy has recently been authorized by the Food and Drug Administration (FDA) for the treatment of melanoma (Julve et al., 2024), and six CAR T cell therapies have been approved by the FDA and by the European Medicines Agency (EMA) for the treatment of hematological malignancies since 2017 (Labanieh and Mackall, 2023). CAR T cells targeting cluster of differentiation (CD) CD19 have been approved for the treatment of acute lymphoblastic leukemia (ALL) (Laetsch et al., 2023, Shah et al., 2021) and B-Non-Hodgkin lymphoma (B-NHL), including diffuse large B cell lymphoma, follicular lymphoma, primary mediastinal large B cell lymphoma and mantle cell lymphoma (Abramson et al., 2020, Jacobson et al., 2022, Schuster et al., 2019, Wang et al., 2020, Wang et al., 2024). In addition, CAR T cells targeting B cell maturation antigen have been approved by both agencies for the treatment of multiple myeloma (Berdeja et al., 2021, Munshi et al., 2021).

1.1 Structure of chimeric antigen receptors

CAR are genetically engineered constructs that enable target antigen recognition and binding through a single-chain variable fragment (scFv) in a major histocompatibility complex (MHC)-unrestricted manner (Labanieh et al., 2023). CAR are composed of an extracellular scFv and spacer, which are connected to intracellular signaling domains (ICD) through a transmembrane domain (Benmebarek et al., 2019, Labanieh et al., 2023). CAR can be categorized into different generations based on the number of ICD incorporated into a receptor's structure. First-generation CAR contain one ICD consisting of a part of the T cell receptor's (TCR) CD3ζ (CD3z) chain (Eshhar et al., 1993). This CD3z chain contains a large proportion of the immunoreceptor tyrosine-based activation motifs (ITAM) essential in initiating TCR activation (signal 1) (Benmebarek et al., 2019). Second-generation CAR contain an additional costimulatory ICD, such as CD28, 4-1BB or inducible T cell costimulator (ICOS) (van der Stegen et al., 2015). These ICD are physiologically responsible for augmenting and sustaining T cell activation upon TCR stimulation (signal 2) and were essential in increasing both expansion and cytokine secretion of first-generation CAR T cells (Labanieh et al., 2023, Maher et al., 2002, van der Stegen et al., 2015). In contrast to naturally occurring TCR, CAR are unable to recognize intracellular antigens and require a higher antigen density

on target cells for activation (Gudipati et al., 2020, Harris et al., 2018, Labanieh et al., 2023). However, since both ICD are connected in cis in a CAR, signals 1 and 2 are activated concurrently upon target antigen binding in CAR T cells (Benmebarek et al., 2019).

1.1.1 Signaling through intracellular costimulatory domains

Signaling through the B7/CD28 immunoglobulin superfamily member CD28 involves activation of phosphoinositide 3-kinase (PI3K) and protein kinase B (AKT) (Chen and Flies, 2013, van der Stegen et al., 2015). In turn, this enhances T cell proliferation and survival through the activation of nuclear factor-κB (NF-κB) and nuclear factor of activated T cells (NFAT) (Chen et al., 2013, van der Stegen et al., 2015). Additionally, PI3K-AKT signaling promotes a metabolic switch to glycolysis (Chen et al., 2013, van der Stegen et al., 2015). While it is unclear whether signaling through a costimulatory ICD in CAR T cells is identical to signaling through endogenous costimulatory receptors, PI3K-AKT signaling has also been reported to be activated in CD28-CD3z (CD28z) CAR T cells (Zhong et al., 2010). Furthermore, endogenous CD28 signaling enhances cell cycle progression through an upregulation of cyclin D (van der Stegen et al., 2015). CD28 signaling also upregulates the expression of additional costimulatory receptors to amplify T cell activation (van der Stegen et al., 2015). Lastly, CD28 signaling enhances effector cytokine production, in particular interleukin (IL)-2 secretion, through the activation of NFAT and T-box transcription factor TBX21 (T-bet) (Chen et al., 2013, van der Stegen et al., 2015).

4-1BB, also known as CD137, is a member of the tumor necrosis factor (TNF) receptor superfamily (van der Stegen et al., 2015). 4-1BB augments cell cycle progression, proliferation and cytokine production by activating TNF receptor-associated factors (TRAF1, TRAF2, TRAF3) (Chen et al., 2013, van der Stegen et al., 2015). TRAF signaling leads to canonical NF-κB and p38 mitogen-activated protein kinase (MAPK) signaling and to the production of effector cytokines (Chen et al., 2013, van der Stegen et al., 2015). Moreover, 4-1BB signaling enhances cell cycle progression through TRAF, extracellular signal-regulated kinase (ERK) and PI3K-AKT-IL-2 signaling (van der Stegen et al., 2015). The latter pathway has also been found to be activated in 4-1BB-CD3z (BBz) CAR T cells (Zhong et al., 2010). Through phosphorylation of adaptor proteins, 4-1BB signaling, like CD28 signaling, amplifies endogenous TCR activation (Nam et al., 2005). Importantly, signaling through 4-1BB was shown to reduce T cell exhaustion and anergy and enhance the survival of CD8+ memory T cells (Habib-Agahi et al., 2007, Pulle et al., 2006, Wang et al., 2012).

Activation of the B7/CD28 immunoglobulin superfamily member ICOS, also referred to as CD278, results in signaling through PI3K-AKT and c-MAF, short for v-MAF avian musculoaponeurotic fibrosarcoma oncogene homolog, pathways (Chen et al., 2013, Simpson et al., 2010, van der Stegen et al., 2015). Unlike CD28, however, ICOS cannot induce relevant IL-2 production as it cannot bind growth factor receptor-bound protein 2 (GRB2) and lymphocyte-specific protein tyrosine kinase (LCK) (Chen et al., 2013, van der Stegen et al., 2015). This difference in cytokine production has also

been reported for ICOS-CD3z (ICOSz) CAR T cells when compared to CD28z-CAR T cells (Guedan et al., 2018). Moreover, ICOS signaling activates B cell lymphoma 6 protein (BCL-6), mediating both a transition from an effector to a memory phenotype as well as a shift away from glycolytic metabolism in T cells (Choi et al., 2011, Oestreich et al., 2014).

1.1.2 Effects of CD28, 4-1BB and ICOS costimulation on CAR T cell function

The ideal costimulation for optimal CAR T cell function might differ based on CAR T cell subset and tumor entity (van der Stegen et al., 2015). FDA-approved CAR T cell therapies include CAR designs incorporating either a CD28 ICD (Jacobson et al., 2022, Shah et al., 2021, Wang et al., 2020) or a 4-1BB ICD (Abramson et al., 2020, Laetsch et al., 2023, Schuster et al., 2019). CD28z- and BBz-CAR T cells targeting CD19 have shown similar complete response and survival rates in patients with ALL and large B cell lymphoma (Davila et al., 2014, Maude et al., 2014, Neelapu et al., 2017, Schuster et al., 2019). In the setting of CLL, however, CD28z-CAR T cells were less efficient (Geyer et al., 2019, Porter et al., 2015). In general, a CD28 ICD mediates faster tumor cell killing (Zhao et al., 2015), while a 4-1BB ICD preferentially enhances CAR T cell persistence, mitochondrial metabolism and memory development (Kawalekar et al., 2016, Long et al., 2015). While ICOSz-CAR T cells have not yet been studied in clinical trials, they were shown to improve CAR T cell persistence in pre-clinical models (Guedan et al., 2014, Guedan et al., 2018).

1.2 Limitations of chimeric antigen receptor T cell therapy

CAR T cell therapy has been established for the treatment of various hematological malignancies. However, its clinical success and application to solid tumors is still limited by treatment-associated complications and tumor relapse. Significant limitations include reduced tumor trafficking due to a suppressive tumor microenvironment or antigen loss on tumor cells as well as insufficient CAR T cell function, for instance through limited persistence, exhaustion or tonic signaling in CAR T cells (Stoiber et al., 2019, Weber et al., 2020). Treatment-associated toxicities include cytokine release syndrome and immune effector cell-associated neurotoxicity syndrome (Stoiber et al., 2019, Weber et al., 2020). Various approaches to reduce these limitations have been proposed, including altering CAR design by incorporating a suicide switch or by overexpressing chemokine receptors (Stoiber et al., 2019, Weber et al., 2020). Modulating CAR affinity to an AND- or NOT-gated or an adaptor CAR structure has also been suggested (Stoiber et al., 2019, Weber et al., 2020). Furthermore, CAR can be targeted to components of the tumor microenvironment or be administered locally to improve tumor trafficking (Adusumilli et al., 2014, Ash et al., 2024). Lastly, preselecting a desired T cell phenotype, such as memory T cells, during CAR T cell manufacturing has been proposed to overcome these treatment limitations (Sabatino et al., 2016).

1.3 CD4+ T cells in chimeric antigen receptor T cell therapy

Conventional CAR T cell infusion products contain a heterogeneous mixture of CD4+ and CD8+ CAR T cells. To date, both higher and lower ratios of CD4+ to CD8+ CAR T cells have been described to improve clinical responses, suggesting that an optimal ratio might depend on CAR target antigen and tumor entity (Cohen et al., 2019, Fraietta et al., 2018, Galli et al., 2023). CD4+ T cells, also known as T helper (Th) cells, have conventionally been regarded as intermediaries amplifying a cytotoxic response mediated by CD8+ T cells (Zander et al., 2019). Accordingly, CD4+ CAR T cells were critical for both expansion and development of a memory phenotype in CD8+ CAR T cells (Lee et al., 2023, Sommermeyer et al., 2016, Wang et al., 2019). However, CD4+ CAR T cells are potent effectors as such (Liadi et al., 2015). In comparison to CD8+ CAR T cells, CD4+ CAR T cells were even shown to be less prone to apoptosis and exhaustion upon tumor encounter or upon additional stimulation through endogenous TCR (Adusumilli et al., 2014, Wang et al., 2018, Yang et al., 2017). Furthermore, it has been suggested that the functional persistence of CAR T cells is mediated predominantly by CD4+ CAR T cells (Adusumilli et al., 2014, Louis et al., 2011, Melenhorst et al., 2022). Consequently, specific CD4+ T cell subsets, such as Th17 and Th9 cells, have been studied in the preclinical setting with the intention of generating more potent, long-lived CAR T effector cells (Guedan et al., 2014, Liu et al., 2020).

1.4 Th9 CD4+ T cells as effector cells for adoptive T cell therapies

1.4.1 Role of Th9 cells in disease

Th9 cells were first described as reprogrammed Th2 cells generated in the presence of transforming growth factor β (TGF-β) (Dardalhon et al., 2008, Veldhoen et al., 2008). They have since been established as critical pro-inflammatory mediators in inflammatory bowel disease and allergy and as effectors of an immune response against helminthic infections (Gerlach et al., 2014, Licona-Limón et al., 2013, Sehra et al., 2015). The role of Th9 cells in cancer is more ambivalent. The infiltration of solid tumors by Th9 cells has been associated with both enhanced and impaired anti-tumor immunity in different tumor entities ranging from breast cancer to hepatocellular carcinoma (Salazar et al., 2020, Tan et al., 2017, Wang et al., 2020, You et al., 2017). Furthermore, peripheral blood Th9 cells have been proposed as potential biomarkers to predict clinical responses to anti-programmed cell death protein blockade (anti-PD-1) with nivolumab in patients with metastatic melanoma (Nonomura et al., 2016).

1.4.2 Differentiation of Th9 cells

The differentiation of naïve CD4+ T cells into effector subsets occurs upon the recognition of an antigen presented by MHC II molecules on antigen-presenting cells (APC) (Kaplan et al., 2015). T helper cell differentiation depends on the local cytokine environment, on costimulation provided by APC and on TCR activation strength (Kaplan et al., 2015, Luckheeram et al., 2012). Importantly, CD4+ T cell subsets retain the ability to re-differentiate, termed T helper cell plasticity (Zhou et al., 2009). Hence,

commitment to a T helper cell lineage is not irreversible. CD4+ T cell differentiation into Th9 cells is initiated in the presence of IL-4, TGF-β and IL-1β (Kaplan et al., 2015). IL-4-STAT6-IRF4/BATF/GATA-3 signaling, IL-2-STAT5-IRF4/PU.1 signaling, TGF-β-SMAD2-4/PU.1 signaling and IL-1β-STAT1-IRF1 signaling are essential for the commitment to a Th9 lineage (Kaplan et al., 2015).

IL-4 leads to the activation of signal transducer and activator of transcription 6 (STAT6), which in turn induces the expression of interferon regulatory factor 4 (IRF4), basic leucine zipper transcription factor ATF-like (BATF) and trans-acting T cell-specific transcription factor GATA-3 (GATA-3) (Goswami et al., 2012, Jabeen et al., 2013, Kaplan et al., 2015). IRF4 and BATF form a complex which binds the IL-9 promoter (Li et al., 2012, Staudt et al., 2010). IRF4 further enhances Th9 differentiation through a downregulation of T-bet, the master regulator of Th1 differentiation (Staudt et al., 2010). GATA-3 inhibits T-bet and forkhead box protein P3 (FOXP3), thus suppressing Th1 and Treg differentiation, respectively (Veldhoen et al., 2008). GATA-3 binding to the IL-9 promoter can be further enhanced through IL-4- and TGF-β-mediated downregulation of DNA-binding protein inhibitor ID-3 (Nakatsukasa et al., 2015).

TGF-β is essential in redirecting CD4+ differentiation from a Th2 to a Th9 phenotype. TGF-β activates SMAD2, SMAD3 and SMAD4 (mothers against decapentaplegic homolog) as well as the transcription factor PU.1 (Chang et al., 2010, Goswami et al., 2012, Jabeen et al., 2013, Tamiya et al., 2013, Wang et al., 2013). SMAD molecules bind the IL-9 promoter and alter its chromatin structure, and SMAD2 and 3 also form a complex with IRF4 (Tamiya et al., 2013, Wang et al., 2013). PU.1 binds the IL-9 promoter directly and can form a complex with IRF4, BATF and IRF8 to further enhance IL-9 transcription (Chang et al., 2010, Humblin et al., 2017).

IL-2 leads to the activation of STAT5, which directly binds the IL-9 promoter and increases its accessibility to BATF binding (Fu et al., 2020, Liao et al., 2014). IL-2/STAT5 signaling also increases expression of IRF4 (Liao et al., 2014). Moreover, STAT5 can inhibit expression of BCL-6, leading to a disinhibition of Th9 differentiation (Liao et al., 2014). STAT5 signaling has also been implicated in the promotion of Th9 differentiation through signaling via mammalian target of rapamycin (mTOR) (Bi et al., 2017).

IL-1β signaling leads to STAT1 activation and subsequent expression of IRF1, which binds the IL-9 promoter (Végran et al., 2014). IL-1β signaling also suppresses BCL-6 expression, disinhibiting Th9 differentiation (Canaria et al., 2022).

1.4.3 Mechanisms of Th9 cell cytotoxicity

Various mechanisms of Th9 cell cytotoxicity have been proposed, including direct tumor cell lysis through effector cytokine secretion as well as recruitment and activation of effector immune cells. Recombinant IL-9 has previously been shown to directly induce the apoptosis of various tumor cell lines (Chauhan et al., 2019, Purwar et al.,

2012). Accordingly, neutralization of IL-9 reduced tumor cell lysis by Th9 cells in a squamous cell carcinoma model *in vitro* and in a murine melanoma model *in vivo* (Kim et al., 2015, Miao et al., 2017, Nakatsukasa et al., 2015, Xue et al., 2019). However, Th9 cells have also been reported to induce tumor lysis independently of IL-9, instead relying on the secretion of granzyme B or IL-21 (Lu et al., 2018, Végran et al., 2014).

In addition, Th9 cells might recruit and activate mast cells, dendritic cells and CD8+ T cells to effectuate an anti-tumor response. In melanoma and colorectal carcinoma models, the absence of mast cells has been reported to abrogate the anti-tumor effects of recombinant IL-9 and Th9 cells *in vivo* (Abdul-Wahid et al., 2016, Purwar et al., 2012). However, in a B-NHL model, mast cell activation mediated through IL-9 was associated with reduced *in vivo* tumor control (Feng et al., 2011). Moreover, mast cell deficiency did not seem to impair the cytolytic capacity of Th9 cells differentiated in the presence of IL-1β (Végran et al., 2014). These conflicting results suggest that the involvement and effect of mast cells on tumor control mediated by Th9 cells might depend on tumor entity. Fittingly, mast cell infiltration itself has been associated with both improved and impaired clinical outcomes in different tumor entities (Hedström et al., 2007, Nonomura et al., 2007, Strouch et al., 2010, Welsh et al., 2005).

Furthermore, Th9 cells have been found to enhance a CD8+-driven anti-tumor response by promoting dendritic cell recruitment and survival and by secreting IL-21 and IL-9 (Kim et al., 2015, Lu et al., 2012, Park et al., 2014, Végran et al., 2014, You et al., 2017). Dendritic cell activation has also been found to promote Th9 differentiation, suggesting a potential cycle of reciprocal activation (Zhao et al., 2016). However, CD8+ T cell depletion has also been reported to have little to no effect on tumor lysis by Th9 cells in murine melanoma models *in vivo* (Lu et al., 2018, Purwar et al., 2012). Overall, Th9-mediated cytotoxicity is a multi-facetted process involving an interplay of various immune effector cells. Its exact mechanisms remain to be conclusively established.

1.4.4 Th9 cells as CAR T cells

Th9 cells have shown promising results as adoptively transferred T cells and as CAR T cells in preclinical tumor models. The adoptive transfer of ovalbumin (OVA)-specific Th9 cells mediated superior tumor control *in vivo* in OVA-expressing melanoma models when compared to Th1, Th2 and Th17 cells (Lu et al., 2012, Lu et al., 2018, Purwar et al., 2012). The addition of IL-1β during Th9 differentiation further enhanced Th9 phenotype and tumor cell killing *in vivo* (Végran et al., 2014, Xue et al., 2019). Additionally, mixed CD4+ and CD8+ CAR T cells that were expanded under Th9-polarizing conditions showed greater *in vivo* clearance of leukemic tumor cells compared to mixed CD4+ and CD8+ CAR T cells expanded under Th1-polarizing conditions (Liu et al., 2020). Interestingly, mesothelin (MSLN)-specific Th9 CAR T cells were the only subset to effectively eliminate tumors containing antigen loss variants in a MSLN-expressing ovarian cancer model *in vivo* (Xue et al., 2021). Th9 CAR T cells could thus potentially possess a distinctive advantage for the treatment of solid tumors,

which exhibit significant antigen heterogeneity and can express antigen loss variants during adoptive T cell transfer (O'Rourke et al., 2017).

1.5 Aims of this thesis

While the addition of IL-1β during T helper cell differentiation has been described to enhance Th9 phenotype and cytotoxicity in murine T cells, its effects on Th9 phenotype in human T cells has not yet been studied (Canaria et al., 2022, Végran et al., 2014, Xue et al., 2019). Furthermore, the suitability of IL-1β-differentiated Th9 cells for CAR T cell therapy remains to be evaluated (Liu et al., 2020). Moreover, both 4-1BB and ICOS ICD have been described to enhance CAR T cell functionality, including the functionality of Th17 and mixed CD4+ CAR T cells (Guedan et al., 2014, Guedan et al., 2018, Kawalekar et al., 2016, Long et al., 2015). Studies of Th9 CAR T cells thus far, however, have only been conducted using a 4-1BB ICD (Liu et al., 2020, Xue et al., 2021).

Therefore, the following project aims were defined:

1. Generation of a comprehensive transcriptional profile of human, IL-1β-differentiated Th9 cells
2. Evaluation of the *in vitro* cytotoxic potential of human, IL-1β-differentiated Th9 CAR T cells
3. Assessment of a potential enhancement of *in vitro* cytotoxicity of human, IL-1β-differentiated Th9 CAR T cells through a CD28, 4-1BB or ICOS ICD

2.1 Materials

2.1.1 Technical equipment

-80°C freezer	HERAfreeze™ HDE series ultra-low temperature freezers	ThermoFisher Scientific, Waltham, MA, USA
Centrifuge	Color sprout plus mini-centrifuge	Biozym, Hessisch Oldendorf, Germany
	Rotina 420R benchtop centrifuge	Hettich, Tuttlingen, Germany
	Fresco™ 17 microcentrifuge	Fisher Scientific, Schwerte, Germany
	Multifuge™ X3	ThermoFisher Scientific, Waltham, MA, USA
Counting chamber	Neubauer improved counting chamber	Marienfeld Superior, Lauda Königshofen, Germany
ELISA plate reader	Tristar 3 multimode reader	Berthold Technologies, Bad Wildbad, Germany
ELISA plate washer	CAPPWash plate washer (12 channel)	CAPP, Nordhausen, Germany
Flow cytometer	BD FACSCanto™ II flow cytometer	BD Biosciences, San Jose, CA, USA
	BD LSRFortessa™ cell analyzer	BD Biosciences, San Jose, CA, USA
Freezing container	Nalgene® Mr. Frosty	Sigma-Aldrich, St. Louis, MO, USA
Incubator	BBD 6220 CO_2 incubator	ThermoFisher Scientific, Waltham, MA, USA
Microscope	Microscope Primovert with binocular tube	Zeiss, Oberkochen, Germany
Pipette	Eppendorf Research® plus pipettes (2.5 µl, 20 µl, 200 µl, 1000 µl)	Eppendorf, Hamburg, Germany
	Multichannel pipette (8 channels) Nichipet EX II (200 µl)	Biozym, Hessisch Oldendorf, Germany
Pipette pump	Pipetus®	Hirschmann, Eberstadt, Germany
Scale	Analytical balance ALJ 160-4AM	Kern, Balingen, Germany
	Precision balance EWJ 6000-1SM	Kern, Balingen, Germany
Shaker	MaxQ™ 4000 benchtop orbital shaker	ThermoFisher Scientific, Waltham, MA, USA
Spectrophotometer	NanoDrop™ 2000/2000c spectrophotometer	ThermoFisher Scientific, Waltham, MA, USA
Sterile hood	Herasafe™ KS, class II biological safety cabinet	ThermoFisher Scientific, Waltham, MA, USA
Test tube racks	Nalgene™ Unwire™ test tube racks (30 mm & 13 mm tubes)	Fisher Scientific, Schwerte, Germany

Vortex mixer	Vortex-Genie 2	Scientific Industries, Inc., Bohemia, NY, USA
Waterbath	Waterbath 1012	Gesellschaft für Labortechnik mbH, Burgwedel, Germany
xCELLigence plate reader	xCELLigence RTCA single plate reader	Agilent, Santa Clara, CA, USA

2.1.2 Consumables

Cell culture flasks	Cellstar® cell culture flask with filter screw cap (25 cm²)	Greiner Bio-One, Frickenhausen, Germany
	Cell culture flask with filter cap (T-75, T-175)	Sarstedt, Nümbrecht, Germany
Cell culture plates	6-well flat bottom cell culture plate	Sarstedt, Nümbrecht, Germany
	Falcon® 24-well flat bottom tissue culture-treated cell culture plate	Corning, Corning, NY, USA
	Falcon® 24-well flat bottom not-treated cell culture plate	Corning, Corning, NY, USA
	96-well round bottom cell culture plate	Sarstedt, Nümbrecht, Germany
	96-well flat bottom cell culture plate	Sarstedt, Nümbrecht, Germany
Cell scraper	Cell scraper	Sarstedt, Nümbrecht, Germany
Cryopreservation tubes	CryoPure tubes (2 ml)	Sarstedt, Nümbrecht, Germany
ELISA plates	96-well half area flat bottom microplate	Corning, Corning, NY, USA
Fixation/permeabilization buffer	BD Cytofix/Cytoperm™	BD Biosciences, San Jose, CA, USA
Flow cytometer setup & tracking beads	CS&T research beads	BD Biosciences, San Jose, CA, USA
Flow cytometry compensation beads	UltraComp eBeads™ compensation beads	Invitrogen™, Waltham, MA, USA
Flow cytometry counting beads	CountBright™ absolute counting beads	ThermoFisher Scientific, Waltham, MA, USA
Injection cannulas	BD Microlance™ 3 injection cannula (20 G, 24 G)	Becton Dickinson, Franklin Lakes, NJ, USA
Microcentrifuge tubes	Eppendorf safe-lock tubes (0.5 mL, 1.5 mL)	Eppendorf, Hamburg, Germany
MiniPrep kit	GeneJET plasmid MiniPrep kit	ThermoFisher Scientific, Waltham, MA, USA

Pipette tips	epT.I.P.S.® standard (200 µl)	Eppendorf, Hamburg, Germany
	SafeSeal SurPhob pipette tips (sterile, with filter) (10 µl, 200 µl, 1000 µl)	Biozym, Hessisch Oldendorf, Germany
RNA isolation kit	RNeasy Plus micro kit	Qiagen, Hilden, Germany
Serological pipettes	Stripette™ serological pipette (5 ml, sterile)	Corning, Corning, NY, USA
	Serological pipette (10 ml, sterile)	Sarstedt, Nümbrecht, Germany
	Serological pipette (25 ml, sterile)	Greiner Bio-One, Frickenhausen, Germany
Syringe	Injekt® syringe (5 ml, 10 ml, 20 ml)	Braun, Melsungen, Germany
Syringe filter	Filtropur S (pore size: 0.2 µm, 0.45 µm)	Sarstedt, Nümbrecht, Germany
Test tubes	Falcon® 5 mL round bottom polystyrene test tube (nonsterile)	Corning, Corning, NY, USA
	Falcon® 5 mL round bottom polystyrene test tube (sterile)	Corning, Corning, NY, USA
	Screw cap tube polypropylene (15 ml, 50 ml)	Sarstedt, Nümbrecht, Germany
Wrapping film	Parafilm™ laboratory wrapping film	ThermoFisher Scientific, Waltham, MA, USA
xCELLigence plates	E-Plate 96 PET	Agilent, Santa Clara, CA, USA

2.1.3 Reagents

Albumin fraction V	Carl Roth, Karlsruhe, Germany
BD FACSFlow™	BD Biosciences, San Jose, CA, USA
BD OptEIA™ TMB substrate reagent set	BD Biosciences, San Jose, CA, USA
Dulbecco's phosphate-buffered saline powder (1X)	PanReac AppliChem ITW Reagents, Darmstadt, Germany
eBioscience™ cell stimulation cocktail (500X)	Invitrogen™, Waltham, MA, USA
eBioscience™ fixable viability dye eFluor™ 780	ThermoFisher Scientific, Waltham, MA, USA
eBioscience™ protein transport inhibitor cocktail (500X)	Invitrogen™, Waltham, MA, USA
Ethylenediaminetetraacetic acid disodium salt solution (EDTA)	Sigma-Aldrich, St. Louis, MO, USA
FlowClean cleaning agent	Beckman Coulter, Brea, CA, USA
Gibco™ Dulbecco's phosphate-buffered saline (no calcium, no magnesium)	ThermoFisher Scientific, Waltham, MA, USA
Heparin-sodium-25000-ratiopharm®	Ratiopharm, Ulm, Germany
HEPES solution	Sigma-Aldrich, St. Louis, MO, USA

Lipofectamine™ 2000 transfection reagent	ThermoFisher Scientific, Waltham, MA, USA
RetroNectin® recombinant human fibronectin fragment	Takara Bio Group, Kusatsu, Japan
Sodium carbonate (Na_2CO_3)	Merck, Darmstadt, Germany
Sodium hydrogen carbonate ($NaHCO_3$)	Carl Roth, Karlsruhe, Germany
Sulphuric acid (1 mol / l)	Carl Roth, Karlsruhe, Germany
Trypan Blue solution	Sigma-Aldrich, St. Louis, MO, USA
Trypsin-EDTA solution 10X	Sigma-Aldrich, St. Louis, MO, USA
Tween® 20	Carl Roth, Karlsruhe, Germany

2.1.4 Buffers

MACS buffer	PBS + 0.5 % BSA + 2 mM EDTA	ELISA washing buffer	20 L ddH_2O (double-distilled water) + 191 g PBS + 10 ml Tween® 20
ELISA coating buffer	1 L ddH_2O (double-distilled water) + 7.19 g $NaHCO_3$ + 1.59 g Na_2CO_3 Adjust pH to 9.5	ELISA buffer (R&D kits)	PBS + 1 % BSA
		ELISA buffer (BD kits)	PBS + 10 % FBS

2.1.5 Cell separation products

CD3 human MicroBeads	Miltenyi Biotec, Bergisch Gladbach, Germany
CD8 human MicroBeads	Miltenyi Biotec, Bergisch Gladbach, Germany
EasySep™ human naïve CD4+ T cell isolation kit II	STEMCELL Technologies, Vancouver, Canada
EasySep™ magnet	STEMCELL Technologies, Vancouver, Canada
Histopaque®-1077	Sigma-Aldrich, St. Louis, MO, USA
LS columns	Miltenyi Biotec, Bergisch Gladbach, Germany
MACS® MultiStand	Miltenyi Biotec, Bergisch Gladbach, Germany
QuadroMACS™ separator	Miltenyi Biotec, Bergisch Gladbach, Germany

2.1.6 Antibodies

Table 1 Fluorochrome-conjugated antibodies

Antibody	Clone	Isotype	Concentration	Company
FITC anti-human/ mouse/rat c-myc	SH1-26E7.1.3	Mouse IgG1	1:100	Miltenyi Biotec, Bergisch Gladbach, Germany
PE anti-human IL-9	MH9A4	Mouse IgG2b, κ	1:100	BioLegend, San Diego, CA, USA
PE/Cyanine7 anti-human IFN-γ	4S.B3	Mouse IgG1, κ	1:100	BioLegend, San Diego, CA, USA

2.1.7 ELISA kits

Human IFN-γ ELISA set	BD Biosciences, San Jose, CA, USA
Human IL-9 DuoSet ELISA	R&D Systems, Minneapolis, MN, USA

2.1.8 Cytokines

Dynabeads™ human T-activator CD3/CD28 for T cell expansion and activation	ThermoFisher Scientific, Waltham, MA, USA
Recombinant human IL-12 p70 (Chinese hamster ovary/CHO-derived)	PeproTech, Cranbury, NJ, USA
Recombinant human IL-1β	PeproTech, Cranbury, NJ, USA
Recombinant human IL-23	PeproTech, Cranbury, NJ, USA
Recombinant human IL-4	PeproTech, Cranbury, NJ, USA
Recombinant human IL-6	R&D Systems, Minneapolis, MN, USA
Recombinant human TGF-β1	PeproTech, Cranbury, NJ, USA
Ultra-LEAF™ purified anti-human IFN-γ antibody	BioLegend, San Diego, CA, USA
Ultra-LEAF™ purified anti-human IL-4 antibody	BioLegend, San Diego, CA, USA

2.1.9 Plasmids

Table 2 CAR constructs

Construct	Target	Transmembrane domain	ICD (signal 2)	ICD (signal 1)
a.MSLN.CD28.CD3z	Mesothelin (human)	CD28	CD28	CD3ζ
a.MSLN.4-1BB.CD3z	Mesothelin (human)	CD8α	4-1BB	CD3ζ
a.MSLN.ICOS.CD3z	Mesothelin (human)	ICOS	ICOS	CD3ζ

2.1.10 Cell lines

Table 3 Cell lines

Cell line	Description	Culture medium	Reference
SUIT-2-MSLN	Mesothelin overexpressing pancreatic adenocarcinoma cell line	DMEM 3+	(Karches et al., 2019)
293Vec-GALV	Amphotropic packaging cell line	DMEM 4+	(Ghani et al., 2009)
293Vec-RD114	Amphotropic packaging cell line	DMEM 4+	

2.1.11 Cell culture media and supplements

2.1.11.1 Cell culture supplements

Dulbecco′s modified Eagle medium (DMEM)	Sigma-Aldrich, St. Louis, MO, USA
Fetal bovine serum (FBS)	ThermoFisher Scientific, Waltham, MA, USA
Human serum	Sigma-Aldrich, St. Louis, MO, USA

IL-15	Miltenyi Biotec, Bergisch Gladbach, Germany
IL-2	Clinigen, Yardley, PA, USA
L-glutamine	Sigma-Aldrich, St. Louis, MO, USA
Non-essential amino acid solution (minimum essential medium/MEM, 100X)	Sigma-Aldrich, St. Louis, MO, USA
Penicillin-streptomycin	Sigma-Aldrich, St. Louis, MO, USA
Roswell Park Memorial Institute (RPMI)-1640 medium	Sigma-Aldrich, St. Louis, MO, USA
Sodium pyruvate solution (100 mM)	Lonza, Basel, Switzerland

2.1.11.2 Cell culture media

Dulbecco's modified Eagle medium 3+ (DMEM 3+)	DMEM + 10 % FBS + 1 % L-glutamine + 1 % Penicillin/streptomycin
Dulbecco's modified Eagle medium 4+ (DMEM 4+)	DMEM + 10 % FBS + 2 % L-glutamine + 1 % Penicillin/streptomycin
xCELLigence assay medium	Tumor cell medium + 1 % Non-essential amino acids + 1 % Sodium pyruvate
Human T cell medium (hTCM)	RPMI-1640 + 2.5 % Human serum + 1 % L-glutamine + 1 % Penicillin/streptomycin + 1 % Non-essential amino acids + 1 % Sodium pyruvate

2.1.12 Software

BD FACSDiva™	BD Biosciences, San Jose, CA, USA
EndNote 20	Clarivate, Philadelphia, PA, USA
FlowJo™ 10	BD, Ashland, OR, USA
GraphPad Prism version 9	GraphPad Software, San Diego, CA, USA
Microsoft Office 2021	Microsoft, Redmond, WA, USA
MicroWin 2010	Labsis Laborsysteme GmbH, Neunkirchen-Seelscheid, Germany
NanoDrop™ 2000/2000c	ThermoFisher Scientific, Waltham, MA, USA
RStudio version 1.4.1717	RStudio, Boston, MA, USA
RTCA software 2.0	Agilent, Santa Clara, CA, USA

2.2 Methods

2.2.1 Cell culture

All cell culture work was performed in S1 or S2 laboratories as appropriate. Cells were cultured in sterile 6-well, 24-well or 96-well flat-bottom plates or in sterile cell culture flasks (T-25, T-75, T-175) at 37 °C with 5 % CO_2 and 95 % humidity. All cell culture work was performed under a sterile cell culture hood. Adherent cell lines were passaged when cells reached a confluency of 70 – 80 % under a microscope. Cells were either detached with a sterile cell scraper or with a 1X trypsin solution (T-25: 2 ml trypsin; T-75: 5 ml trypsin; T-175: 8 ml trypsin), washed once with PBS and resuspended in the appropriate medium.

2.2.2 Cell counting

Cells were counted using Neubauer improved cell counting chambers. Prior to counting, adherent cells were detached and resuspended in an appropriate volume for counting. For counting, cells were diluted 1:10 in Trypan Blue, and 10 µl of this 1:10 dilution was added to the counting chamber. For low cell counts, cells were diluted 1:2. To determine accurate cell counts, all four large squares of the Neubauer counting chamber, each containing 16 smaller squares, were counted. Absolute cell counts in 10^6 cells / ml were determined as the product of the number of cells counted per large square and the dilution factor multiplied by 10^4. Viability was assessed by determining the proportion of live cells to the total number of cells. Cells were only used for assays if their viability was greater than 80 %.

2.2.3 Cryopreservation of cells

Prior to cryopreservation, cells were washed twice in PBS, counted, and resuspended in FBS. 100 µl of DMSO was added to every cryopreservation tube, followed by 900 µl of the cell suspension. Cryos were immediately transferred to a Mr. Frosty and placed in a -80 °C freezer. Approximately 5 x 10^6 cells were preserved per cryopreservation tube. Cryopreserved cells were stored at -80 °C for short-term storage and below -140 °C in the vapor phase of a liquid nitrogen tank for long-term storage.

2.2.4 Generation of producer cell lines

Producer cell lines stably produce retroviral virus, ensuring the reproducibility of retroviral transductions. Plasmid-DNA containing the CAR construct was first amplified using a MiniPrep kit according to the manufacturer's protocol. A 293Vec-Galv retroviral packaging cell line was then transfected with the amplified plasmid-DNA. The supernatant produced by the packaging cell line was subsequently used to transduce a 293Vec-RD114 packaging cell line to generate RD114-construct producers. For retroviral transductions, fresh virus supernatant was collected from producer cell lines at a cell confluency of 70 – 80 %.

2.2.5 Isolation of primary human peripheral blood mononuclear cells, naïve CD4+ T cells and CD3+ T cells

Primary human peripheral blood mononuclear cells (PBMC) were isolated from the blood of healthy donors using a Histopaque®-1077 gradient and were further sorted for CD3+ T cells or naïve CD4+ T cells. Human T cell medium (hTCM) was used for the culture of primary human T cells, and anti-CD3/CD28 Dynabeads were added to the cell suspension at a cell to bead ratio of 3:1 for T cell activation.

CD3+ T cells were isolated from healthy donor PBMC using a magnetic activated cell sorting approach (MACS) with CD3 MicroBeads and LS columns. CD3+ T cells were resuspended in hTCM supplemented with human IL-2 1:50 and human IL-15 1:20000 at a concentration of 0.25 – 1 x 10^6 cells / ml.

Naïve CD4+ T cells were isolated from healthy donor PBMC through negative selection using an EasySep™ human naïve CD4+ T cell isolation kit. Naïve CD4+ T cells were resuspended in hTCM supplemented with human IL-2 1:100 and human IL-15 1:20000 at a concentration of 0.25 x 10^6 cells / ml.

2.2.6 Retroviral transduction of human T cells

Non-tissue culture treated 24-well-plates were coated with RetroNectin one day prior to retroviral transduction. Primary human T cells were retrovirally transduced on day two after isolation using fresh virus supernatant generated by producer cell lines. Naïve CD4+ T cells were transduced at a concentration of 0.25 x 10^6 cells / ml. CD3+ T cells were transduced at a concentration of 0.25 – 1 x 10^6 cells / ml. Transduction efficiency was measured one day after transduction, and in case of insufficient transduction efficiency, T cells were retrovirally transduced once again. T cells were expanded every two days and cultured at a concentration of 0.25 – 1 x 10^6 cells / ml.

2.2.7 Polarization of naïve CD4+ T cells

To induce the differentiation of naïve CD4+ T cells, subset-specific polarizing cytokines were added to cell suspensions every two days. Th1 cells were differentiated using IL-12 (5 ng / ml, only on day 0) and αIL-4 (10 μg / ml). Th2 cells were polarized using IL-4 (20 ng / ml) and αIFN-γ (10 μg / ml). Th9 and Th9+ cells were differentiated using IL-4 (20 ng / ml), TGF-β (2 ng / ml), αIFN-γ (10 μg / ml) and, in the case of Th9+ cells, IL-1β (10 ng / ml). Th17 cells were polarized using IL-6 (10 ng / ml), IL-23 (20 ng / ml), IL-1β (10 ng / ml), αIL-4 (10 μg / ml) and αIFN-γ (10 μg / ml). Correct polarization was analyzed using ELISA and flow cytometry.

2.2.8 Flow cytometry

Flow cytometry (FACS, fluorescence activated cell sorting) enables the detection and sorting of cells based on the binding of fluorochrome-coupled antibodies. Cells were

first stained for cell surface antigens (antibody concentration 1:100). A fixable viability dye at a concentration of 1:1000 was included in this step to differentiate live from dead cells. Subsequently, cells were either washed and resuspended in PBS for immediate FACS analysis or fixed and permeabilized to stain for intracellular antigens (antibody concentration 1:100). Fixed and stained cells were washed and resuspended in permeabilization buffer with 2 % FBS prior to FACS analysis. To assess CD4+ T cell polarization, antibodies detecting interferon-γ (IFN-γ) and IL-9 were used. To measure transduction efficiency, a FITC-conjugated antibody detecting c-myc was used.

2.2.9 Cytokine secretion assay

An enzyme-linked immunosorbent assay (ELISA) enables the detection of cytokines or other secreted molecules in the supernatant of the cells of interest. Supernatants were first incubated with a plate-bound capture antibody. After washing, detection antibodies were added and subsequently coupled to streptavidin-horseradish peroxidase. After stopping the reaction with sulfuric acid, absorbance was measured. A nonlinear least squares regression based on the absorbance values of a standard was used to infer cytokine secretion from absorbance measurements.

2.2.10 Proliferation assay

Naïve CD4+ T cells were cultured in polarizing medium at a concentration of 0.25×10^6 cells / ml. 200 µl of the cell suspension was added to every well of a 96-well-plate. Every two days, 100 µl of supernatants were collected to assess cytokine secretion. Cells were resuspended in the remaining 100 µl and stained with a fixable viability dye. Proliferation was assessed using counting beads for flow cytometry. Cells in the remaining wells were split 1:2 and resuspended in 150 µl of polarizing medium.

2.2.11 Real-time cytotoxicity assay

Prior to xCELLigence measurements, T cells were retrovirally transduced on day two after isolation and expanded for a total of six days. xCELLigence measurements enable the real-time and continual assessment of tumor cell adhesion, proliferation and lysis. Changes in electrical impedance resulting from target cell adhesion or detachment are translated into a unit-free measure, the cell index. After blanking with an electrically conductive medium, 3×10^4 MSLN-overexpressing SUIT-2-MSLN tumor cells were seeded per well in a 96-well xCELLigence plate. Once the tumor cells had entered a linear phase of proliferation, 6×10^4 CAR T cells or untransduced T cells were added per well for an effector to target ratio of 2:1.

2.2.12 RNA sequencing

To prepare samples for ribonucleic acid (RNA) extraction, DynaBeads were removed from the cell suspension, and cells were washed twice. RNA was extracted using a RNeasy micro kit according to the manufacturer's protocol. In brief, samples were lysed

and homogenized and subsequently resuspended in ethanol. Purified RNA was bound to a silica membrane, washed and eluted in water. To check the quality of the isolated RNA, RNA concentration was measured using a NanoDrop instrument, and the integrity of the isolated RNA was assessed using a Bioanalyzer.

RNA was isolated on day 7 after primary T cell isolation. The following subsets were analyzed for RNA sequencing: Th1, Th2, Th9, Th9+, Th17. RNA sequencing and the bioinformatic analysis of the sequencing results were performed by our collaborators at the Technical University of Munich (principal investigator Prof. Dr. Roland Rad).

2.2.13 RNA sequencing analysis

For the analysis of the transcriptional profiles of different T helper cell subsets, DESeq2 log2 fold changes with *apeglm*-shrinkage and adjusted p-values were used. For gene set enrichment analysis (GSEA), pathways from the Reactome Pathway Database and normalized enrichment scores (NES) were used (Gillespie et al., 2021). Gene expression was considered significant if $p < 0.01$.

For the calculation of expression scores, gene signatures were either downloaded from the Molecular Signatures Database or adapted from previous publications. The gene sets “HALLMARK_APOPTOSIS”, “GOBP_ALPHA_BETA_T_CELL_ PROLIFERATION_GO 0046633”, “HALLMARK_GLYCOLYSIS” and “HALLMARK_ OXIDATIVE_PHOSPHORYLATION” were downloaded from the Molecular Signatures Database (Ashburner et al., 2000, Carbon et al., 2008, Liberzon et al., 2015, Subramanian et al., 2005, The Gene Ontology Consortium et al., 2023). Gene signatures of a 4-1BB ICD phenotype (Boroughs et al., 2020, Long et al., 2015), CD28 ICD phenotype (Long et al., 2015), effector phenotype (Sheih et al., 2020, Willinger et al., 2005) and exhaustion (Sheih et al., 2020, Wherry et al., 2007) were adapted from previous publications. Expression scores were calculated by forming the sum of the *apeglm*-shrunken log2 fold changes of all significantly up- or downregulated genes in a gene set. Only fold changes < -1 or > 1 were considered.

2.2.14 Statistical analysis

FACS data was analyzed using BD FACSDiva and FlowJo software. xCELLigence data was analyzed using RTCA software. ELISA data was analyzed using MicroWin software. NanoDrop data was analyzed using NanoDrop 2000/2000c software. GraphPad Prism was used to make figures 1, 4, 5, 8, 13 and 14. The packages ggplot2 (Wickham, 2016), ggrepel (Slowikowski, 2021), cowplot (Wilke, 2020) and fmsb (Nakazawa, 2023) in RStudio (R Core Team, 2021) were used to generate figures 2, 3, 6, 7, 9, 10 and 11. Figure 12 was created using Microsoft Office PowerPoint. Analyses of differences between groups were performed using one-way analysis of variance (ANOVA) with correction for multiple testing by the Turkey method or using two-way ANOVA with correction for multiple testing by the Bonferroni method. Unless otherwise stated, a p-value cutoff of $p < 0.05$ was used to determine statistical significance.

Results

3.1 Incubation of naïve CD4+ T cells with polarizing cytokines results in effective polarization of T helper cell subsets

Naïve CD4+ T cells were incubated with polarizing cytokines to induce their differentiation towards either a Th1, Th2, Th9, Th9+ or Th17 phenotype. To confirm effective polarization, the secretion of subset-specific cytokines was determined using flow cytometry and ELISA. The percentage of IFN-γ-positive T cells was increased in the Th1 subset compared to the Th2, Th9, Th9+ and Th17 subsets on day seven after isolation (Fig. 1a). Likewise, the percentage of IL-9-positive T cells was higher in the Th9+ subset compared to the Th1, Th2, Th9 and Th17 subsets (Fig. 1b). While the percentage of IL-9-positive T cells also seemed to be higher in the Th9 subset relative to the Th1, Th2 and Th17 subsets, this effect was not statistically significant (Fig. 1b).

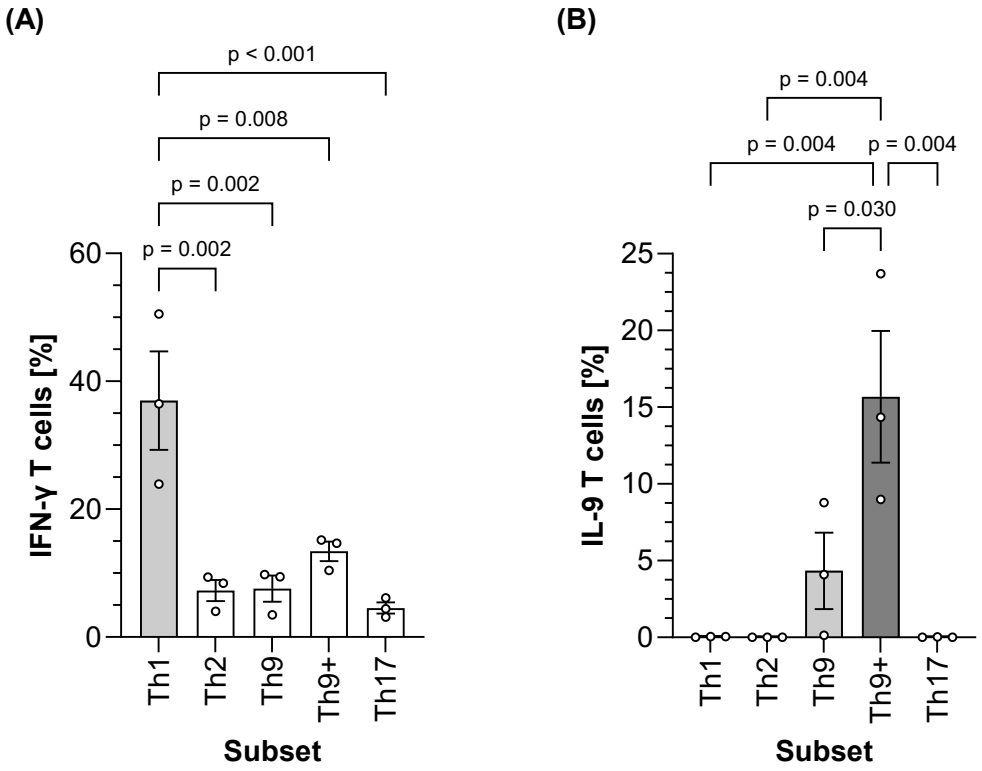

Figure 1 Incubation with polarizing cytokines results in effective polarization of T helper cell subsets

Human CD4+ T cells were polarized towards a Th1, Th2, Th9, Th9+ or Th17 phenotype. IFN-γ and IL-9 expression were measured in the abovementioned subsets on day 7 after isolation using flow cytometry. Depicted in (A) are mean percentages of IFN-γ-positive cells ± SEM in Th1, Th2, Th9, Th9+ and Th17 cells of three (n = 3) independent donors. The Th1 subset is highlighted in grey. Depicted in (B) are mean percentages of IL-9-positive cells ± SEM in the abovementioned subsets of three (n = 3) independent donors. The Th9 and Th9+ subsets are highlighted in grey. Each point represents one donor. For each donor, measurements were performed in duplicates. Analyses of differences between groups were performed using one-way analysis of variance (ANOVA) with correction for multiple testing by the Turkey method.

To confirm effective polarization on a gene expression level, RNA was extracted from CD4+ T cells polarized towards either a Th1, Th2, Th9, Th9+ or Th17 phenotype and sequenced on day seven after isolation. For every T helper cell subset, a set of subset-defining genes was defined to include cytokines characteristically produced by a subset as well as lineage-driving transcription factors. An upregulation of these subset-defining genes could be found in every T helper cell subset (Table 4).

Table 4 Gene expression of T helper cell subset-defining genes
CD4+ T cells were polarized towards either a Th1, Th2, Th9, Th9+ or Th17 phenotype. RNA was extracted from each group on day 7 after isolation and sequenced. Data was pooled for three (n = 3) independent donors. Subset-defining genes were defined as transcription factors essential for driving polarization towards a T helper cell lineage or as cytokines characteristically produced by a subset. Fold changes represent log2 fold changes with *apeglm*-shrinkage. All fold changes are depicted relative to the Th1 subset. To determine significance, a p-value cutoff of p = 0.05 was used. Fold changes that did not reach statistical significance are depicted in grey and annotated with the term (ns).

Comparison: Th1 vs. subset	Gene	*Apeglm*-adjusted log2 fold change	Adjusted p-value
Th2	IFN-γ	-4.604	3.52E-88
	IL-2	-3.168	0.002
	Tbx21	-4.283	2.79E-15
	Tnf	-1.032	0.014
	Gata3	1.247	1.61E-09
	IL-13	0.068	0.764 (ns)
	IL-5	1.073	0.049
	Irf4	0.085	0.767 (ns)
Th9	IFN-γ	-4.358	8.24E-80
	IL-2	-2.980	0.002
	Tbx21	-4.901	8.63E-14
	Tnf	-0.258	0.421 (ns)
	IL-9	1.820	0.004
	Irf4	0.075	0.840 (ns)
Th9+	IFN-γ	-4.015	2.28E-70
	IL-2	-3.796	3.93E-04
	Tbx21	-3.964	2.67E-15
	Tnf	0.590	0.101 (ns)
	IL-9	3.505	3.47E-08
	Irf4	0.080	0.832 (ns)
Th17	IFN-γ	-2.734	6.79E-34
	IL-2	-0.033	0.376 (ns)
	Tbx21	-2.504	1.53E-08
	Tnf	-0.065	0.437 (ns)
	IL-17F	3.387	7.54E-11
	IL-21	-0.097	0.213 (ns)
	IL-22	0.019	0.730 (ns)

IFN-γ and Tbx21 were upregulated in the Th1 subset compared to the Th2, Th9, Th9+ and Th17 subsets. IL-2 was upregulated in the Th1 subset compared to every subset except for Th17. Tnf, encoding TNF-α, was upregulated in the Th1 subset relative to the Th2 subset. IL-5 and Gata3 were upregulated in the Th2 subset compared to the Th1 subset. IL-17F was upregulated in the Th17 subset compared to the Th1 subset (Table 4).

Table 5 Gene expression of IL-9 in different T helper cell subsets
CD4+ T cells were polarized towards either a Th1, Th2, Th9, Th9+ or Th17 phenotype. RNA was extracted from each group on day 7 after isolation and sequenced. Data was pooled for three (n = 3) independent donors. Gene expression data for IL-9 is shown for Th9 and Th9+ cells, each compared to Th1, Th2 or Th17 cells. Fold changes represent log2 fold changes with *apeglm*-shrinkage. To determine significance, a p-value cutoff of p = 0.05 was used. Fold changes that did not reach statistical significance are depicted in grey and annotated with the term (ns).

Population	Comparison to subset	*Apeglm*-adjusted log2 fold change	Adjusted p-value
Th9	Th1	1.820	0.004
	Th2	0.072	7.35E-04
	Th9+	-0.016	0.410 (ns)
	Th17	1.986	0.002
Th9+	Th1	3.505	3.47E-08
	Th2	4.125	5.47E-10
	Th17	3.646	1.23E-08

IL-9 was upregulated in the Th9 subset compared to Th1 and Th17 cells and in the Th9+ subset compared to Th1, Th2 and Th17 cells. IL-9 was not differentially expressed between the Th9 and Th9+ subsets. While statistically significant, the *apeglm*-adjusted log2 fold change of IL-9 between conventional Th9 and Th2 cells was less than one (Table 5).

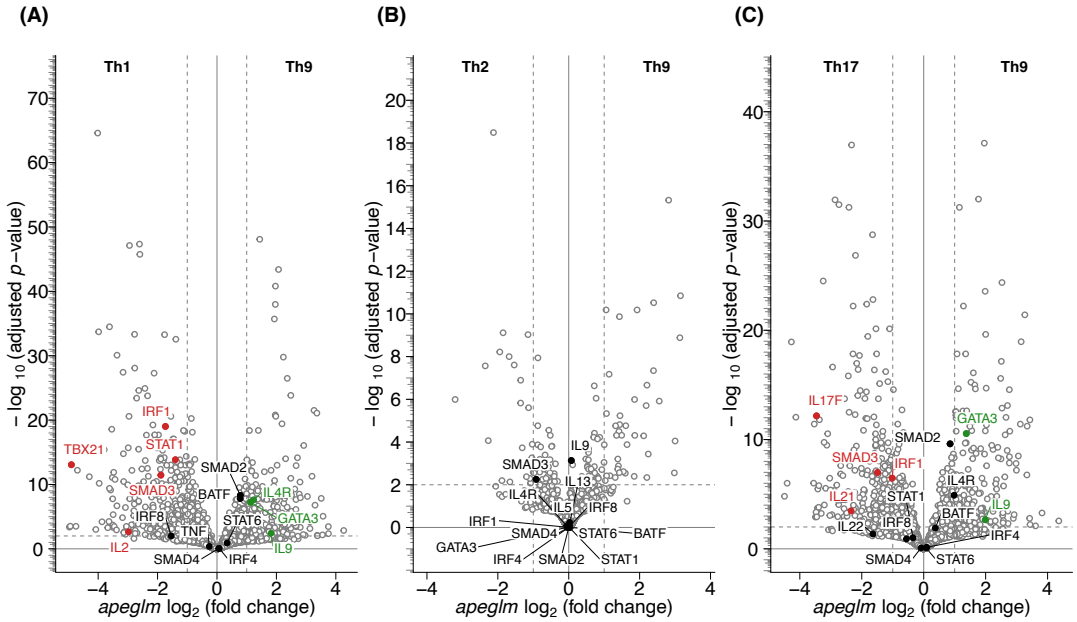

Figure 2 Th9-defining genes are differentially expressed by Th9 cells compared to Th1 and Th17 cells

CD4+ T cells were polarized towards either a Th1, Th2, Th9, Th9+ or Th17 phenotype. RNA was extracted from each group on day 7 after isolation and sequenced. Depicted here is the gene expression profile of Th9 cells compared to (A) Th1 cells, (B) Th2 cells, or (C) Th17 cells. Data was pooled for three (n = 3) independent donors. For each comparison, subset-defining genes are highlighted. Genes characteristic of a Th9 lineage are consistently highlighted in green (adjusted fold change > 1 and $p < 0.01$), while those characteristic of either a (A) Th1, (B) Th2, or (C) Th17 lineage are highlighted in red (adjusted fold change < -1 and $p < 0.01$). Subset-defining genes which were not differentially expressed are highlighted in black (-1 < adjusted fold change < 1 and/or $p > 0.01$). Fold changes represent log2 fold changes with *apeglm*-shrinkage and are depicted on the x-axis. Adjusted p-values were logarithmically transformed and are depicted on the y-axis. To determine significance, a p-value cutoff of $p = 0.01$ was used.

Irf4 was not upregulated in the Th9 or Th9+ subsets compared to the Th1, Th2 and Th17 subsets (Fig. 2 and 3). Gata3 was upregulated in the Th9 and Th9+ subsets compared to the Th1 and Th17 subsets (Fig. 2 and 3). Il4r, encoding IL-4 receptor, was upregulated in the Th9 subset compared to the Th1 subset (Fig. 2). IL-5 and IL-13 were upregulated in the Th9+ subset compared to the Th2 subset (Fig. 3). No subset-defining genes were differentially expressed between the Th9 and Th2 subsets (Fig. 2).

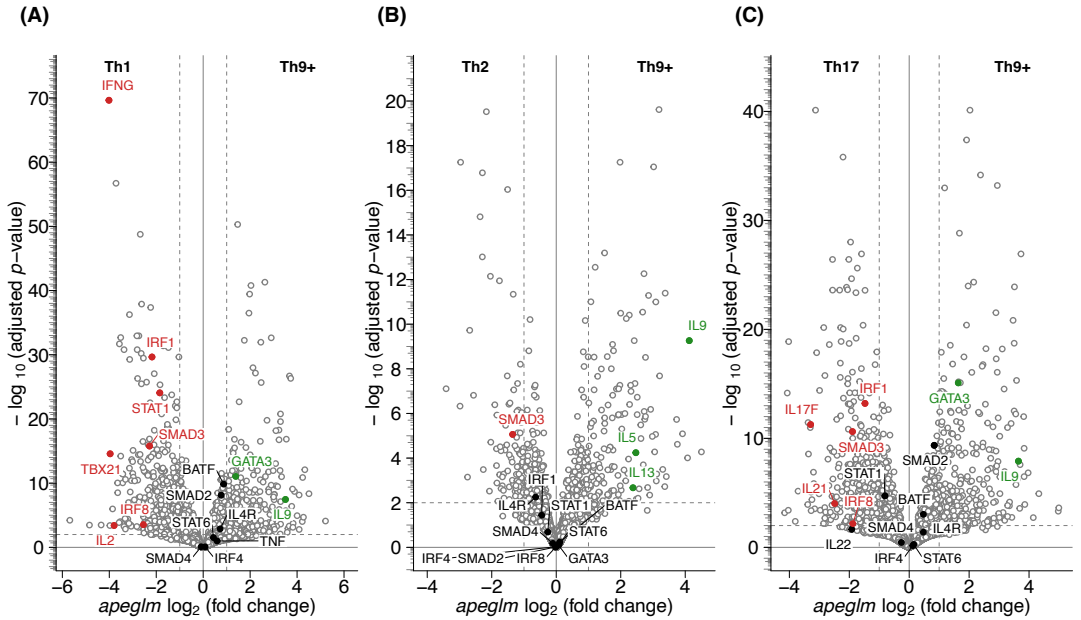

Figure 3 Th9-defining genes are differentially expressed by Th9+ cells compared to Th1, Th2 and Th17 cells

CD4+ T cells were polarized towards either a Th1, Th2, Th9, Th9+ or Th17 phenotype. RNA was extracted from each group on day 7 after isolation and sequenced. Depicted here is the gene expression profile of Th9+ cells compared to (A) Th1 cells, (B) Th2 cells, or (C) Th17 cells. Data was pooled for three (n = 3) independent donors. For each comparison, subset-defining genes are highlighted. Genes characteristic of a Th9 lineage are consistently highlighted in green (adjusted fold change > 1 and $p < 0.01$), while those characteristic of either a (A) Th1, (B) Th2, or (C) Th17 lineage are highlighted in red (adjusted fold change < -1 and $p < 0.01$). Subset-defining genes which were not differentially expressed are highlighted in black (-1 < adjusted fold change < 1 and/or $p > 0.01$). Fold changes represent log2 fold changes with *apeglm*-shrinkage and are depicted on the x-axis. Adjusted p-values were logarithmically transformed and are depicted on the y-axis. To determine significance, a p-value cutoff of $p = 0.01$ was used.

To determine whether cytokine secretion is stable throughout the polarization process, the secretion of IFN-γ and IL-9 was measured in supernatants every two days using ELISA. The secretion of IFN-γ by Th1 cells as well as the secretion of IL-9 by Th9 and Th9+ cells were variable throughout the polarization process. IFN-γ secretion by Th1 cells was highest on day four after isolation (Fig. 4a). IL-9 secretion by Th9 and Th9+ cells was highest between days four and six after isolation (Fig. 4b-c).

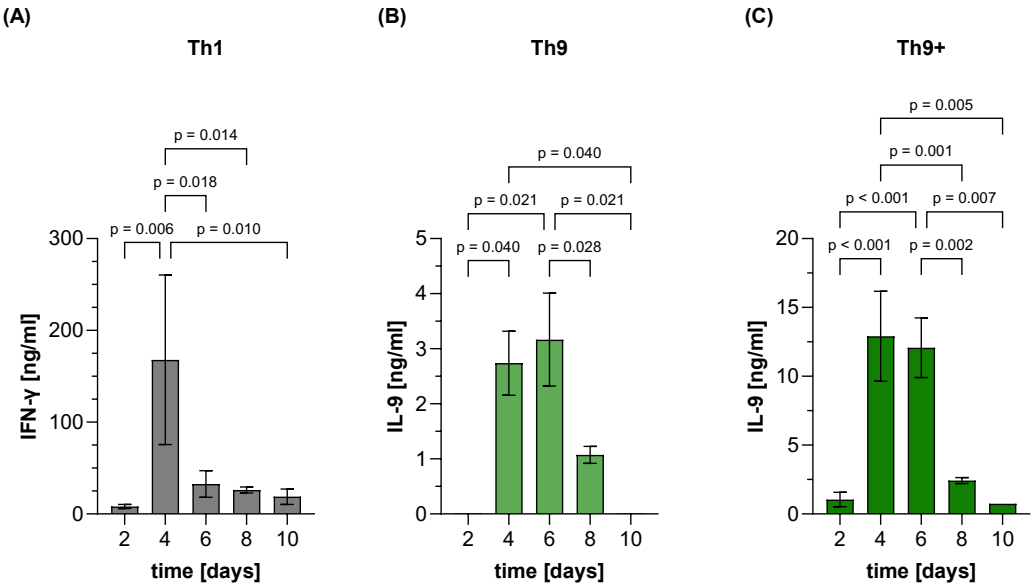

Figure 4 Cytokine secretion is variable and highest four to six days after polarization
CD4+ T cells were polarized towards a Th1, Th9 or Th9+ phenotype. Supernatants were collected on days 2, 4, 6, 8 and 10 after isolation. IFN-γ and IL-9 secretion were measured using ELISA. Depicted in (A) is mean IFN-γ secretion ± SEM in Th1 cells. Depicted in (B) and (C) is mean IL-9 secretion ± SEM in (B) Th9 and (C) Th9+ cells, respectively. Shown here is data of one donor representative of three (n = 3) independent donors. For each donor, measurements were performed in triplicates. Analyses of differences between groups were performed using one-way ANOVA with correction for multiple testing by the Turkey method.

IL-1β has been shown to enhance the differentiation of murine CD4+ T cells towards a Th9 phenotype (Végran et al., 2014). To assess polarization efficacy between conventional Th9 and Th9+ cells, IL-9 secretion was compared between both subsets. IL-9 secretion was higher in the Th9+ condition on days four and six after isolation (Fig. 5).

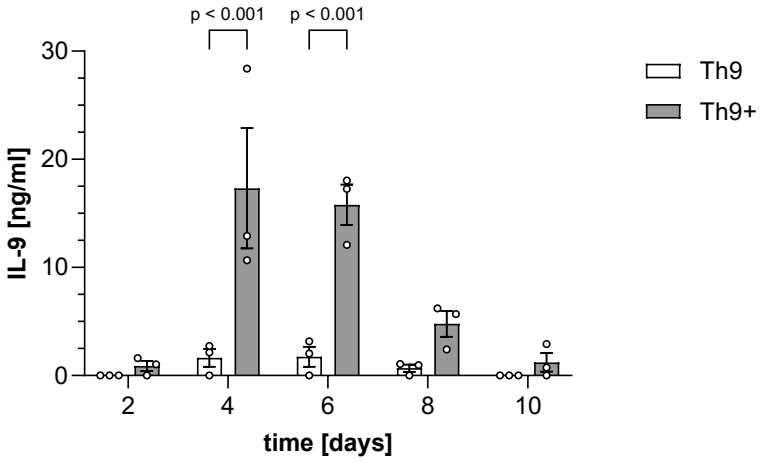

Figure 5 Incubation with IL-1β enhances T cell polarization towards a Th9 phenotype
CD4+ T cells were polarized towards a Th9 phenotype in the presence (Th9+) or absence (Th9) of IL-1β. Supernatants were collected on days 2, 4, 6, 8 and 10 after isolation. IL-9 secretion was measured using ELISA. Depicted here is mean IL-9 secretion ± SEM of three (n = 3) independent donors. Each point represents one donor. For each donor, measurements were

performed in triplicates. Analyses of differences between groups were performed using two-way ANOVA with correction for multiple testing by the Bonferroni method.

To further evaluate the influence of IL-1β on human Th9 differentiation, the gene expression profiles of conventional Th9 and Th9+ cells were compared (Fig. 6). Three genes were differentially expressed using an *apeglm*-shrunken log2 fold change cutoff of one and an adjusted p-value cutoff of 0.01 (Fig. 6). Zc3h12a, encoding monocyte chemotactic protein-induced protein 1 (MCPIP-1), as well as Basp1, encoding brain acid soluble protein 1, were upregulated in the Th9+ subset. Clic3, encoding chloride intracellular channel protein 3, was upregulated in the Th9 subset.

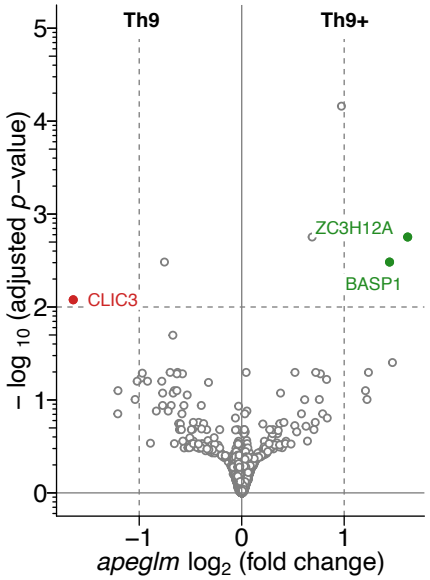

Figure 6 Zc3h12a, Basp1 and Clic3 are differentially expressed in the Th9+ and Th9 subsets
CD4+ T cells were polarized towards either a Th1, Th2, Th9, Th9+ or Th17 phenotype. RNA was extracted from each group on day 7 after isolation and sequenced. Depicted here is the gene expression profile of Th9+ cells compared to Th9 cells. Data was pooled for three (n = 3) independent donors. Genes upregulated in Th9+ cells are highlighted in green (adjusted fold change > 1 and p < 0.01), and those upregulated in Th9 cells are highlighted in red (adjusted fold change < -1 and p < 0.01). Fold changes represent log2 fold changes with *apeglm*-shrinkage and are depicted on the x-axis. Adjusted p-values were logarithmically transformed and are depicted on the y-axis. To determine significance, a p-value cutoff of p = 0.01 was used.

To further characterize these differences, GSEA based on the Reactome Pathway Database was performed (Fig. 7). In the Th9 subset, gene sets associated with protein translation, including cellular responses to amino acid deficiency, and with G-protein-mediated signaling were upregulated. In the Th9+ subset, gene sets associated with interleukin signaling, particularly interleukin-1 signaling, and with cell cycle and DNA replication were upregulated. In addition, gene sets related to organelle biogenesis, including cilium assembly, and NF-κB pathway activation were upregulated in this subset. Furthermore, gene sets related to TNF receptor (TNFR) signaling, Hedgehog signaling and apoptosis were upregulated in the Th9+ subset.

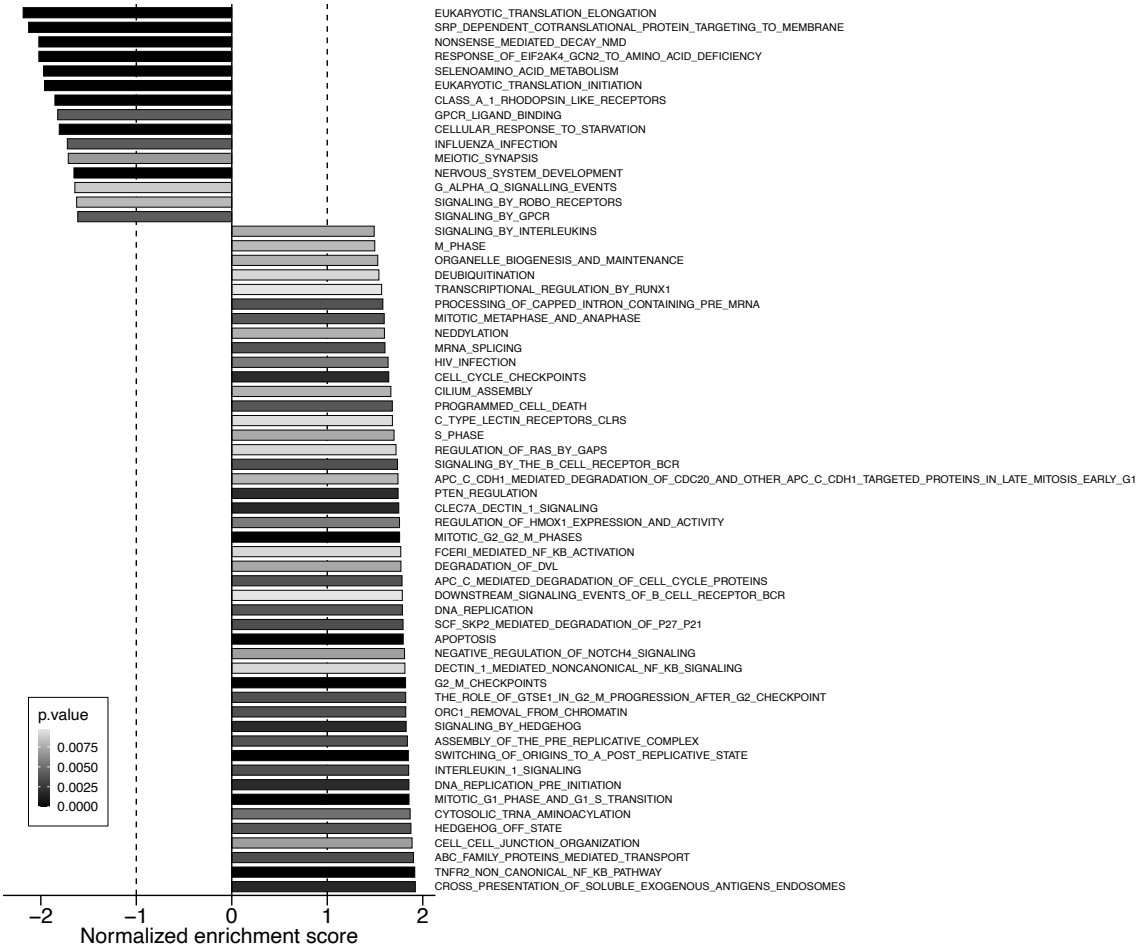

Figure 7 Gene sets associated with interleukin signaling and cell cycle regulation are enriched in the Th9+ subset relative to the conventional Th9 subset
CD4+ T cells were polarized towards either a Th1, Th2, Th9, Th9+ or Th17 phenotype. RNA was extracted from each group on day 7 after isolation and sequenced. Depicted here is the differential expression of gene sets based on the Reactome Pathway Database in the Th9 and Th9+ subsets. Data was pooled for three (n = 3) independent donors. To determine relative gene set expression, normalized enrichment scores (NES) were used (Th9: NES < -1; Th9+: NES > 1). Only pathways whose NES was significant ($p < 0.01$) are displayed. For each gene set, bar shading corresponds to p-values.

3.2 Th9+ cells exhibit an efficient and sustained proliferative capacity

Since reduced CAR T cell persistence is a key factor limiting the success of CAR T cell therapy (Fraietta et al., 2018), the proliferative capacity of Th1, Th2, Th9, Th9+ and Th17 cells was analyzed. To determine proliferative capacity, the ratio of live cells to counting beads was measured using flow cytometry over the course of ten days. The only subsets presenting increases in cell number between days two and eight were Th2 and Th9+ cells (Fig. 8). While Th1, Th9 and Th17 cells also seemed to proliferate, this difference was not statistically significant.

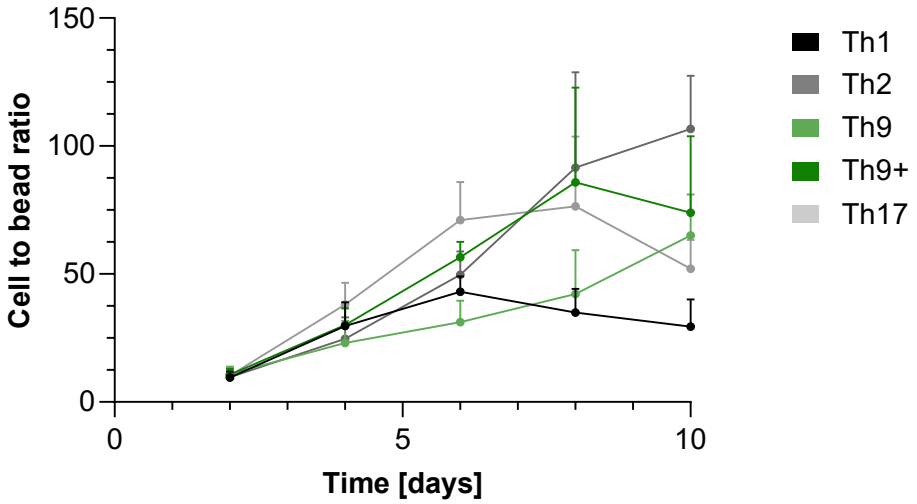

Figure 8 Th9+ cells exhibit an efficient and sustained proliferative capacity
CD4+ T cells were polarized towards either a Th1, Th2, Th9, Th9+ or Th17 phenotype. Proliferative capacity was measured using flow cytometry by analyzing the ratio of live cells to counting beads. For each donor, measurements were performed in duplicates. Depicted here are mean cell to bead ratios ± SEM of three (n = 3) independent donors for the abovementioned subsets. Analyses of differences between groups were performed using two-way ANOVA with correction for multiple testing by the Bonferroni method. The following comparisons were significant: Th2 day 2 vs. day 8 $p = 0.026$, day 2 vs. day 10 $p = 0.005$, and day 4 vs. day 10 $p = 0.008$. Th9+ day 2 vs. day 8 $p = 0.020$. All other comparisons were not significant.

3.3 Th9+ cells exhibit an advantageous phenotypic and metabolic profile for CAR T cell therapy

We next sought to further characterize the transcriptional phenotype of Th9+ cells by comparing it to the gene expression profile of Th1 cells. To this end, GSEA based on the Reactome Pathway Database was performed (Fig. 9). In the Th9+ subset, gene sets associated with metabolic and biosynthetic processes were upregulated, including fatty acid and amino acid metabolism and oxidative phosphorylation. In the Th1 subset, gene sets associated with an inflammatory response and signaling by interferons and interleukins were upregulated. In addition, gene sets associated with cellular senescence and programmed cell death were upregulated in Th1 cells.

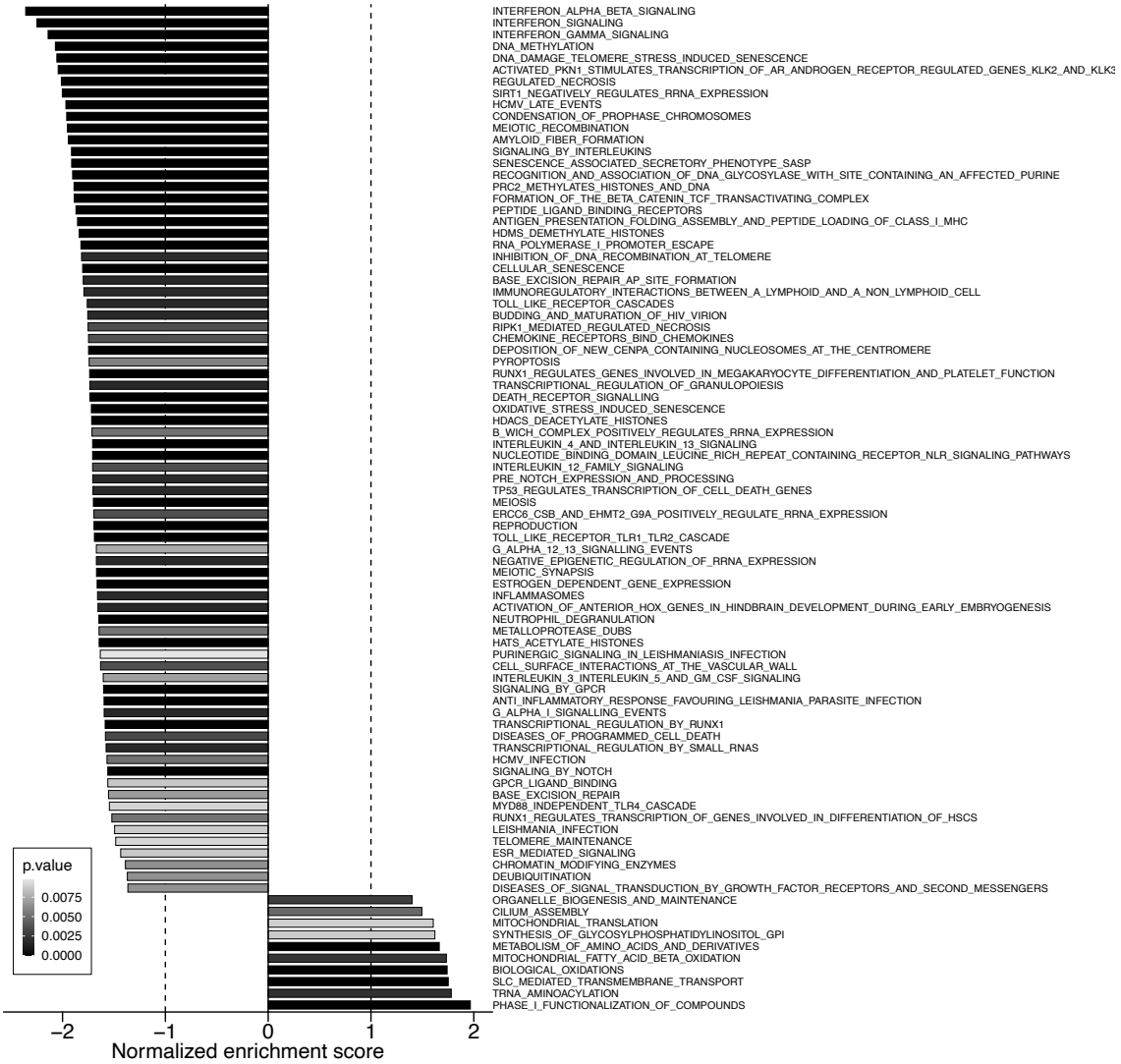

Figure 9 Gene sets associated with mitochondrial metabolism are enriched in the Th9+ subset relative to the Th1 subset
CD4+ T cells were polarized towards either a Th1, Th2, Th9, Th9+ or Th17 phenotype. RNA was extracted from each group on day 7 after isolation and sequenced. Depicted here is the differential expression of gene sets based on the Reactome Pathway Database in the Th1 and Th9+ subsets. Data was pooled for three (n = 3) independent donors. To determine relative gene set expression, normalized enrichment scores (NES) were used (Th1: NES < -1; Th9+: NES > 1). Only pathways whose NES was significant ($p < 0.01$) are displayed. For each gene set, bar shading corresponds to p-values.

To explore whether a Th9+ subset exhibits a favorable phenotypic profile for CAR T cell therapy, the expression of genes associated with factors contributing to CAR T cell therapy success or failure was compared between Th9+ and Th1 cells. Factors associated with enhanced CAR T cell function include a sufficient proliferative capacity, a metabolic profile favoring oxidative phosphorylation over anaerobic processes and a central memory phenotype (Chen et al., 2021, Fraietta et al., 2018, Melenhorst et al., 2022). Factors associated with CAR T cell therapy failure include T cell exhaustion, apoptosis and an effector phenotype (Deng et al., 2020, Finney et al., 2019, Fraietta et al., 2018). For each subset, an expression scored was calculated for each factor by forming the sum of the fold changes of all significantly upregulated

genes in that gene set (Fig. 10). Genes related to apoptosis (expression scores: Th1: 37.872; Th9+: 8.530), exhaustion (Th1: 22.895; Th9+: 5.230), effector phenotype (Th1: 22.687; Th9+: 2.081) and proliferation (Th1: 16.423; Th9+: 2.112) were upregulated in the Th1 subset. Genes associated with oxidative phosphorylation (Th1: 1.153; Th9+: 10.568) were upregulated in the Th9+ subset. Genes associated with glycolysis (Th1: 8.441; Th9+: 9.765) were expressed in a similar manner in both subsets (Fig. 10).

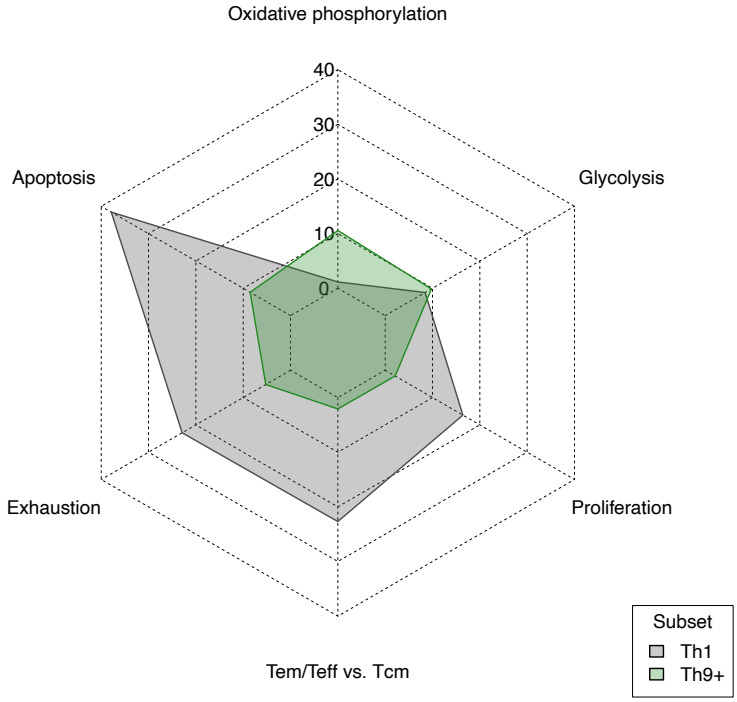

Figure 10 Genes associated with CAR T cell therapy failure are upregulated to a greater extent in the Th1 subset compared to the Th9+ subset
CD4+ T cells were polarized towards either a Th1, Th2, Th9, Th9+ or Th17 phenotype. RNA was extracted from each group on day 7 after isolation and sequenced. Data was pooled for three (n = 3) independent donors. Depicted here are expression scores of factors associated with CAR T cell therapy failure (apoptosis, exhaustion, Tem/Teff vs. Tcm phenotype, glycolysis) or with enhanced CAR T cell persistence (proliferation, oxidative phosphorylation) in the Th1 and Th9+ subsets. For each subset, an expression score was calculated for each factor by forming the sum of *apeglm*-shrunken log2 fold changes of all significantly upregulated genes ($p < 0.01$) associated with that specific factor. Expression scores for the Th1 subset are depicted in grey, expression scores for the Th9+ subset in green.

The transcriptional profile described for 4-1BB-based CAR T cells closely resembles that of Th9+ cells, notably in terms of metabolism, memory phenotype and susceptibility to exhaustion (Boroughs et al., 2020, Long et al., 2015). We next sought to analyze the differential expression of a 4-1BB ICD and a CD28 ICD gene signature in Th1 and Th9+ cells. The 4-1BB ICD gene signature was adapted from Long et al. and Boroughs et al. and comprised 4511 genes associated with 4-1BB ICD signaling in BBz-CAR T cells (Boroughs et al., 2020, Long et al., 2015). The CD28 ICD gene signature was adapted from Long et al. and included 5338 genes associated with CD28 ICD signaling in CD28z-CAR T cells (Long et al., 2015). For each subset, an expression scored was calculated for each gene signature by forming the sum of the

fold changes of all significantly upregulated genes in that gene set. The expression score of a 4-1BB ICD gene signature was higher in Th9+ cells (Th1: 170.495; Th9+: 237.693). The expression score of a CD28 ICD gene signature was higher in Th1 cells (Th1: 329.879; Th9+: 85.901) (Fig. 11).

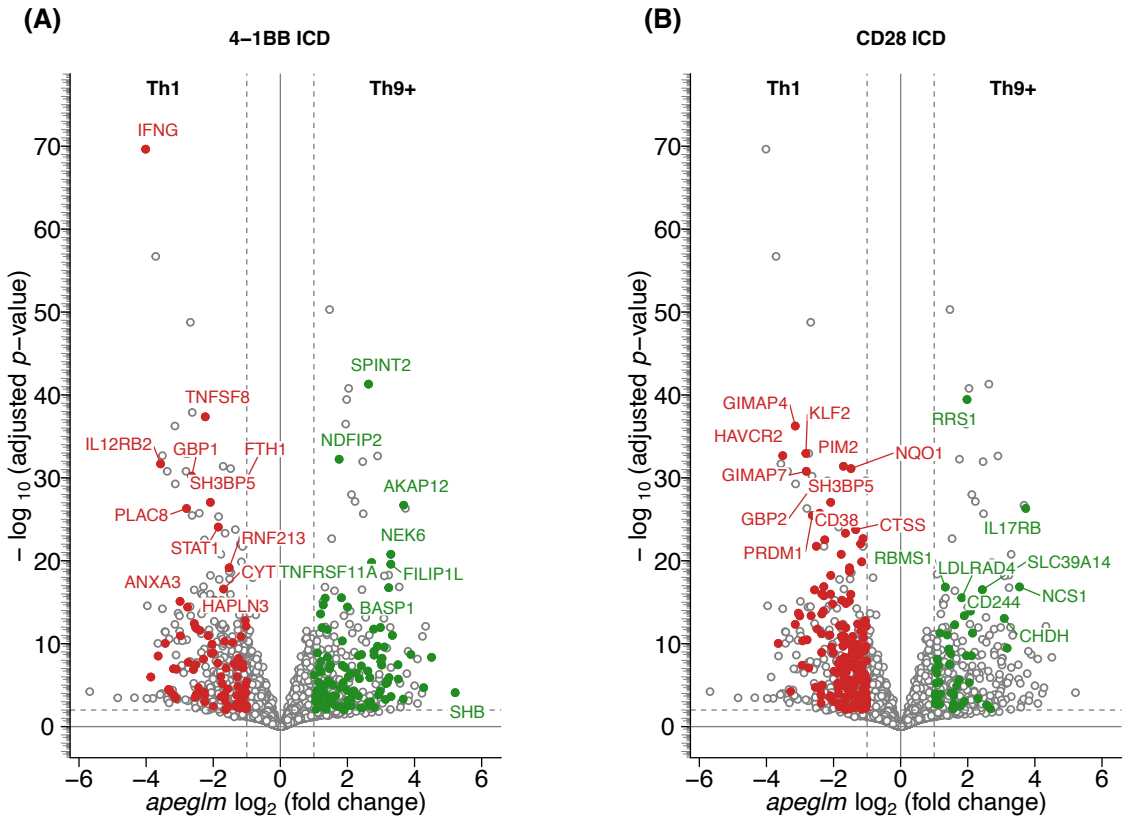

Figure 11 Genes associated with a 4-1BB ICD gene signature are upregulated in the Th9+ subset, and genes associated with a CD28 ICD gene signature are upregulated in the Th1 subset

CD4+ T cells were polarized towards either a Th1, Th2, Th9, Th9+ or Th17 phenotype. RNA was extracted from each group on day 7 after isolation and sequenced. Data was pooled for three (n = 3) independent donors. Depicted here is the expression of genes associated with either a (A) 4-1BB ICD gene signature or with a (B) CD28 ICD gene signature in the Th1 and Th9+ subsets. Genes upregulated in Th9+ cells are highlighted in green (adjusted fold change > 1 and p < 0.01), and those upregulated in Th1 cells are highlighted in red (adjusted fold change < -1 and p < 0.01). Fold changes represent log2 fold changes with *apeglm*-shrinkage and are depicted on the x-axis. Adjusted p-values were logarithmically transformed and are depicted on the y-axis. To determine significance, a p-value cutoff of p = 0.01 was used.

3.4 Th9+ CAR T cells effectively control tumor growth *in vitro*

Due to their phenotypic profile, we hypothesized that Th9+ CAR T cells would exhibit a superior functionality when transduced with a 4-1BB ICD or ICOS ICD instead of a CD28 ICD. To test this hypothesis, every T helper cell subset was transduced with a second-generation CAR directed towards MSLN containing either a CD28, 4-1BB or ICOS ICD. All T helper cell subsets could be effectively transduced with each CAR (Fig. 12). Transduction efficiencies were highest for the CD28z-CAR across subsets, followed by the BBz-CAR and the ICOSz-CAR.

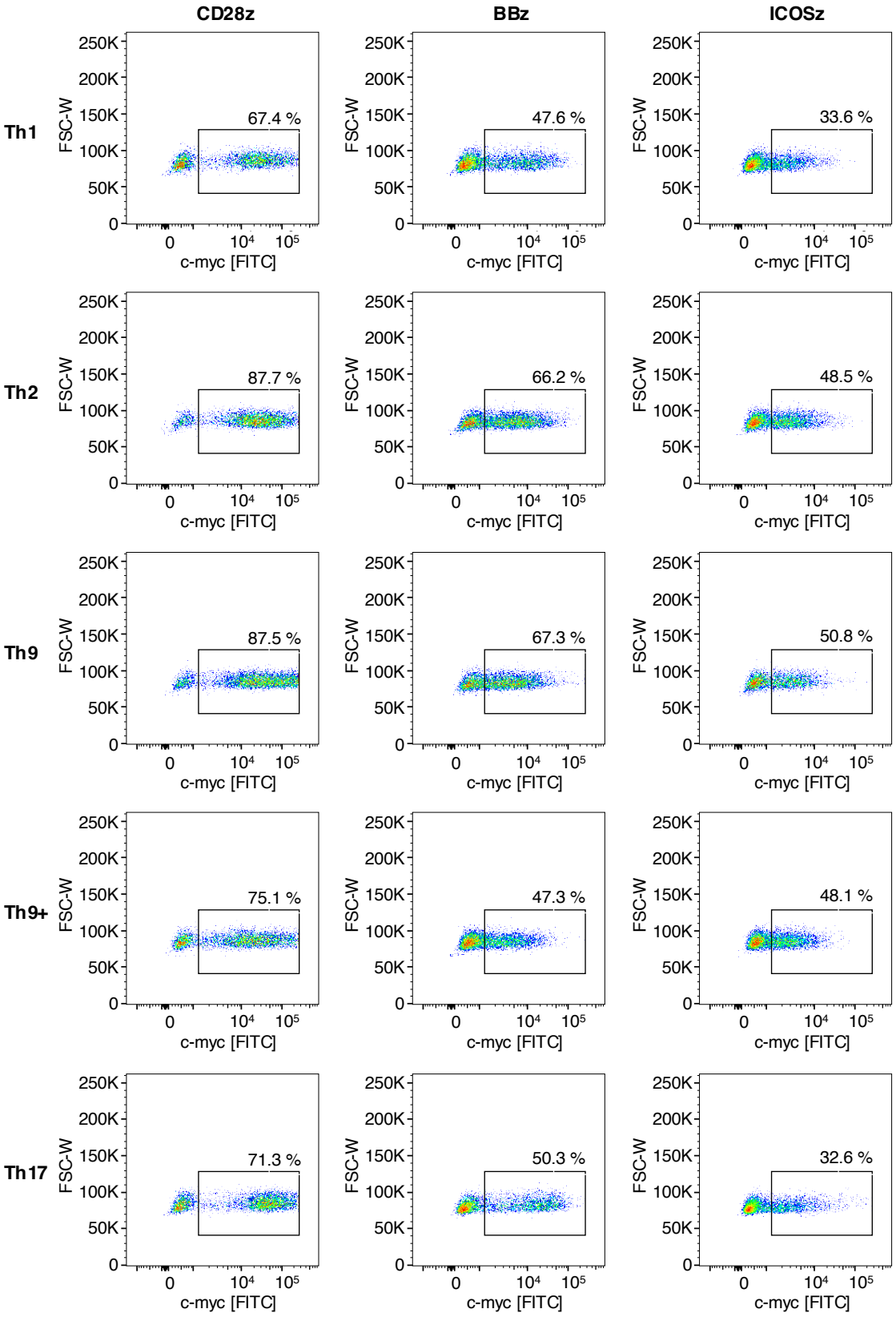

Figure 12 All T helper cell subsets can be effectively transduced with an aMSLN.CD28.CD3z CAR, an aMSLN.4-1BB.CD3z CAR or an aMSLN.ICOS.CD3z CAR
CD4+ T cells were polarized towards a Th1, Th2, Th9, Th9+ or Th17 phenotype and transduced with either an aMSLN.CD28.CD3z CAR, an aMSLN.4-1BB.CD3z CAR or an aMSLN.ICOS.CD3z CAR. Transduction efficiency was measured on day 6 after isolation using

a c-myc staining for flow cytometry. Depicted here are transduction efficiencies of one donor representative of three (n = 3) independent donors. For each donor, measurements were performed in duplicates.

To assess their functionality, CAR T cells were incubated with a MSLN-overexpressing SUIT-2-MSLN pancreatic cancer cell line. Tumor cell killing was determined using a real-time impedance-based cytotoxicity assay (xCELLigence). MSLN was selected as a target antigen as it is highly differentially expressed on solid tumors and is associated with cancer aggressiveness in a variety of tumor entities (Beatty et al., 2018, Kachala et al., 2014, Servais et al., 2012, Tozbikian et al., 2014).

In Figure 13, tumor cell lysis by T helper CAR T cells is shown for one representative donor. Tumor cell killing could be observed in every CD4+ CAR T cell condition (Fig. 13). No tumor cell killing occurred when untransduced T cells, irrespective of T cell subset, were incubated with tumor cells.

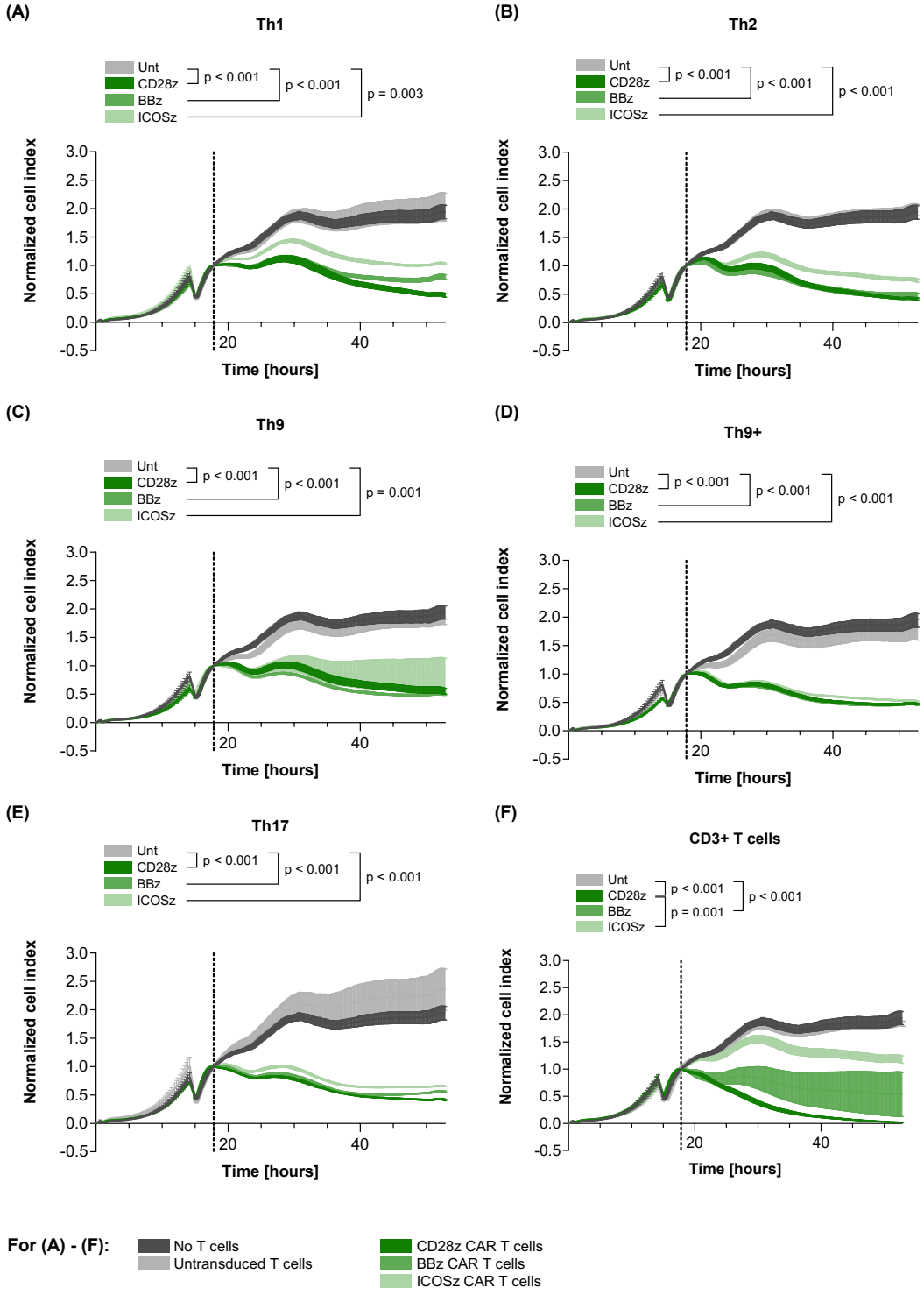

Figure 13 All T helper CAR T cell subsets can effectively kill tumor cells
CD4+ T cells were polarized towards a (A) Th1, (B) Th2, (C) Th9, (D) Th9+ or (E) Th17 phenotype. CD3+ T cells (F) were isolated as a control. All subsets were transduced with either an aMSLN.CD28.CD3z CAR, an aMSLN.4-1BB.CD3z CAR or an aMSLN.ICOS.CD3z CAR. SUIT-2-MSLN tumor cell killing was measured using xCELLigence technology. Tumor cells were added at 0 h, and T cells were added at 17.8 h (dashed line). All conditions were adjusted for transduction efficiency to ensure a comparable ratio of transduced CAR T cells to tumor cells between conditions. Cell indices were normalized to the time point of T cell addition (t = 17.8 h). Depicted here are mean values ± SEM of normalized cell indices of one donor representative of three (n = 3) independent donors. For each donor, measurements were performed in triplicates,

except for the CD3+ T cell BBz- and ICOSz-CAR conditions, which were performed in duplicates. p-values were calculated for the final time point (t = 35 h) using one-way ANOVA with correction for multiple testing by the Turkey method.

To better objectify the cytotoxic capacity of T helper CAR T cell subsets between donors, maximal tumor cell lysis was assessed at 35 hours after T cell addition. Maximal cytotoxicity was calculated as the complement to 100% of the ratio of normalized cell indices of the CAR T cell condition to the tumor only condition. Tumor cell lysis was significant in all conditions except for the Th2 ICOSz-CAR, Th17 ICOSz-CAR and CD3+ T cell ICOSz-CAR conditions (Fig. 14, table 6). Overall, cytotoxicity was highest in the CD28z conditions, followed by the BBz conditions and ICOSz conditions. Whilst not significant, Th9+ CAR T cells seemed to have the highest mean cytotoxicity in the BBz and ICOSz conditions compared to other subsets.

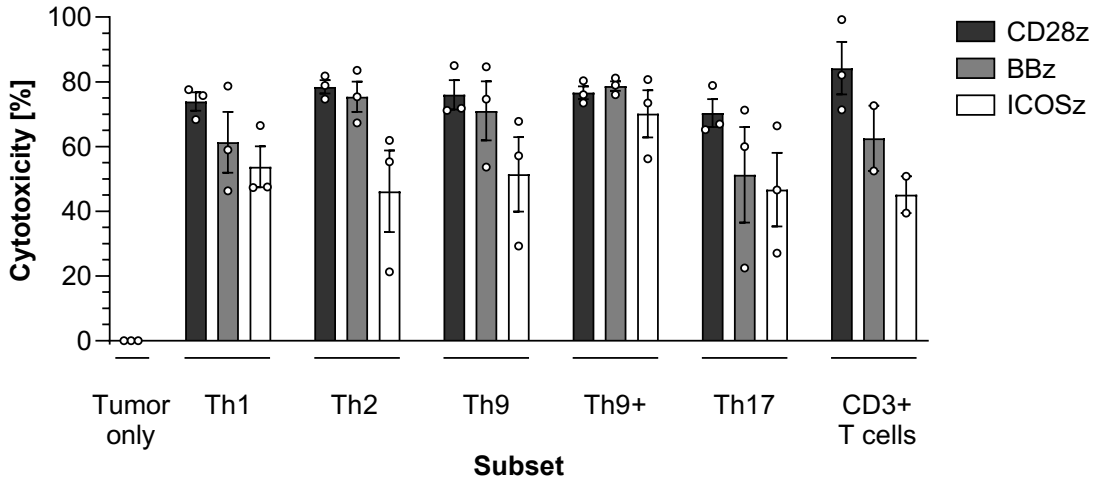

Figure 14 Cytotoxic capacity of T helper CAR T cells varies based on CAR ICD
CD4+ T cells were polarized towards a Th1, Th2, Th9, Th9+ or Th17 phenotype. CD3+ T cells were isolated as a control. All subsets were transduced with either an aMSLN.CD28.CD3z CAR, an aMSLN.4-1BB.CD3z CAR or an aMSLN.ICOS.CD3z CAR. SUIT-2-MSLN tumor cell killing was measured using xCELLigence technology. Tumor cells were added at 0 h, and T cells were added at 17.8 h. Cell indices were normalized to the time point of T cell addition (t = 17.8 h). Maximal cytotoxicity was calculated as the complement to 100% of the ratio of the normalized cell indices of the CAR T cell condition compared to the tumor only condition at 35 h after T cell addition. Depicted here are mean maximal cytotoxicity values ± SEM of three (n = 3) independent donors. Each point represents one donor. For each donor, measurements were performed in triplicates. Analyses of differences between groups were performed using one-way ANOVA with correction for multiple testing by the Turkey method. p-values for comparisons between the tumor only and different CAR T cell conditions are shown in table 6. Comparisons between different CAR T cell conditions did not reach statistical significance.

Table 6 Cytotoxic capacity of T helper CAR T cells based on CAR ICD
For experimental details, see figure 14. Depicted here are mean maximal cytotoxicity values ± SEM and corresponding adjusted p-values for the CAR T cell vs. tumor only conditions of three (n = 3) independent donors. For each donor, measurements were performed in triplicates. Analyses of differences between groups were performed using one-way ANOVA with correction for multiple testing by the Turkey method. Values that did not reach statistical significance are depicted in grey and annotated with the term (ns).

CAR T cell condition		Cytotoxicity [%]	Adjusted p-value
CD28z	Th1	73.907 ± 2.837	< 0.001
	Th2	78.406 ± 2.072	< 0.001
	Th9	75.968 ± 4.527	< 0.001
	Th9+	76.616 ± 1.999	< 0.001
	Th17	70.332 ± 4.284	< 0.001
	CD3+ T cells	84.222 ± 8.128	< 0.001
BBz	Th1	61.293 ± 9.405	0.003
	Th2	75.396 ± 4.673	< 0.001
	Th9	70.968 ± 9.129	< 0.001
	Th9+	78.691 ± 1.488	< 0.001
	Th17	51.214 ± 14.773	0.034
	CD3+ T cells	62.530 ± 10.113	0.012
ICOSz	Th1	53.753 ± 6.342	0.020
	Th2	46.148 ± 12.608	0.096 (ns)
	Th9	51.398 ± 11.486	0.033
	Th9+	70.108 ± 7.263	< 0.001
	Th17	46.642 ± 11.349	0.087 (ns)
	CD3+ T cells	45.098 ± 5.718	0.259 (ns)

Discussion

The clinical success of CAR T cell therapy depends on a variety of factors. These include efficient on-target antigen recognition and tumor cell lysis, CAR T cell persistence as well as minimal T cell dysfunction. We sought to investigate the role of IL-1β in enhancing human Th9 differentiation and cytotoxicity and to further examine the suitability of an IL-1β-differentiated Th9+ subset for CAR T cell therapy.

4.1 Effects of IL-1β on Th9 polarization

Differentiating naïve CD4+ T cells in the presence of IL-1β enhanced a Th9 phenotype on a secretory and a transcriptional level, in line with previous reports (Végran et al., 2014). IL-9 levels detected in supernatants of Th9 cells polarized in the presence of IL-1β were more than eightfold higher than those detected in supernatants of conventional Th9 cells. Intriguingly, the expression of IL-9 was not upregulated in the Th9+ subset relative to the conventional Th9 subset. Cytokine secretion dynamics, including a peak in IL-9 secretion between days four and six of polarization, resembled previously published reports (Tan et al., 2010). In both conventional Th9 and Th9+ cells, Th9-defining genes such as IL-9 and Gata3 were upregulated in comparison to Th1 and Th17 cells. When comparing the relative expression of subset-defining genes between the Th2 and both Th9 subsets, however, we found striking differences. Th9-defining genes such as IL-5 and IL-13 were upregulated in the Th9+ subset relative to the Th2 subset. However, there was no significant difference in their expression between conventional Th9 cells and Th2 cells. Even though Th2 and Th9 differentiation are closely related, the absence of an upregulation of Th9-defining genes in conventional Th9 cells compared to Th2 cells is surprising (Veldhoen et al., 2008). Nevertheless, these findings might be a byproduct of the *apeglm* fold change shrinkage applied to log2 fold changes during statistical analysis. *apeglm*-shrinkage alters fold changes to reduce the overestimation of effect sizes of small or highly variable sequenced read counts during RNA sequencing analysis (Zhu et al., 2018).

4.1.1 Upregulation of Zc3h12a and Basp1in IL-1β-differentiated Th9 cells

Only three genes were highly differentially expressed between the Th9+ and the conventional Th9 subsets after *in vitro* polarization. Zc3h12a and Basp1 were upregulated in the Th9+ subset, while Clic3 was upregulated in the conventional Th9 subset. Upregulation of Zc3h12a, encoding MCPIP-1 or Regnase-1, most likely represents a direct effect of IL-1β signaling during Th9+ differentiation. IL-1β can induce the transcription of Zc3h12a in a NF-κB-dependent manner (Skalniak et al., 2009). MCPIP-1 subsequently acts as a RNase for the degradation of pro-inflammatory cytokines including IL-1β (Mizgalska et al., 2009). MCPIP-1 also acts as a negative regulator of NF-κB activation after IL-1β stimulation, thus limiting uncontrolled inflammation through IL-1β signaling (Skalniak et al., 2009). Basp1 encodes brain acid soluble protein 1 and has been described to translocate from the nucleus to the cytoplasm in cells undergoing apoptosis (Ohsawa et al., 2008). It has also been

reported to inhibit a Myc target gene network involved in the promotion of cell cycle progression, protein synthesis and mitochondrial metabolism (Dang et al., 2006, Hartl et al., 2020). Since gene sets related to cell cycle progression and apoptosis were enriched in the Th9+ subset compared to the Th9 subset, upregulation of Basp1 could represent a regulatory mechanism activated in this subset.

An upregulation of Clic3, encoding chloride intracellular channel protein 3, has been described for various tumors, where it promotes tumor cell invasion (Hernandez-Fernaud et al., 2017, Macpherson et al., 2014). The role of Clic3 in T cell biology, however, has not yet been extensively studied.

4.1.2 Enrichment of gene sets associated with pro-inflammatory signaling in IL-1β-differentiated Th9 cells

GSEA based on the Reactome Pathway Database revealed an enrichment of pathways associated with pro-inflammatory signaling, cell cycle progression, organelle biogenesis and apoptosis in Th9+ cells in comparison to conventional Th9 cells. As could be expected, pathways related to IL-1 signaling were enriched in the Th9+ subset relative to conventional Th9 cells. IL-1 signaling mainly involves the activation of NF-κB, c-Jun N-terminal kinase and p38 mitogen-activated protein kinase pathways (Weber et al., 2010, Xue et al., 2019). Signaling through NF-κB can also be activated by TNF receptors such as TNFR2 to promote cellular proliferation (Faustman and Davis, 2010). Pathways associated with TNFR-mediated NF-κB signaling were also enriched in the Th9+ subset, as previously described (Xue et al., 2019). Furthermore, pathways related to programmed cell death were enriched in the Th9+ subset relative to the Th9 subset, which could be interpreted as a result of a more pronounced pro-inflammatory phenotype of Th9+ cells.

4.1.3 Enrichment of gene sets associated with cellular proliferation in IL-1β-differentiated Th9 cells

Furthermore, pathways related to DNA replication and cellular proliferation were enriched in Th9+ cells relative to conventional Th9 cells. These transcriptional changes mirror a sustained proliferative capacity found in this subset. Th9 cells, including Th9 CAR T cells, have previously been described to have an enhanced proliferative capacity compared to other T helper cell subsets *in vitro* and *in vivo* (Liu et al., 2020, Lu et al., 2018). This effect has been attributed to enhanced PU.1-TRAF6-NF-κB signaling in Th9 cells (Lu et al., 2018).

CAR T cell persistence is a prerequisite for CAR T cell therapy success and requires sufficient CAR T cell expansion and minimal T cell dysfunction. Clinical CAR T cell expansion, including CD4+ CAR T cell expansion, has been found to correlate with response to CAR T cell therapy (Finney et al., 2019, Fraietta et al., 2018, Jain et al., 2021, Louis et al., 2011, Maude et al., 2014). Moreover, in the setting of CLL, the extent of *in vitro* proliferation of CAR T cells during clinical manufacturing directly

correlated with their clinical expansion (Fraietta et al., 2018). Insufficient persistence of CAR T cells still represents a large barrier in the treatment of solid tumors such as glioblastoma or malignant pleural mesothelioma (Haas et al., 2019, O'Rourke et al., 2017, Vitanza et al., 2021). Hence, a sustained proliferative capacity, as seen in the Th9+ subset, could be advantageous to CAR T cell therapy in solid tumors.

4.1.4 Enrichment of gene sets associated with organelle biogenesis in IL-1β-differentiated Th9 cells

Furthermore, pathways enhancing organelle biogenesis, including ribosome biogenesis and cilium assembly, and pathways promoting gene expression were enriched in the Th9+ subset compared to the conventional Th9 subset (Cai et al., 2015). The primary cilium is the locus for multiple intracellular signaling pathways, including Wnt and Hedgehog signaling (Berbari et al., 2009). Intriguingly, a Hedgehog-off signature was enriched in the Th9+ subset compared to the conventional Th9 subset. Constitutive activation of Hedgehog signaling has been suggested to inhibit the proliferation of mature T cells upon TCR engagement (Rowbotham et al., 2007). In the tumor setting, however, activation of Hedgehog signaling in T cells has been proposed to enhance immunological synapse formation and *in vitro* tumor lysis (de la Roche et al., 2013). A Hedgehog-off signature in Th9+ cells could thus be interpreted in relation to their enhanced proliferative capacity. However, Hedgehog signaling has also been reported to be involved in CD4+ T cell differentiation, particularly in Th17 differentiation (Hanna et al., 2022). In this subset, Hedgehog signaling also enhanced the development of a stem-cell-like phenotype under stimulation with IL-6- but not IL-1β (Hanna et al., 2022). However, Hedgehog signaling has not yet been studied in Th9 cells (Hanna and de la Roche, 2024). Thus, the potential consequences of its relative downregulation through the addition of IL-1β during Th9 differentiation remain to be explored.

4.1.5 Enrichment of gene sets associated with cellular stress in conventional Th9 cells

Furthermore, adaptive pathways to cellular stress, referred to as an integrated stress response (ISR), seem to be enriched in conventional Th9 cells in comparison to Th9+ cells. The ISR is activated by various cellular stressors, such as amino acid deprivation, endoplasmic reticulum stress and hypoxia, and is characterized by the phosphorylation of eukaryotic translation initiation factor 2 α (EIF-2α) (Holcik and Sonenberg, 2005, Pakos-Zebrucka et al., 2016). Its initial activation aims to maintain cellular homeostasis and survival by reducing global protein synthesis and stimulating autophagy (Holcik et al., 2005, Pakos-Zebrucka et al., 2016, Rutkowski et al., 2006, Ye et al., 2010). A prolonged ISR in response to sustained and severe stress, however, can lead to the induction of cell death (Holcik et al., 2005, Pakos-Zebrucka et al., 2016).

Overall, the transcriptional profile of Th9+ cells compared to Th9 cells suggests that differentiation in the presence of IL-1β generates a fitter Th9 subset. As a next step, we sought to evaluate the functionality of Th9+ cells for CAR T cell therapy.

4.2 Transcriptional profile of IL-1β-differentiated Th9 cells relative to Th1 cells

4.2.1 Enrichment of gene sets associated with pro-inflammatory signaling in Th1 cells

4.2.1.1 Enrichment of gene sets associated with interleukin-1 signaling in Th1 cells

GSEA comparing Th9+ cells to Th1 cells revealed an expected enrichment of pathways associated with pro-inflammatory signaling in the Th1 subset relative to the Th9+ subset. Surprisingly, pathways related to IL-4 and IL-13 signaling were also enriched in the Th1 subset relative to the Th9+ subset. As IL-4 signaling and IL-13 production are typically associated with a Th2 phenotype, this finding was unexpected (Veldhoen et al., 2008).

CD4+ T cells can acquire different phenotypes depending on the environment they are exposed to. A shift towards a Th1-like phenotype was critical for adoptively transferred Th17 cells directed towards tyrosinase related protein 1 (TRP-1) or transduced with a MSLN-CAR (Guedan et al., 2014, Muranski et al., 2011). These cells shifted towards a Th1/Th17 phenotype upon target antigen encounter *in vitro* and *in vivo,* and their tumor cell killing was impaired in IFN-γ and Tbx21 knockout mice (Guedan et al., 2014, Muranski et al., 2011). However, it is unclear whether a shift towards a Th1 phenotype is a critical component of Th9-mediated cytotoxicity. Th9 cells targeting myelin oligodendrocyte glycoprotein adopted a Th9/Th1 phenotype *in vivo* in a murine model of autoimmune encephalitis (Jäger et al., 2009). Likewise, Th9 CAR T cells switched to a Th1-like phenotype *in vivo* in a murine leukemia model (Liu et al., 2020). OVA-specific Th9 and IL-1β-induced Th9 cells, however, maintained a Th9 phenotype upon adoptive transfer in murine pulmonary melanoma models (Lu et al., 2012, Végran et al., 2014). Their cytotoxicity was unaffected when IFN-γ was knocked out Th9 cells (Végran et al., 2014).

Moreover, different ICD have been suggested to promote the development of different T helper phenotypes in CD4+ T cells *in vitro* (Guedan et al., 2018). A combined Th1/Th2 phenotype has been described in CD28z-CAR T cells, a Th1 phenotype with an isolated additional secretion of IL-13 in BBz-CAR T cells and a Th1/Th17 phenotype in ICOSz-CAR T cells (Guedan et al., 2018).

Whether a Th1-like phenotype represents an advantage or a disadvantage for CAR T cell therapy remains to be conclusively determined. IFN-γ/IFN-γ receptor signaling has been suggested to enhance tumor cell killing by CAR T cells in various solid tumor models, including glioblastoma, ovarian cancer and pancreatic cancer (Larson et al., 2022). This anti-tumor effect has been attributed to enhanced CAR T cell adhesion through intercellular adhesion molecule 1 (ICAM-1) (Larson et al., 2022). In

hematological malignancies, however, IFN-γ/IFN-γ receptor signaling did not seem to affect CAR T cell cytotoxicity (Bailey et al., 2022, Larson et al., 2022). As a matter of fact, stimulating pro-inflammatory type I interferon response genes during CAR T cell production was associated with poor clinical CAR T cell persistence in patients with B-ALL (Chen et al., 2021). Thus, the benefit of the development of a Th1-like phenotype might depend on the degree of its activation and on tumor entity.

4.2.1.2 Enrichment of gene sets associated with toll-like receptor signaling in Th1 cells

Furthermore, pathways related to toll-like receptor (TLR) signaling, inflammasome activation and pyroptosis were upregulated in Th1 cells relative to Th9+ cells. Activation of TLR in response to pathogen- or damage-associated molecular patterns initiates a pro-inflammatory response, including a release of type I interferons (Kabelitz, 2007, Uematsu and Akira, 2007). Furthermore, TLR can prime inflammasomes and induce pyroptosis (Guo et al., 2015, Liu et al., 2016). While classically associated with an innate immune response, TLR are also expressed on T cells and can enhance their proliferation (Hornung et al., 2002, Kabelitz, 2007, Quigley et al., 2009). Moreover, various components of inflammasomes and TLR activation have been reported to affect CD4+ T cell differentiation (Linder and Hornung, 2022). TLR2 stimulation has mainly been described to induce Th1 differentiation; however, it has also been reported to enhance Th17 and Th9 differentiation (Imanishi et al., 2007, Karim et al., 2017, Nyirenda et al., 2011). In addition, incorporating a TLR2 ICD or co-expressing a TLR4 construct in CAR T cells enhanced their anti-tumor responses *in vivo* in various tumor models (Lai et al., 2018, Mikolič et al., 2024). Thus, an enrichment of TLR signaling in Th1 cells could be a reflection of a general activation of pro-inflammatory pathways in this subset and might potentially further promote their phenotypic differentiation.

4.2.2 Enrichment of gene sets associated with T cell dysfunction in Th1 cells

4.2.2.1 Enrichment of gene sets associated with apoptosis in Th1 cells

We found an enrichment of pathways related to programmed cell death in the Th1 subset relative to the Th9+ subset, which was reflected in a more than quadrupled apoptosis score. These results mirror previously published reports demonstrating that Th9 CAR T cells were less prone to apoptosis compared to Th1 CAR T cells in a murine leukemia model (Liu et al., 2020). Moreover, we found a transcriptional upregulation of genes associated with exhaustion in the Th1 subset, reflected in a quadrupled exhaustion score. These results are consistent with previous reports, which found that IFN-γ signaling could promote exhaustion *in vitro* (Bailey et al., 2022). In line with these findings, Th1 CAR T cells were shown to upregulate inhibitory receptors such as PD-1 to a greater extent than Th9 CAR T cells in a murine leukemia model *in vivo* (Liu et al., 2020). Moreover, during *in vitro* expansion, Th9 CAR T cells showed a higher expression of c-jun (Liu et al., 2020), which has been associated with reversing exhaustion in CAR T cells (Lynn et al., 2019).

Both programmed cell death and hyporesponsive T cell states such as exhaustion and senescence have been associated with clinical CAR T cell failure in hematological malignancies (Deng et al., 2020, Finney et al., 2019, Fraietta et al., 2018). CAR T cell apoptosis was shown to be mediated through Fas/Fas ligand signaling in response to tumor exposure *in vivo* and occurred even in the absence of CAR activation (Tschumi et al., 2018). However, Fas signaling has also been shown to enhance the anti-tumor effects of CAR T cells, for instance by inducing the lysis of target-antigen-negative tumor cells in a testicular cancer model *in vitro* (Hong et al., 2018).

Moreover, Fas has been suggested to be involved in non-apoptotic signaling. Fas signaling has been proposed to enhance Th9 differentiation through protein kinase C (PKCβ) and NF-κB activation and to promote Th17 differentiation through STAT1 inhibition (Meyer Zu Horste et al., 2018, Shen et al., 2019). Accordingly, Fas signaling might assume different roles during differentiation and effector programs in CD4+ T cells.

4.2.2.2 Enrichment of gene sets associated with T cell exhaustion in Th1 cells

T cell exhaustion describes the progressive loss of effector function of T cells upon chronic antigen stimulation (Wherry and Kurachi, 2015). This process is marked by a sustained upregulation of inhibitory receptors, an impaired effector response, a failure to acquire a memory phenotype and altered metabolism (Baitsch et al., 2011, Doering et al., 2012, Pauken and Wherry, 2015, Wherry et al., 2007, Wherry et al., 2015). Importantly, exhaustion represents a potentially reversible state (Weber et al., 2021, Wherry et al., 2015). CD4+ T cell exhaustion shares many common features of CD8+ T cell exhaustion and further involves the loss of a Th1-like effector phenotype with concomitant upregulation of IL-10 and IL-21 (Crawford et al., 2014). Due to suppressive tumor microenvironments, T cell exhaustion represents a significant barrier for adoptive cellular therapies in solid tumors (Jiang et al., 2015).

Intriguingly, transcription factors critical for Th9 differentiation, notably IRF4 and BATF, have been linked to both the promotion and prevention of exhaustion in T cells. IRF4 enhanced effector function and clonal expansion in CD8+ T cells *in vivo* in a murine influenza model (Man et al., 2013). However, IRF4 was also shown to promote CD8+ T cell exhaustion in a murine chronic lymphocytic choriomeningitis virus (LCMV) infection model (Man et al., 2017). Similarly, BATF knockout in MSLN-CAR T cells enhanced their anti-tumor effect *in vivo* in squamous cell and pancreatic carcinoma models (Zhang et al., 2022). Conversely, BATF overexpression in CD19-CAR T cells was associated with superior *in vivo* tumor control and reduced expression of inhibitory receptors in a CD19-expressing melanoma model (Seo et al., 2021).

4.2.2.3 Enrichment of gene sets associated with T cell senescence in Th1 cells

Pathways related to cellular senescence were enriched in the Th1 subset relative to the Th9+ subset. During cellular senescence, cells undergo cell cycle arrest as well as characteristic changes in morphology, chromatin structure and secretome in response

to stimuli such as persistent DNA damage, cellular stress or reactive oxygen species (ROS) (Kuilman et al., 2010, Ruhland and Alspach, 2021). Tumor cells can induce T cell senescence in the tumor microenvironment, promoting cancer immune evasion (Montes et al., 2008, Ye et al., 2014). Changes in secretome during senescence are referred to as the senescence-associated secretory phenotype (SASP) (Ye and Peng, 2015). A SASP includes both pro-inflammatory cytokines, such as IL-6, IL-8, IFN-γ and TNF-α, and anti-inflammatory cytokines, such as IL-10 and TGF-β (Ye et al., 2015). Secretion of a SASP can further uphold a senescent phenotype in an autocrine manner (Ruhland et al., 2021). An enrichment of senescence-associated pathways including a SASP in the Th1 subset could therefore reflect a pro-inflammatory profile of Th1 cells as well as early signs of T cell dysfunction.

4.2.2.4 Enrichment of gene sets related to an effector phenotype in Th1 cells

While chronic antigen stimulation can lead to T cell dysfunction, CAR T cells can also adapt to antigen stimulation by developing a functional memory phenotype. We found a skewing towards an effector phenotype in the Th1 subset compared to the Th9+ subset, reflected by a tenfold increase in effector vs. central memory score. In line with these results, Th9 CAR T cells have been shown to be enriched in a central memory gene signature during *in vitro* expansion (Liu et al., 2020). However, they have also been reported to shift towards an effector memory and terminally differentiated effector memory phenotype upon adoptive transfer in a murine leukemia model (Liu et al., 2020). The development of a stem cell memory or central memory phenotype has been described to improve therapeutic responses to TIL and CAR T cell therapy (Deng et al., 2020, Fraietta et al., 2018, Krishna et al., 2020). A higher proportion of central memory T cells in CAR T cell infusion products also correlated with clinical CAR T cell persistence in patients with ALL and neuroblastoma (Chen et al., 2021, Louis et al., 2011). Selectively enriching a stem cell memory-like T cell population during CD8+ CAR T cell production enhanced *in vivo* tumor control in murine leukemia and Burkitt lymphoma models (Sabatino et al., 2016, Sommermeyer et al., 2016).

4.2.3 Enrichment of gene sets associated with mitochondrial metabolism in IL-1β-differentiated Th9 cells

T cell memory and dysfunction are intricately linked to cellular metabolism. Naïve T cells mainly rely on mitochondrial fatty acid oxidation as a source of energy (Rangel Rivera et al., 2021). Upon activation, they undergo metabolic reprogramming, increasing glucose uptake and glycolysis (Macintyre et al., 2014, Rangel Rivera et al., 2021, van der Windt et al., 2012). During memory development, T cells become less dependent on glycolysis and increase mitochondrial biogenesis and mitochondrial fatty acid oxidation through TRAF6 activation (Pearce et al., 2009, Sukumar et al., 2013, van der Windt et al., 2012). Mitochondria in effector T cells exist in a fragmented state, also referred to as fission (Buck et al., 2016), which has been associated with increased ROS production (Yu et al., 2006). Central memory T cells, on the other hand, contain fused mitochondria, favoring a close association of electron transport chain

complexes, oxidative phosphorylation and fatty acid oxidation (Buck et al., 2016, Yu et al., 2006). Moreover, memory T cells show an increased spare respiratory capacity, defined as the difference between maximal and basal oxygen consumption rates, which improves a cell's ability to tolerate cellular stress (Teijeira et al., 2018, van der Windt et al., 2012).

Many pathways related to mitochondrial metabolism and protein synthesis were enriched in the Th9+ subset relative to the Th1 subset, which was further illustrated by an almost tenfold increase in oxidative phosphorylation score in the Th9+ subset. Glycolysis scores, on the other hand, were similar between both subsets. These results closely align with previous findings demonstrating that Th9 CAR T cells had a more pronounced respiratory capacity during *in vitro* expansion compared to Th1 CAR T cells (Liu et al., 2020). Th9 CAR T cells also increased their mitochondrial mass upon an *in vivo* tumor challenge in a murine leukemia model (Liu et al., 2020). Moreover, T-bet, the master regulator of Th1 differentiation, was shown to inhibit the suppression of glycolysis-related genes typically mediated by BCL-6 (Oestreich et al., 2014).

Like a central memory phenotype, increased mitochondrial mass and biogenesis have been associated with improved clinical persistence and response to CAR T cell therapy (van Bruggen et al., 2019). Increased mitochondrial respiration has also been suggested to enhance the infiltration of solid tumors by CD8+ T cells *in vitro* (Simula et al., 2024). Intriguingly, a recent study investigating persisting CD19-CAR T cells, which were isolated from a patient with CLL who had received CAR T cells ten years earlier and had subsequently achieved complete remission, found an upregulation of oxidative phosphorylation pathways in these cells (Melenhorst et al., 2022). Coincidentally, these persisting CAR T cells were exclusively CD4+ (Melenhorst et al., 2022).

4.2.3.1 Metabolic reprogramming during T cell exhaustion and senescence

Mitochondrial dysfunction has been reported to be both a cause and a consequence of T cell exhaustion. Inducing mitochondrial dysfunction in T cells led to a shift from mitochondrial respiration to aerobic glycolysis, giving rise to an exhausted T cell phenotype in a murine LCMV infection model (Wu et al., 2023). Furthermore, TIL isolated from murine melanoma models and from patients with renal cell carcinoma exhibited fragmented mitochondria and a reduced respiratory capacity (Scharping et al., 2016, Siska et al., 2017, Yu et al., 2020). In addition, these cells showed an insufficient response to ROS marked by a downregulation of superoxide dismutase 2 (SOD2), which is responsible for protecting mitochondrial DNA from oxidative damage (Che et al., 2016, Siska et al., 2017). Notably, these effects were less pronounced in CD4+ TIL compared to CD8+ TIL (Scharping et al., 2016, Siska et al., 2017).

Mitochondrial dysfunction has also been described during the development of cellular senescence. During this process, mitochondrial production of ROS has been described to be increased and catabolic lipid metabolism to be downregulated (Liu et al., 2021, Moiseeva et al., 2009).

4.3 *In vitro* cytotoxicity of CD4+ chimeric antigen receptor T cells

4.3.1 Enrichment of a 4-1BB ICD gene signature in IL-1β-differentiated Th9 cells

The gene expression profile of Th9+ cells is highly reminiscent of a phenotype previously described for CAR T cells transduced with a 4-1BB ICD, especially in regard to cellular metabolism, memory phenotype, susceptibility to T cell dysfunction and persistence (Boroughs et al., 2020, Long et al., 2015). We thus sought to investigate whether genes related to a 4-1BB ICD phenotype were enriched in Th9+ cells at baseline. An enrichment of such a phenotype could be suggestive of a potential functional synergism of a 4-1BB ICD in Th9 CAR T cells.

Signaling through endogenous 4-1BB and a 4-1BB ICD enhances mitochondrial metabolism. It increases mitochondrial and spare respiratory capacity and upregulates genes involved in mitochondrial replication, oxidative phosphorylation and long-chain fatty acids uptake (Kawalekar et al., 2016, Long et al., 2015, Teijeira et al., 2018). Signaling through endogenous CD28 and a CD28 ICD, on the other hand, has been shown to favor glucose uptake and glycolysis (Frauwirth et al., 2002, Kawalekar et al., 2016). These metabolic changes were associated with an enrichment of a central memory phenotype in BBz-CAR T cells and an effector memory phenotype in CD28z-CAR T cells (Kawalekar et al., 2016). Notably, clinical CAR T cell persistence has been reported for both CD28z- and BBz-CAR T cells (CD28z: (Brentjens et al., 2013, Jain et al., 2021), BBz: (Finney et al., 2019, Fraietta et al., 2018, Maude et al., 2014)). A 4-1BB ICD, however, has been suggested to promote CAR T cell persistence more significantly in preclinical models (Long et al., 2015). In line with this, changing one amino acid residue of a CD28 ICD to direct CAR T cells towards a central memory phenotype improved their *in vivo* persistence and anti-tumor activity (Guedan et al., 2020). Lastly, while tonic signaling occurs in both CD28z- and BBz-CAR T cells, 4-1BB-based CAR T cells appear to be less prone to tonic signaling (Frigault et al., 2015, Gomes-Silva et al., 2017, Long et al., 2015, Sun et al., 2020). Intriguingly, tonic signaling through a 4-1BB ICD has even been reported to improve CAR T cell functionality by enhancing immune synapse formation and stability in a murine leukemia model (Singh et al., 2021).

We found a pronounced upregulation of a CD28 ICD gene signature in Th1 cells with an approximately fourfold increase in CD28 ICD gene expression score. A 4-1BB ICD gene signature, on the other hand, was slightly upregulated in Th9+ cells. However, when interpreting these results, it is important to keep in mind that the experimental conditions used to generate both gene signatures were slightly different from those we used for RNA sequencing. These gene signatures were generated at later time points during *in vitro* differentiation (day 9 or 15 after isolation) and using different CAR target antigens (ganglioside G2 or CD19) (Boroughs et al., 2020, Long et al., 2015). Moreover, different forms of stimulation were used (anti-CD3/CD28 beads with or without additional stimulation with irradiated NALM-6 leukemia tumor cells) (Boroughs et al., 2020, Long et al., 2015). Activation of CD4+ T cells with anti-CD3/CD28 beads has been suggested to induce different T helper cell phenotypes compared to physiological stimulation with APC (Tan et al., 2014). Moreover, Long et al. did not

differentiate between CD4+ and CD8+ gene signatures (Long et al., 2015). Nonetheless, these results indicate a higher upregulation of genes associated with 4-1BB costimulation in the Th9+ subset, which led us to hypothesize that Th9+ BBz-CAR T cells would outperform other T helper cell subsets in functional assays.

4.3.2 Effective lysis of a mesothelin-overexpressing SUIT-2-MSLN pancreatic cancer cell line *in vitro* by CD4+ chimeric antigen receptor T cells

Due to a less pronounced upregulation of phenotypes associated with CAR T cell therapy failure in untransduced Th9+ cells, we hypothesized that these cells would be more suitable effectors for CAR T cell therapy. We could confirm effective transduction of all CD4+ T cell subsets with a MSLN-CAR incorporating either a CD28z, BBz or ICOSz ICD. Transduction efficiencies were comparable with previously published transduction efficiencies of a MSLN-directed CD28z-CAR (Adusumilli et al., 2021). As transduction efficiencies were consistently higher for the CD28z-CAR compared to the BBz- and ICOSz-CAR, CAR T cell numbers were normalized for functional assays. All CD4+ CAR T cells showed effective tumor cell clearance *in vitro* in a MSLN-overexpressing SUIT-2-MSLN pancreatic cancer model. However, tumor cell lysis was not statistically significant for Th2 and Th17 CAR T cells transduced with an ICOSz-CAR, which might be a result of inter-donor variability. Tumor cell lysis was CAR-dependent, as untransduced CD4+ T cells did not mediate tumor cell lysis. Strikingly, ICOSz-CAR T cells appeared to be less efficient at clearing tumor cells compared to CD28z- and BBz-CAR T cells.

Enhancing a Th9 phenotype through the addition of IL-1β during differentiation has been shown to increase Th9-mediated cytotoxicity in murine pulmonary melanoma models *in vivo* (Végran et al., 2014, Xue et al., 2019). Intriguingly, the cytotoxic capacity of Th9+ CAR T cells seemed to be equally high irrespective of ICD. Th9+ CAR T cells even seemed to surpass all other subsets when transduced with a BBz or ICOSz ICD. However, the lack of statistically significant differences in *in vitro* cytotoxicity between CD4+ CAR T cell subsets led us to question whether we would see differences in cytotoxicity using different experimental setups. Different target antigens, different tumor cell lines or lower effector to target ratios might help unmask potential differences in cytotoxicity. Furthermore, assessing a response to sustained antigen exposure or potential interactions with other immune effector cells through long-term assays might provide valuable insights into Th9+ CAR T cell cytotoxicity (Guedan et al., 2018, Wang et al., 2019).

4.4 Conclusion and outlook

In conclusion, this project provides new insights into the transcriptional profile of human Th9 cells differentiated in the presence of IL-1β and their suitability as effector cells for CAR T cell therapy. Effective subset polarization could be confirmed for Th1, Th2, conventional Th9, IL-1β-differentiated Th9, and Th17 cells on a transcriptional level.

The transcriptional profile of Th9+ cells, with a relative enrichment of pathways related to organelle biogenesis and cell cycle progression compared to Th9 cells, suggests that differentiation in the presence of IL-1β enhances Th9 fitness. In comparison to Th1 cells, the gene expression profile of Th9+ cells pointed to a less pronounced upregulation of phenotypes associated with CAR T cell therapy failure, such as programmed cell death, exhaustion, senescence and effector phenotype differentiation. Furthermore, genes related to 4-1BB ICD signaling were enriched in Th9+ cells compared to Th1 cells. Functional assays showed effective tumor cell lysis of a SUIT-2-MSLN pancreatic cancer cell line *in vitro* by Th1, Th2, conventional Th9, Th9+, and Th17 cells transduced with a MSLN-directed CAR containing either a CD28 ICD, a 4-1BB ICD or an ICOS ICD, except for Th2 and Th17 CAR T cells transduced with an ICOSz-CAR. While the differences in cytotoxicity between CD4+ CAR T cell subsets were not statistically significant, Th9+ CAR T cells seemed to outperform other subsets, especially when transduced with a 4-1BB ICD. A potential synergism of a 4-1BB ICD in Th9+ CAR T cells warrants further investigation. In particular, the effects of sustained antigen exposure on Th9+ CAR T cell function and potential interactions of Th9+ CAR T cells with other immune effector cells remain to be explored.

Summary

Chimeric antigen receptor (CAR) therapy has revolutionized the treatment of hematological malignancies. However, treatment-associated complications and tumor relapse still limit its clinical success and represent a barrier to its application to solid tumors (Weber et al., 2020). Th9 CAR T cells mediated superior tumor control in murine models (Liu et al., 2020, Xue et al., 2021). The addition of IL-1β during murine Th9 differentiation has been suggested to enhance Th9 phenotype and cytotoxicity (Végran et al., 2014, Xue et al., 2019). This project aimed to further investigate the transcriptional profile of human Th9 cells differentiated in the presence of IL-1β and to examine the suitability of an IL-1β-differentiated Th9 subset for CAR T cell therapy. Gene set enrichment analysis revealed an enrichment of pathways related to IL-1 signaling, cellular proliferation and organelle biogenesis in IL-1β-differentiated Th9 cells relative to conventional Th9 cells during *in vitro* polarization. Adaptive pathways to cellular stress were enriched in the conventional Th9 subset. Th2 and IL-1β-differentiated Th9 cells were the only subsets to significantly proliferate during *in vitro* differentiation. Further transcriptional profiling of the IL-1β-differentiated Th9 subset revealed an enrichment of pathways associated with mitochondrial metabolism in IL-1β-differentiated Th9 cells relative to Th1 cells. Pathways associated with pro-inflammatory signaling, effector phenotype differentiation, programmed cell death, exhaustion and senescence were enriched in the Th1 subset. Genes related to 4-1BB intracellular costimulatory domain signaling were enriched in IL-1β-differentiated Th9 cells compared to Th1 cells. Effective lysis of a mesothelin-overexpressing SUIT-2-MSLN pancreatic cancer cell line could be confirmed *in vitro* for Th1, Th2, conventional Th9, IL-1β-differentiated Th9, and Th17 cells transduced with either an aMSLN.CD28.CD3z CAR, an aMSLN.4-1BB.CD3z CAR or an aMSLN.ICOS.CD3z CAR. While these differences in cytotoxicity between CD4+ CAR T cell subsets were not statistically significant, IL-1β-differentiated Th9 CAR T cells seemed to outperform other subsets – albeit not significantly – when transduced with a 4-1BB or ICOS intracellular costimulatory domain.

Summary (in German)

Die *chimeric antigen receptor* (CAR) T-Zell-Therapie hat die Behandlung hämatologischer Tumore revolutioniert. Behandlungsbedingte Komplikationen und Tumorrezidive begrenzen jedoch weiterhin ihr Therapieergebnis und stellen ein Hindernis für ihre Anwendung bei soliden Tumoren dar (Weber et al., 2020). Th9-CAR-T-Zellen bewirkten in Mausmodellen eine bessere Tumorkontrolle (Liu et al., 2020, Xue et al., 2021). Die Differenzierung mittels IL-1β verstärkte den Phänotyp und die Zytotoxizität von murinen Th9-Zellen (Végran et al., 2014, Xue et al., 2019). Ziel dieses Projekts war es, das transkriptionelle Profil von humanen Th9-Zellen, die mittels IL-1β differenziert wurden, weiter zu untersuchen und die Eignung dieses Th9-Subsets für die Anwendung als CAR-T-Zellen zu prüfen. Im Vergleich zu konventionellen Th9-Zellen zeigte eine *gene set enrichment* Analyse von IL-1β-differenzierten Th9-Zellen während der *in-vitro*-Differenzierung eine Hochregulierung von Signalwegen, welche für die Signalübertragung von IL-1, Proliferation und die Biogenese von Organellen zuständig sind. In konventionellen Th9-Zellen waren dahingegen adaptive Signalwege als Folge von zellulärem Stress hochreguliert. Th2 und IL-1β-differenzierte Th9-Zellen waren die einzigen T-Helferzell-Subsets, die während der *in-vitro*-Differenzierung signifikant proliferierten. Weitere *gene set enrichment* Analysen der IL-1β-differenzierten Th9-Zellen im Vergleich zu Th1-Zellen zeigten im IL-1β-differenzierten Th9-Subset eine Hochregulierung von Signalwegen, welche für eine mitochondriale Stoffwechsellage relevant sind. Im Th1-Subset waren dahingegen Signalwege hochreguliert, die mit Inflammation, einer Differenzierung zu Effektor-Zellen, programmiertem Zelltod, T-Zell Erschöpfung und zellulärer Seneszenz verbunden sind. Ein Genprofil, welches mit der intrazellulären kostimulatorischen Domäne 4-1BB zusammenhängt, war in IL-1β-differenzierten Th9-Zellen im Vergleich zu Th1-Zellen verstärkt exprimiert. Th1-, Th2-, konventionelle Th9-, IL-1β-differenzierte Th9- und Th17-CAR-T-Zellen, welche entweder einen aMSLN.CD28.CD3z-CAR, einen aMSLN.4 1BB.CD3z-CAR oder einen aMSLN.ICOS.CD3z-CAR exprimierten, konnten eine Mesothelin-exprimierende SUIT-2-MSLN-Tumorzelllinie *in vitro* fast vollständig lysieren. Während die Unterschiede in der Zytotoxizität der verschiedenen CD4+-CAR -T-Zell-Subsets statistisch nicht signifikant waren, schienen IL-1β-differenzierte Th9-CAR-T-Zellen die zytotoxischen Fähigkeiten der anderen T-Helferzell-Subsets in Zusammenhang mit einer 4-1BB oder ICOS intrazellulären kostimulatorischen Domäne zu übertreffen, wenngleich dies nur eine Tendenz und keinen statistisch signifikanten Unterschied darstellte.

References

A. Abdul-Wahid, M. Cydzik, A. Prodeus, M. Alwash, M. Stanojcic, M. Thompson, E. H. Huang, J. E. Shively, S. D. Gray-Owen and J. Gariépy: Induction of antigen-specific TH 9 immunity accompanied by mast cell activation blocks tumor cell engraftment;
Int J Cancer, 2016; 4, 139, 841-53.

J. S. Abramson, M. L. Palomba, L. I. Gordon, M. A. Lunning, M. Wang, J. Arnason, A. Mehta, E. Purev, D. G. Maloney, C. Andreadis, A. Sehgal, S. R. Solomon, N. Ghosh, T. M. Albertson, J. Garcia, A. Kostic, M. Mallaney, K. Ogasawara, K. Newhall, Y. Kim, D. Li and T. Siddiqi: Lisocabtagene maraleucel for patients with relapsed or refractory large B-cell lymphomas (TRANSCEND NHL 001): a multicentre seamless design study;
Lancet, 2020; 10254, 396, 839-852.

P. S. Adusumilli, L. Cherkassky, J. Villena-Vargas, C. Colovos, E. Servais, J. Plotkin, D. R. Jones and M. Sadelain: Regional delivery of mesothelin-targeted CAR T cell therapy generates potent and long-lasting CD4-dependent tumor immunity;
Sci Transl Med, 2014; 261, 6, 261ra151.

P. S. Adusumilli, M. G. Zauderer, I. Rivière, S. B. Solomon, V. W. Rusch, R. E. O'Cearbhaill, A. Zhu, W. Cheema, N. K. Chintala, E. Halton, J. Pineda, R. Perez-Johnston, K. S. Tan, B. Daly, J. A. Araujo Filho, D. Ngai, E. McGee, A. Vincent, C. Diamonte, J. L. Sauter, S. Modi, D. Sikder, B. Senechal, X. Wang, W. D. Travis, M. Gönen, C. M. Rudin, R. J. Brentjens, D. R. Jones and M. Sadelain: A Phase I Trial of Regional Mesothelin-Targeted CAR T-cell Therapy in Patients with Malignant Pleural Disease, in Combination with the Anti-PD-1 Agent Pembrolizumab;
Cancer Discov, 2021; 11, 11, 2748-2763.

S. L. Ash, R. Orha, H. Mole, M. Dinesh-Kumar, S. P. Lee, F. K. Turrell and C. M. Isacke: Targeting the activated microenvironment with endosialin (CD248)-directed CAR-T cells ablates perivascular cells to impair tumor growth and metastasis;
J Immunother Cancer, 2024; 2, 12.

M. Ashburner, C. A. Ball, J. A. Blake, D. Botstein, H. Butler, J. M. Cherry, A. P. Davis, K. Dolinski, S. S. Dwight, J. T. Eppig, M. A. Harris, D. P. Hill, L. Issel-Tarver, A. Kasarskis, S. Lewis, J. C. Matese, J. E. Richardson, M. Ringwald, G. M. Rubin and G. Sherlock: Gene Ontology: tool for the unification of biology;
Nature Genetics, 2000; 1, 25, 25-29.

S. R. Bailey, S. Vatsa, R. C. Larson, A. A. Bouffard, I. Scarfò, M. C. Kann, T. R. Berger, M. B. Leick, M. Wehrli, A. Schmidts, H. Silva, K. A. Lindell, A. Demato, K. M. E. Gallagher, M. J. Frigault and M. V. Maus: Blockade or Deletion of IFNγ Reduces Macrophage Activation without Compromising CAR T-cell Function in Hematologic Malignancies;
Blood Cancer Discov, 2022; 2, 3, 136-153.

L. Baitsch, P. Baumgaertner, E. Devêvre, S. K. Raghav, A. Legat, L. Barba, S. Wieckowski, H. Bouzourene, B. Deplancke, P. Romero, N. Rufer and D. E. Speiser: Exhaustion of tumor-specific $CD8^+$ T cells in metastases from melanoma patients;
J Clin Invest, 2011; 6, 121, 2350-60.

G. L. Beatty, M. H. O'Hara, S. F. Lacey, D. A. Torigian, F. Nazimuddin, F. Chen, I. M. Kulikovskaya, M. C. Soulen, M. McGarvey, A. M. Nelson, W. L. Gladney, B. L. Levine, J. J. Melenhorst, G. Plesa and C. H. June: Activity of Mesothelin-Specific Chimeric Antigen Receptor T Cells Against Pancreatic Carcinoma Metastases in a Phase 1 Trial;
Gastroenterology, 2018; 1, 155, 29-32.

M. R. Benmebarek, C. H. Karches, B. L. Cadilha, S. Lesch, S. Endres and S. Kobold: Killing Mechanisms of Chimeric Antigen Receptor (CAR) T Cells;
Int J Mol Sci, 2019; 6, 20.

N. F. Berbari, A. K. O'Connor, C. J. Haycraft and B. K. Yoder: The primary cilium as a complex signaling center;
Curr Biol, 2009; 13, 19, R526-35.

J. G. Berdeja, D. Madduri, S. Z. Usmani, A. Jakubowiak, M. Agha, A. D. Cohen, A. K. Stewart, P. Hari, M. Htut, A. Lesokhin, A. Deol, N. C. Munshi, E. O'Donnell, D. Avigan, I. Singh, E. Zudaire, T. M. Yeh, A. J. Allred, Y. Olyslager, A. Banerjee, C. C. Jackson, J. D. Goldberg, J. M. Schecter, W. Deraedt, S. H. Zhuang, J. Infante, D. Geng, X. Wu, M. J. Carrasco-Alfonso, M. Akram, F. Hossain, S. Rizvi, F. Fan, Y. Lin, T. Martin and S. Jagannath: Ciltacabtagene autoleucel, a B-cell maturation antigen-directed chimeric antigen receptor T-cell therapy in patients with relapsed or refractory multiple myeloma (CARTITUDE-1): a phase 1b/2 open-label study;
Lancet, 2021; 10297, 398, 314-324.

E. Bi, X. Ma, Y. Lu, M. Yang, Q. Wang, G. Xue, J. Qian, S. Wang and Q. Yi: Foxo1 and Foxp1 play opposing roles in regulating the differentiation and antitumor activity of T(H)9 cells programmed by IL-7;
Sci Signal, 2017; 500, 10.

A. C. Boroughs, R. C. Larson, N. D. Marjanovic, K. Gosik, A. P. Castano, C. B. M. Porter, S. J. Lorrey, O. Ashenberg, L. Jerby, M. Hofree, G. Smith-Rosario, R. Morris, J. Gould, L. S. Riley, T. R. Berger, S. J. Riesenfeld, O. Rozenblatt-Rosen, B. D. Choi, A. Regev and M. V. Maus: A Distinct Transcriptional Program in Human CAR T Cells Bearing the 4-1BB Signaling Domain Revealed by scRNA-Seq;
Molecular Therapy, 2020; 12, 28, 2577-2592.

R. J. Brentjens, M. L. Davila, I. Riviere, J. Park, X. Wang, L. G. Cowell, S. Bartido, J. Stefanski, C. Taylor, M. Olszewska, O. Borquez-Ojeda, J. Qu, T. Wasielewska, Q. He, Y. Bernal, I. V. Rijo, C. Hedvat, R. Kobos, K. Curran, P. Steinherz, J. Jurcic, T. Rosenblat, P. Maslak, M. Frattini and M. Sadelain: CD19-targeted T cells rapidly induce molecular remissions in adults with chemotherapy-refractory acute lymphoblastic leukemia;
Sci Transl Med, 2013; 177, 5, 177ra38.

M. D. Buck, D. O'Sullivan, R. I. Klein Geltink, J. D. Curtis, C. H. Chang, D. E. Sanin, J. Qiu, O. Kretz, D. Braas, G. J. van der Windt, Q. Chen, S. C. Huang, C. M. O'Neill, B. T. Edelson, E. J. Pearce, H. Sesaki, T. B. Huber, A. S. Rambold and E. L. Pearce: Mitochondrial Dynamics Controls T Cell Fate through Metabolic Programming;
Cell, 2016; 1, 166, 63-76.

X. Cai, L. Gao, L. Teng, J. Ge, Z. M. Oo, A. R. Kumar, D. G. Gilliland, P. J. Mason, K. Tan and N. A. Speck: Runx1 Deficiency Decreases Ribosome Biogenesis and Confers Stress Resistance to Hematopoietic Stem and Progenitor Cells;
Cell Stem Cell, 2015; 2, 17, 165-77.

D. A. Canaria, M. G. Clare, B. Yan, C. B. Campbell, Z. A. Ismaio, N. L. Anderson, S. Park, A. L. Dent, M. Kazemian and M. R. Olson: IL-1β promotes IL-9-producing Th cell differentiation in IL-2-limiting conditions through the inhibition of BCL6;
Front Immunol, 2022; 13, 1032618.

S. Carbon, A. Ireland, C. J. Mungall, S. Shu, B. Marshall, S. Lewis, t. A. Hub and t. W. P. W. Group: AmiGO: online access to ontology and annotation data;
Bioinformatics, 2008; 2, 25, 288-289.

H. C. Chang, S. Sehra, R. Goswami, W. Yao, Q. Yu, G. L. Stritesky, R. Jabeen, C. McKinley, A. N. Ahyi, L. Han, E. T. Nguyen, M. J. Robertson, N. B. Perumal, R. S. Tepper, S. L. Nutt and M. H. Kaplan: The transcription factor PU.1 is required for the development of IL-9-producing T cells and allergic inflammation;
Nat Immunol, 2010; 6, 11, 527-34.

S. R. Chauhan, P. G. Singhal, U. Sharma, K. Bandil, K. Chakraborty and M. Bharadwaj: Th9 cytokines curb cervical cancer progression and immune evasion;
Hum Immunol, 2019; 12, 80, 1020-1025.

M. Che, R. Wang, X. Li, H. Y. Wang and X. F. S. Zheng: Expanding roles of superoxide dismutases in cell regulation and cancer;
Drug Discov Today, 2016; 1, 21, 143-149.

G. M. Chen, C. Chen, R. K. Das, P. Gao, C. H. Chen, S. Bandyopadhyay, Y. Y. Ding, Y. Uzun, W. Yu, Q. Zhu, R. M. Myers, S. A. Grupp, D. M. Barrett and K. Tan: Integrative Bulk and Single-Cell Profiling of Premanufacture T-cell Populations Reveals Factors Mediating Long-Term Persistence of CAR T-cell Therapy;
Cancer Discov, 2021; 9, 11, 2186-2199.

L. Chen and D. B. Flies: Molecular mechanisms of T cell co-stimulation and co-inhibition;
Nat Rev Immunol, 2013; 4, 13, 227-42.

Y. S. Choi, R. Kageyama, D. Eto, T. C. Escobar, R. J. Johnston, L. Monticelli, C. Lao and S. Crotty: ICOS receptor instructs T follicular helper cell versus effector cell differentiation via induction of the transcriptional repressor Bcl6;
Immunity, 2011; 6, 34, 932-46.

A. D. Cohen, A. L. Garfall, E. A. Stadtmauer, J. J. Melenhorst, S. F. Lacey, E. Lancaster, D. T. Vogl, B. M. Weiss, K. Dengel, A. Nelson, G. Plesa, F. Chen, M. M. Davis, W. T. Hwang, R. M. Young, J. L. Brogdon, R. Isaacs, I. Pruteanu-Malinici, D. L. Siegel, B. L. Levine, C. H. June and M. C. Milone: B cell maturation antigen-specific CAR T cells are clinically active in multiple myeloma;
J Clin Invest, 2019; 6, 129, 2210-2221.

A. Crawford, J. M. Angelosanto, C. Kao, T. A. Doering, P. M. Odorizzi, B. E. Barnett and E. J. Wherry: Molecular and transcriptional basis of $CD4^+$ T cell dysfunction during chronic infection;
Immunity, 2014; 2, 40, 289-302.

C. V. Dang, K. A. O'Donnell, K. I. Zeller, T. Nguyen, R. C. Osthus and F. Li: The c-Myc target gene network;
Semin Cancer Biol, 2006; 4, 16, 253-64.

V. Dardalhon, A. Awasthi, H. Kwon, G. Galileos, W. Gao, R. A. Sobel, M. Mitsdoerffer, T. B. Strom, W. Elyaman, I. C. Ho, S. Khoury, M. Oukka and V. K. Kuchroo: IL-4 inhibits TGF-beta-induced Foxp3+ T cells and, together with TGF-beta, generates IL-9+ IL-10+ Foxp3(-) effector T cells;
Nat Immunol, 2008; 12, 9, 1347-55.

M. L. Davila, I. Riviere, X. Wang, S. Bartido, J. Park, K. Curran, S. S. Chung, J. Stefanski, O. Borquez-Ojeda, M. Olszewska, J. Qu, T. Wasielewska, Q. He, M. Fink, H. Shinglot, M. Youssif, M. Satter, Y. Wang, J. Hosey, H. Quintanilla, E. Halton, Y. Bernal, D. C. Bouhassira, M. E. Arcila, M. Gonen, G. J. Roboz, P. Maslak, D. Douer, M. G. Frattini, S. Giralt, M. Sadelain and R. Brentjens: Efficacy and toxicity management of 19-28z CAR T cell therapy in B cell acute lymphoblastic leukemia;
Sci Transl Med, 2014; 224, 6, 224ra25.

M. de la Roche, A. T. Ritter, K. L. Angus, C. Dinsmore, C. H. Earnshaw, J. F. Reiter and G. M. Griffiths: Hedgehog signaling controls T cell killing at the immunological synapse;
Science, 2013; 6163, 342, 1247-50.

Q. Deng, G. Han, N. Puebla-Osorio, M. C. J. Ma, P. Strati, B. Chasen, E. Dai, M. Dang, N. Jain, H. Yang, Y. Wang, S. Zhang, R. Wang, R. Chen, J. Showell, S. Ghosh, S. Patchva, Q. Zhang, R. Sun, F. Hagemeister, L. Fayad, F. Samaniego, H. C. Lee, L. J. Nastoupil, N. Fowler, R. Eric Davis, J. Westin, S. S. Neelapu, L. Wang and M. R. Green: Characteristics of anti-CD19 CAR T cell infusion products associated with efficacy and toxicity in patients with large B cell lymphomas;
Nat Med, 2020; 12, 26, 1878-1887.

T. A. Doering, A. Crawford, J. M. Angelosanto, M. A. Paley, C. G. Ziegler and E. J. Wherry: Network analysis reveals centrally connected genes and pathways involved in CD8+ T cell exhaustion versus memory;
Immunity, 2012; 6, 37, 1130-44.

Z. Eshhar, T. Waks, G. Gross and D. G. Schindler: Specific activation and targeting of cytotoxic lymphocytes through chimeric single chains consisting of antibody-binding domains and the gamma or zeta subunits of the immunoglobulin and T-cell receptors;
Proc Natl Acad Sci U S A, 1993; 2, 90, 720-4.

D. Faustman and M. Davis: TNF receptor 2 pathway: drug target for autoimmune diseases;
Nature Reviews Drug Discovery, 2010; 6, 9, 482-493.

L. L. Feng, J. M. Gao, P. P. Li and X. Wang: IL-9 contributes to immunosuppression mediated by regulatory T cells and mast cells in B-cell non-hodgkin's lymphoma;
J Clin Immunol, 2011; 6, 31, 1084-94.

O. C. Finney, H. M. Brakke, S. Rawlings-Rhea, R. Hicks, D. Doolittle, M. Lopez, R. B. Futrell, R. J. Orentas, D. Li, R. A. Gardner and M. C. Jensen: CD19 CAR T cell product and disease attributes predict leukemia remission durability;
J Clin Invest, 2019; 5, 129, 2123-2132.

J. A. Fraietta, S. F. Lacey, E. J. Orlando, I. Pruteanu-Malinici, M. Gohil, S. Lundh, A. C. Boesteanu, Y. Wang, R. S. O'Connor, W. T. Hwang, E. Pequignot, D. E. Ambrose, C. Zhang, N. Wilcox, F. Bedoya, C. Dorfmeier, F. Chen, L. Tian, H. Parakandi, M. Gupta, R. M. Young, F. B. Johnson, I. Kulikovskaya, L. Liu, J. Xu, S. H. Kassim, M. M. Davis, B. L. Levine, N. V. Frey, D. L. Siegel, A. C. Huang, E. J. Wherry, H. Bitter, J. L. Brogdon, D. L. Porter, C. H. June and J. J. Melenhorst: Determinants of response and resistance to CD19 chimeric antigen receptor (CAR) T cell therapy of chronic lymphocytic leukemia;
Nat Med, 2018; 5, 24, 563-571.

K. A. Frauwirth, J. L. Riley, M. H. Harris, R. V. Parry, J. C. Rathmell, D. R. Plas, R. L. Elstrom, C. H. June and C. B. Thompson: The CD28 signaling pathway regulates glucose metabolism;
Immunity, 2002; 6, 16, 769-77.

M. J. Frigault, J. Lee, M. C. Basil, C. Carpenito, S. Motohashi, J. Scholler, O. U. Kawalekar, S. Guedan, S. E. McGettigan, A. D. Posey, Jr., S. Ang, L. J. Cooper, J. M. Platt, F. B. Johnson, C. M. Paulos, Y. Zhao, M. Kalos, M. C. Milone and C. H. June: Identification of chimeric antigen receptors that mediate constitutive or inducible proliferation of T cells;
Cancer Immunol Res, 2015; 4, 3, 356-67.

Y. Fu, J. Wang, G. Panangipalli, B. J. Ulrich, B. Koh, C. Xu, R. Kharwadkar, X. Chu, Y. Wang, H. Gao, W. Wu, J. Sun, R. S. Tepper, B. Zhou, S. C. Janga, K. Yang and M. H. Kaplan: STAT5 promotes accessibility and is required for BATF-mediated plasticity at the Il9 locus;
Nat Commun, 2020; 1, 11, 4882.

E. Galli, S. Bellesi, I. Pansini, G. Di Cesare, C. Iacovelli, R. Malafronte, E. Maiolo, P. Chiusolo, S. Sica, F. Sorà and S. Hohaus: The CD4/CD8 ratio of infused CD19-CAR-T is a prognostic factor for efficacy and toxicity;
Br J Haematol, 2023; 4, 203, 564-570.

K. Gerlach, Y. Hwang, A. Nikolaev, R. Atreya, H. Dornhoff, S. Steiner, H. A. Lehr, S. Wirtz, M. Vieth, A. Waisman, F. Rosenbauer, A. N. McKenzie, B. Weigmann and M. F. Neurath: TH9 cells that express the transcription factor PU.1 drive T cell-mediated colitis via IL-9 receptor signaling in intestinal epithelial cells;
Nat Immunol, 2014; 7, 15, 676-86.

M. B. Geyer, I. Rivière, B. Sénéchal, X. Wang, Y. Wang, T. J. Purdon, M. Hsu, S. M. Devlin, M. L. Palomba, E. Halton, Y. Bernal, D. G. van Leeuwen, M. Sadelain, J. H. Park and R. J. Brentjens: Safety and tolerability of conditioning chemotherapy followed by CD19-targeted CAR T cells for relapsed/refractory CLL;
JCI Insight, 2019; 9, 5.

K. Ghani, X. Wang, P. O. de Campos-Lima, M. Olszewska, A. Kamen, I. Rivière and M. Caruso: Efficient human hematopoietic cell transduction using RD114- and GALV-pseudotyped retroviral vectors produced in suspension and serum-free media;
Hum Gene Ther, 2009; 9, 20, 966-74.

M. Gillespie, B. Jassal, R. Stephan, M. Milacic, K. Rothfels, A. Senff-Ribeiro, J. Griss, C. Sevilla, L. Matthews, C. Gong, C. Deng, T. Varusai, E. Ragueneau, Y. Haider, B. May, V. Shamovsky, J. Weiser, T. Brunson, N. Sanati, L. Beckman, X. Shao, A. Fabregat, K. Sidiropoulos, J. Murillo, G. Viteri, J. Cook, S. Shorser, G. Bader, E. Demir, C. Sander, R. Haw, G. Wu, L. Stein, H. Hermjakob and P. D'Eustachio: The reactome pathway knowledgebase 2022;
Nucleic Acids Research, 2021; D1, 50, D687-D692.

D. Gomes-Silva, M. Mukherjee, M. Srinivasan, G. Krenciute, O. Dakhova, Y. Zheng, J. M. S. Cabral, C. M. Rooney, J. S. Orange, M. K. Brenner and M. Mamonkin: Tonic 4-1BB Costimulation in Chimeric Antigen Receptors Impedes T Cell Survival and Is Vector-Dependent;
Cell Rep, 2017; 1, 21, 17-26.

R. Goswami, R. Jabeen, R. Yagi, D. Pham, J. Zhu, S. Goenka and M. H. Kaplan: STAT6-dependent regulation of Th9 development;
J Immunol, 2012; 3, 188, 968-75.

V. Gudipati, J. Rydzek, I. Doel-Perez, V. D. R. Gonçalves, L. Scharf, S. Königsberger, E. Lobner, R. Kunert, H. Einsele, H. Stockinger, M. Hudecek and J. B. Huppa: Inefficient CAR-proximal signaling blunts antigen sensitivity;
Nat Immunol, 2020; 8, 21, 848-856.

S. Guedan, X. Chen, A. Madar, C. Carpenito, S. E. McGettigan, M. J. Frigault, J. Lee, A. D. Posey, Jr., J. Scholler, N. Scholler, R. Bonneau and C. H. June: ICOS-based chimeric antigen receptors program bipolar TH17/TH1 cells;
Blood, 2014; 7, 124, 1070-80.

S. Guedan, A. D. Posey, Jr., C. Shaw, A. Wing, T. Da, P. R. Patel, S. E. McGettigan, V. Casado-Medrano, O. U. Kawalekar, M. Uribe-Herranz, D. Song, J. J. Melenhorst, S. F. Lacey, J. Scholler, B. Keith, R. M. Young and C. H. June: Enhancing CAR T cell persistence through ICOS and 4-1BB costimulation;
JCI Insight, 2018; 1, 3.

S. Guedan, A. Madar, V. Casado-Medrano, C. Shaw, A. Wing, F. Liu, R. M. Young, C. H. June and A. D. Posey, Jr.: Single residue in CD28-costimulated CAR-T cells limits long-term persistence and antitumor durability;
J Clin Invest, 2020; 6, 130, 3087-3097.

H. Guo, J. B. Callaway and J. P. Y. Ting: Inflammasomes: mechanism of action, role in disease, and therapeutics;
Nature Medicine, 2015; 7, 21, 677-687.

A. R. Haas, J. L. Tanyi, M. H. O'Hara, W. L. Gladney, S. F. Lacey, D. A. Torigian, M. C. Soulen, L. Tian, M. McGarvey, A. M. Nelson, C. S. Farabaugh, E. Moon, B. L. Levine, J. J. Melenhorst, G. Plesa, C. H. June, S. M. Albelda and G. L. Beatty: Phase I Study of Lentiviral-Transduced Chimeric Antigen Receptor-Modified T Cells Recognizing Mesothelin in Advanced Solid Cancers;
Mol Ther, 2019; 11, 27, 1919-1929.

M. Habib-Agahi, T. T. Phan and P. F. Searle: Co-stimulation with 4-1BB ligand allows extended T-cell proliferation, synergizes with CD80/CD86 and can reactivate anergic T cells;
Int Immunol, 2007; 12, 19, 1383-94.

J. Hanna, F. Beke, L. M. O'Brien, C. Kapeni, H. C. Chen, V. Carbonaro, A. B. Kim, K. Kishore, T. E. Adolph, M. O. Skjoedt, K. Skjoedt, M. de la Roche and M. de la Roche: Cell-autonomous Hedgehog signaling controls Th17 polarization and pathogenicity;
Nat Commun, 2022; 1, 13, 4075.

J. Hanna and M. de la Roche: Hedgehog signalling in CD4(+) T helper cell polarisation;
Int J Biochem Cell Biol, 2024; 168, 106518.

D. T. Harris, M. V. Hager, S. N. Smith, Q. Cai, J. D. Stone, P. Kruger, M. Lever, O. Dushek, T. M. Schmitt, P. D. Greenberg and D. M. Kranz: Comparison of T Cell Activities Mediated by Human TCRs and CARs That Use the Same Recognition Domains;
J Immunol, 2018; 3, 200, 1088-1100.

M. Hartl, K. Puglisi, A. Nist, P. Raffeiner and K. Bister: The brain acid-soluble protein 1 (BASP1) interferes with the oncogenic capacity of MYC and its binding to calmodulin;
Mol Oncol, 2020; 3, 14, 625-644.

G. Hedström, M. Berglund, D. Molin, M. Fischer, G. Nilsson, U. Thunberg, M. Book, C. Sundström, R. Rosenquist, G. Roos, M. Erlanson, R. M. Amini and G. Enblad: Mast cell infiltration is a favourable prognostic factor in diffuse large B-cell lymphoma;
Br J Haematol, 2007; 1, 138, 68-71.

J. R. Hernandez-Fernaud, E. Ruengeler, A. Casazza, L. J. Neilson, E. Pulleine, A. Santi, S. Ismail, S. Lilla, S. Dhayade, I. R. MacPherson, I. McNeish, D. Ennis, H. Ali, F. G. Kugeratski, H. Al Khamici, M. van den Biggelaar, P. V. van den Berghe, C. Cloix, L. McDonald, D. Millan, A. Hoyle, A. Kuchnio, P. Carmeliet, S. M. Valenzuela, K. Blyth, H. Yin, M. Mazzone, J. C. Norman and S. Zanivan: Secreted CLIC3 drives cancer progression through its glutathione-dependent oxidoreductase activity;
Nat Commun, 2017; 8, 14206.

M. Holcik and N. Sonenberg: Translational control in stress and apoptosis;
Nat Rev Mol Cell Biol, 2005; 4, 6, 318-27.

L. K. Hong, Y. Chen, C. C. Smith, S. A. Montgomery, B. G. Vincent, G. Dotti and B. Savoldo: CD30-Redirected Chimeric Antigen Receptor T Cells Target CD30(+) and CD30(-) Embryonal Carcinoma via Antigen-Dependent and Fas/FasL Interactions;
Cancer Immunol Res, 2018; 10, 6, 1274-1287.

V. Hornung, S. Rothenfusser, S. Britsch, A. Krug, B. Jahrsdörfer, T. Giese, S. Endres and G. Hartmann: Quantitative expression of toll-like receptor 1-10 mRNA in cellular subsets of human peripheral blood mononuclear cells and sensitivity to CpG oligodeoxynucleotides;
J Immunol, 2002; 9, 168, 4531-7.

E. Humblin, M. Thibaudin, F. Chalmin, V. Derangère, E. Limagne, C. Richard, R. A. Flavell, S. Chevrier, S. Ladoire, H. Berger, R. Boidot, L. Apetoh, F. Végran and F. Ghiringhelli: IRF8-dependent molecular complexes control the Th9 transcriptional program;
Nat Commun, 2017; 1, 8, 2085.

P. Hunter: The fourth pillar: Despite some setbacks in the clinic, immunotherapy has made notable progress toward becoming an additional therapeutic option against cancer;
EMBO Rep, 2017; 11, 18, 1889-1892.

T. Imanishi, H. Hara, S. Suzuki, N. Suzuki, S. Akira and T. Saito: Cutting edge: TLR2 directly triggers Th1 effector functions;
J Immunol, 2007; 11, 178, 6715-9.

R. Jabeen, R. Goswami, O. Awe, A. Kulkarni, E. T. Nguyen, A. Attenasio, D. Walsh, M. R. Olson, M. H. Kim, R. S. Tepper, J. Sun, C. H. Kim, E. J. Taparowsky, B. Zhou and M. H. Kaplan: Th9 cell development requires a BATF-regulated transcriptional network;
J Clin Invest, 2013; 11, 123, 4641-53.

C. A. Jacobson, J. C. Chavez, A. R. Sehgal, B. M. William, J. Munoz, G. Salles, P. N. Munshi, C. Casulo, D. G. Maloney, S. de Vos, R. Reshef, L. A. Leslie, I. Yakoub-Agha, O. O. Oluwole, H. C. H. Fung, J. Rosenblatt, J. M. Rossi, L. Goyal, V. Plaks, Y. Yang, R. Vezan, M. P. Avanzi and S. S. Neelapu: Axicabtagene ciloleucel in relapsed or refractory indolent non-Hodgkin lymphoma (ZUMA-5): a single-arm, multicentre, phase 2 trial;
Lancet Oncol, 2022; 1, 23, 91-103.

A. Jäger, V. Dardalhon, R. A. Sobel, E. Bettelli and V. K. Kuchroo: Th1, Th17, and Th9 effector cells induce experimental autoimmune encephalomyelitis with different pathological phenotypes;
J Immunol, 2009; 11, 183, 7169-77.

M. D. Jain, H. Zhao, X. Wang, R. Atkins, M. Menges, K. Reid, K. Spitler, R. Faramand, C. Bachmeier, E. A. Dean, B. Cao, J. C. Chavez, B. Shah, A. Lazaryan, T. Nishihori, M. Hussaini, R. J. Gonzalez, J. E. Mullinax, P. C. Rodriguez, J. R. Conejo-Garcia, C. Anasetti, M. L. Davila and F. L. Locke: Tumor interferon signaling and suppressive myeloid cells are associated with CAR T-cell failure in large B-cell lymphoma;
Blood, 2021; 19, 137, 2621-2633.

Y. Jiang, Y. Li and B. Zhu: T-cell exhaustion in the tumor microenvironment;
Cell Death Dis, 2015; 6, 6, e1792.

M. Julve, M. P. Lythgoe, J. Larkin and A. J. S. Furness: Lifileucel: the first cellular therapy approved for solid tumours;
Trends Cancer, 2024; 6, 10, 475-477.

D. Kabelitz: Expression and function of Toll-like receptors in T lymphocytes;
Curr Opin Immunol, 2007; 1, 19, 39-45.

S. S. Kachala, A. J. Bograd, J. Villena-Vargas, K. Suzuki, E. L. Servais, K. Kadota, J. Chou, C. S. Sima, E. Vertes, V. W. Rusch, W. D. Travis, M. Sadelain and P. S. Adusumilli: Mesothelin overexpression is a marker of tumor aggressiveness and is associated with reduced recurrence-free and overall survival in early-stage lung adenocarcinoma;
Clin Cancer Res, 2014; 4, 20, 1020-8.

M. H. Kaplan, M. M. Hufford and M. R. Olson: The development and in vivo function of T helper 9 cells;
Nat Rev Immunol, 2015; 5, 15, 295-307.

C. H. Karches, M. R. Benmebarek, M. L. Schmidbauer, M. Kurzay, R. Klaus, M. Geiger, F. Rataj, B. L. Cadilha, S. Lesch, C. Heise, R. Murr, J. Vom Berg, M. Jastroch, D. Lamp, J. Ding, P. Duewell, G. Niederfellner, C. Sustmann, S. Endres, C. Klein and S. Kobold: Bispecific Antibodies Enable Synthetic Agonistic Receptor-Transduced T Cells for Tumor Immunotherapy;
Clin Cancer Res, 2019; 19, 25, 5890-5900.

A. F. Karim, S. M. Reba, Q. Li, W. H. Boom and R. E. Rojas: Toll like Receptor 2 engagement on CD4(+) T cells promotes TH9 differentiation and function;
Eur J Immunol, 2017; 9, 47, 1513-1524.

O. U. Kawalekar, R. S. O'Connor, J. A. Fraietta, L. Guo, S. E. McGettigan, A. D. Posey, Jr., P. R. Patel, S. Guedan, J. Scholler, B. Keith, N. W. Snyder, I. A. Blair, M. C. Milone and C. H. June: Distinct Signaling of Coreceptors Regulates Specific Metabolism Pathways and Impacts Memory Development in CAR T Cells;
Immunity, 2016; 2, 44, 380-90.

I.-K. Kim, B.-S. Kim, C.-H. Koh, J.-W. Seok, J.-S. Park, K.-S. Shin, E.-A. Bae, G.-E. Lee, H. Jeon, J. Cho, Y. Jung, D. Han, B. S. Kwon, H.-Y. Lee, Y. Chung and C.-Y. Kang: Glucocorticoid-induced tumor necrosis factor receptor–related protein co-stimulation facilitates tumor regression by inducing IL-9–producing helper T cells;
Nature Medicine, 2015; 9, 21, 1010-1017.

S. Krishna, F. J. Lowery, A. R. Copeland, E. Bahadiroglu, R. Mukherjee, L. Jia, J. T. Anibal, A. Sachs, S. O. Adebola, D. Gurusamy, Z. Yu, V. Hill, J. J. Gartner, Y. F. Li, M. Parkhurst, B. Paria, P. Kvistborg, M. C. Kelly, S. L. Goff, G. Altan-Bonnet, P. F. Robbins and S. A. Rosenberg: Stem-like CD8 T cells mediate response of adoptive cell immunotherapy against human cancer;
Science, 2020; 6522, 370, 1328-1334.

T. Kuilman, C. Michaloglou, W. J. Mooi and D. S. Peeper: The essence of senescence;
Genes Dev, 2010; 22, 24, 2463-79.

L. Labanieh and C. L. Mackall: CAR immune cells: design principles, resistance and the next generation;
Nature, 2023; 7949, 614, 635-648.

T. W. Laetsch, S. L. Maude, S. Rives, H. Hiramatsu, H. Bittencourt, P. Bader, A. Baruchel, M. Boyer, B. De Moerloose, M. Qayed, J. Buechner, M. A. Pulsipher, G. D. Myers, H. E. Stefanski, P. L. Martin, E. Nemecek, C. Peters, G. Yanik, S. L. Khaw, K. L. Davis, J. Krueger, A. Balduzzi, N. Boissel, R. Tiwari, D. O'Donovan and S. A. Grupp: Three-Year Update of Tisagenlecleucel in Pediatric and Young Adult Patients With Relapsed/Refractory Acute Lymphoblastic Leukemia in the ELIANA Trial;
J Clin Oncol, 2023; 9, 41, 1664-1669.

Y. Lai, J. Weng, X. Wei, L. Qin, P. Lai, R. Zhao, Z. Jiang, B. Li, S. Lin, S. Wang, Q. Wu, Z. Tang, P. Liu, D. Pei, Y. Yao, X. Du and P. Li: Toll-like receptor 2 costimulation potentiates the antitumor efficacy of CAR T Cells;
Leukemia, 2018; 3, 32, 801-808.

R. C. Larson, M. C. Kann, S. R. Bailey, N. J. Haradhvala, P. M. Llopis, A. A. Bouffard, I. Scarfó, M. B. Leick, K. Grauwet, T. R. Berger, K. Stewart, P. V. Anekal, M. Jan, J. Joung, A. Schmidts, T. Ouspenskaia, T. Law, A. Regev, G. Getz and M. V. Maus: CAR T cell killing requires the IFNγR pathway in solid but not liquid tumours;
Nature, 2022; 7906, 604, 563-570.

S. Y. Lee, D. H. Lee, W. Sun, F. Cervantes-Contreras, R. S. Basom, F. Wu, S. Liu, R. Rai, H. R. Mirzaei, S. O'Steen, D. J. Green, M. Shadman and B. G. Till: CD8(+) chimeric antigen receptor T cells manufactured in absence of CD4(+) cells exhibit hypofunctional phenotype;
J Immunother Cancer, 2023; 11, 11.

P. Li, R. Spolski, W. Liao, L. Wang, T. L. Murphy, K. M. Murphy and W. J. Leonard: BATF-JUN is critical for IRF4-mediated transcription in T cells;
Nature, 2012; 7421, 490, 543-6.

I. Liadi, H. Singh, G. Romain, N. Rey-Villamizar, A. Merouane, J. R. Adolacion, P. Kebriaei, H. Huls, P. Qiu, B. Roysam, L. J. Cooper and N. Varadarajan: Individual Motile CD4(+) T Cells Can Participate in Efficient Multikilling through Conjugation to Multiple Tumor Cells;
Cancer Immunol Res, 2015; 5, 3, 473-82.

W. Liao, R. Spolski, P. Li, N. Du, E. E. West, M. Ren, S. Mitra and W. J. Leonard: Opposing actions of IL-2 and IL-21 on Th9 differentiation correlate with their differential regulation of BCL6 expression;
Proc Natl Acad Sci U S A, 2014; 9, 111, 3508-13.

A. Liberzon, C. Birger, H. Thorvaldsdóttir, M. Ghandi, J. P. Mesirov and P. Tamayo: The Molecular Signatures Database (MSigDB) hallmark gene set collection;
Cell Syst, 2015; 6, 1, 417-425.

P. Licona-Limón, J. Henao-Mejia, A. U. Temann, N. Gagliani, I. Licona-Limón, H. Ishigame, L. Hao, D. R. Herbert and R. A. Flavell: Th9 Cells Drive Host Immunity against Gastrointestinal Worm Infection;
Immunity, 2013; 4, 39, 744-57.

A. Linder and V. Hornung: Inflammasomes in T cells;
J Mol Biol, 2022; 4, 434, 167275.

L. Liu, E. Bi, X. Ma, W. Xiong, J. Qian, L. Ye, P. Su, Q. Wang, L. Xiao, M. Yang, Y. Lu and Q. Yi: Enhanced CAR-T activity against established tumors by polarizing human T cells to secrete interleukin-9;
Nat Commun, 2020; 1, 11, 5902.

X. Liu, Z. Zhang, J. Ruan, Y. Pan, V. G. Magupalli, H. Wu and J. Lieberman: Inflammasome-activated gasdermin D causes pyroptosis by forming membrane pores;
Nature, 2016; 7610, 535, 153-158.

X. Liu, C. L. Hartman, L. Li, C. J. Albert, F. Si, A. Gao, L. Huang, Y. Zhao, W. Lin, E. C. Hsueh, L. Shen, Q. Shao, D. F. Hoft, D. A. Ford and G. Peng: Reprogramming lipid metabolism prevents effector T cell senescence and enhances tumor immunotherapy;
Science Translational Medicine, 2021; 587, 13, eaaz6314.

A. H. Long, W. M. Haso, J. F. Shern, K. M. Wanhainen, M. Murgai, M. Ingaramo, J. P. Smith, A. J. Walker, M. E. Kohler, V. R. Venkateshwara, R. N. Kaplan, G. H. Patterson, T. J. Fry, R. J. Orentas and C. L. Mackall: 4-1BB costimulation ameliorates T cell exhaustion induced by tonic signaling of chimeric antigen receptors;
Nat Med, 2015; 6, 21, 581-90.

C. U. Louis, B. Savoldo, G. Dotti, M. Pule, E. Yvon, G. D. Myers, C. Rossig, H. V. Russell, O. Diouf, E. Liu, H. Liu, M. F. Wu, A. P. Gee, Z. Mei, C. M. Rooney, H. E. Heslop and M. K. Brenner: Antitumor activity and long-term fate of chimeric antigen receptor-positive T cells in patients with neuroblastoma;
Blood, 2011; 23, 118, 6050-6.

Y. Lu, S. Hong, H. Li, J. Park, B. Hong, L. Wang, Y. Zheng, Z. Liu, J. Xu, J. He, J. Yang, J. Qian and Q. Yi: Th9 cells promote antitumor immune responses in vivo;
J Clin Invest, 2012; 11, 122, 4160-71.

Y. Lu, Q. Wang, G. Xue, E. Bi, X. Ma, A. Wang, J. Qian, C. Dong and Q. Yi: Th9 Cells Represent a Unique Subset of CD4(+) T Cells Endowed with the Ability to Eradicate Advanced Tumors;
Cancer Cell, 2018; 6, 33, 1048-1060.e7.

R. V. Luckheeram, R. Zhou, A. D. Verma and B. Xia: CD4+T Cells: Differentiation and Functions;
Journal of Immunology Research, 2012; 1, 2012, 925135.

R. C. Lynn, E. W. Weber, E. Sotillo, D. Gennert, P. Xu, Z. Good, H. Anbunathan, J. Lattin, R. Jones, V. Tieu, S. Nagaraja, J. Granja, C. F. A. de Bourcy, R. Majzner, A. T. Satpathy, S. R. Quake, M. Monje, H. Y. Chang and C. L. Mackall: c-Jun overexpression in CAR T cells induces exhaustion resistance;
Nature, 2019; 7786, 576, 293-300.

A. N. Macintyre, V. A. Gerriets, A. G. Nichols, R. D. Michalek, M. C. Rudolph, D. Deoliveira, S. M. Anderson, E. D. Abel, B. J. Chen, L. P. Hale and J. C. Rathmell: The glucose transporter Glut1 is selectively essential for CD4 T cell activation and effector function;
Cell Metab, 2014; 1, 20, 61-72.

I. R. Macpherson, E. Rainero, L. E. Mitchell, P. V. van den Berghe, C. Speirs, M. A. Dozynkiewicz, S. Chaudhary, G. Kalna, J. Edwards, P. Timpson and J. C. Norman: CLIC3 controls recycling of late endosomal MT1-MMP and dictates invasion and metastasis in breast cancer;
J Cell Sci, 2014; Pt 18, 127, 3893-901.

J. Maher, R. J. Brentjens, G. Gunset, I. Rivière and M. Sadelain: Human T-lymphocyte cytotoxicity and proliferation directed by a single chimeric TCRzeta /CD28 receptor;
Nat Biotechnol, 2002; 1, 20, 70-5.

K. Man, M. Miasari, W. Shi, A. Xin, D. C. Henstridge, S. Preston, M. Pellegrini, G. T. Belz, G. K. Smyth, M. A. Febbraio, S. L. Nutt and A. Kallies: The transcription factor IRF4 is essential for TCR affinity-mediated metabolic programming and clonal expansion of T cells;
Nat Immunol, 2013; 11, 14, 1155-65.

K. Man, S. S. Gabriel, Y. Liao, R. Gloury, S. Preston, D. C. Henstridge, M. Pellegrini, D. Zehn, F. Berberich-Siebelt, M. A. Febbraio, W. Shi and A. Kallies: Transcription Factor IRF4 Promotes CD8(+) T Cell Exhaustion and Limits the Development of Memory-like T Cells during Chronic Infection;
Immunity, 2017; 6, 47, 1129-1141.e5.

S. L. Maude, N. Frey, P. A. Shaw, R. Aplenc, D. M. Barrett, N. J. Bunin, A. Chew, V. E. Gonzalez, Z. Zheng, S. F. Lacey, Y. D. Mahnke, J. J. Melenhorst, S. R. Rheingold, A. Shen, D. T. Teachey, B. L. Levine, C. H. June, D. L. Porter and S. A. Grupp: Chimeric antigen receptor T cells for sustained remissions in leukemia;
N Engl J Med, 2014; 16, 371, 1507-17.

J. J. Melenhorst, G. M. Chen, M. Wang, D. L. Porter, C. Chen, M. A. Collins, P. Gao, S. Bandyopadhyay, H. Sun, Z. Zhao, S. Lundh, I. Pruteanu-Malinici, C. L. Nobles, S. Maji, N. V. Frey, S. I. Gill, A. W. Loren, L. Tian, I. Kulikovskaya, M. Gupta, D. E. Ambrose, M. M. Davis, J. A. Fraietta, J. L. Brogdon, R. M. Young, A. Chew, B. L. Levine, D. L. Siegel, C. Alanio, E. J. Wherry, F. D. Bushman, S. F. Lacey, K. Tan and C. H. June: Decade-long leukaemia remissions with persistence of CD4(+) CAR T cells;
Nature, 2022; 7897, 602, 503-509.

G. Meyer Zu Horste, D. Przybylski, M. A. Schramm, C. Wang, A. Schnell, Y. Lee, R. Sobel, A. Regev and V. K. Kuchroo: Fas Promotes T Helper 17 Cell Differentiation and Inhibits T Helper 1 Cell Development by Binding and Sequestering Transcription Factor STAT1;
Immunity, 2018; 3, 48, 556-569.e7.

B. P. Miao, R. S. Zhang, H. J. Sun, Y. P. Yu, T. Chen, L. J. Li, J. Q. Liu, J. Liu, H. Q. Yu, M. Zhang, Z. G. Liu and P. C. Yang: Inhibition of squamous cancer growth in a mouse model by Staphylococcal enterotoxin B-triggered Th9 cell expansion;
Cell Mol Immunol, 2017; 4, 14, 371-379.

V. Mikolič, J. Pantović-Žalig, Š. Malenšek, M. Sever, D. Lainšček and R. Jerala: Toll-like receptor 4 signaling activation domains promote CAR T cell function against solid tumors;
Mol Ther Oncol, 2024; 2, 32, 200815.

D. Mizgalska, P. Wegrzyn, K. Murzyn, A. Kasza, A. Koj, J. Jura, B. Jarzab and J. Jura: Interleukin-1-inducible MCPIP protein has structural and functional properties of RNase and participates in degradation of IL-1beta mRNA;
Febs j, 2009; 24, 276, 7386-99.

O. Moiseeva, V. Bourdeau, A. Roux, X. Deschênes-Simard and G. Ferbeyre: Mitochondrial dysfunction contributes to oncogene-induced senescence;
Mol Cell Biol, 2009; 16, 29, 4495-507.

C. L. Montes, A. I. Chapoval, J. Nelson, V. Orhue, X. Zhang, D. H. Schulze, S. E. Strome and B. R. Gastman: Tumor-induced senescent T cells with suppressor function: a potential form of tumor immune evasion;
Cancer Res, 2008; 3, 68, 870-9.

N. C. Munshi, L. D. Anderson, Jr., N. Shah, D. Madduri, J. Berdeja, S. Lonial, N. Raje, Y. Lin, D. Siegel, A. Oriol, P. Moreau, I. Yakoub-Agha, M. Delforge, M. Cavo, H. Einsele, H. Goldschmidt, K. Weisel, A. Rambaldi, D. Reece, F. Petrocca, M. Massaro, J. N. Connarn, S. Kaiser, P. Patel, L. Huang, T. B. Campbell, K. Hege and J. San-Miguel: Idecabtagene Vicleucel in Relapsed and Refractory Multiple Myeloma;
N Engl J Med, 2021; 8, 384, 705-716.

P. Muranski, Z. A. Borman, S. P. Kerkar, C. A. Klebanoff, Y. Ji, L. Sanchez-Perez, M. Sukumar, R. N. Reger, Z. Yu, S. J. Kern, R. Roychoudhuri, G. A. Ferreyra, W. Shen, S. K. Durum, L. Feigenbaum, D. C. Palmer, P. A. Antony, C. C. Chan, A. Laurence, R. L. Danner, L. Gattinoni and N. P. Restifo: Th17 cells are long lived and retain a stem cell-like molecular signature;
Immunity, 2011; 6, 35, 972-85.

H. Nakatsukasa, D. Zhang, T. Maruyama, H. Chen, K. Cui, M. Ishikawa, L. Deng, P. Zanvit, E. Tu, W. Jin, B. Abbatiello, N. Goldberg, Q. Chen, L. Sun, K. Zhao and W. Chen: The DNA-binding inhibitor Id3 regulates IL-9 production in CD4(+) T cells;
Nat Immunol, 2015; 10, 16, 1077-84.

M. Nakazawa: fmsb: Functions for Medical Statistics Book with some Demographic Data;
2023; R package version 0.7.5, available from https://CRAN.R-project.org/package=fmsb [accessed 01 Nov 2023].

K. O. Nam, H. Kang, S. M. Shin, K. H. Cho, B. Kwon, B. S. Kwon, S. J. Kim and H. W. Lee: Cross-linking of 4-1BB activates TCR-signaling pathways in CD8+ T lymphocytes;
J Immunol, 2005; 4, 174, 1898-905.

S. S. Neelapu, F. L. Locke, N. L. Bartlett, L. J. Lekakis, D. B. Miklos, C. A. Jacobson, I. Braunschweig, O. O. Oluwole, T. Siddiqi, Y. Lin, J. M. Timmerman, P. J. Stiff, J. W. Friedberg, I. W. Flinn, A. Goy, B. T. Hill, M. R. Smith, A. Deol, U. Farooq, P. McSweeney, J. Munoz, I. Avivi, J. E. Castro, J. R. Westin, J. C. Chavez, A. Ghobadi, K. V. Komanduri, R. Levy, E. D. Jacobsen, T. E. Witzig, P. Reagan, A. Bot, J. Rossi, L. Navale, Y. Jiang, J. Aycock, M. Elias, D. Chang, J. Wiezorek and W. Y. Go: Axicabtagene Ciloleucel CAR T-Cell Therapy in Refractory Large B-Cell Lymphoma;
N Engl J Med, 2017; 26, 377, 2531-2544.

N. Nonomura, H. Takayama, K. Nishimura, D. Oka, Y. Nakai, M. Shiba, A. Tsujimura, M. Nakayama, K. Aozasa and A. Okuyama: Decreased number of mast cells infiltrating into needle biopsy specimens leads to a better prognosis of prostate cancer;
Br J Cancer, 2007; 7, 97, 952-6.

Y. Nonomura, A. Otsuka, C. Nakashima, J. A. Seidel, A. Kitoh, T. Dainichi, S. Nakajima, Y. Sawada, S. Matsushita, M. Aoki, T. Takenouchi, T. Fujimura, N. Hatta, S. Koreeda, S. Fukushima, T. Honda and K. Kabashima: Peripheral blood Th9 cells are a possible pharmacodynamic biomarker of nivolumab treatment efficacy in metastatic melanoma patients;
Oncoimmunology, 2016; 12, 5, e1248327.

M. H. Nyirenda, L. Sanvito, P. J. Darlington, K. O'Brien, G. X. Zhang, C. S. Constantinescu, A. Bar-Or and B. Gran: TLR2 stimulation drives human naive and effector regulatory T cells into a Th17-like phenotype with reduced suppressive function;
J Immunol, 2011; 5, 187, 2278-90.

D. M. O'Rourke, M. P. Nasrallah, A. Desai, J. J. Melenhorst, K. Mansfield, J. J. D. Morrissette, M. Martinez-Lage, S. Brem, E. Maloney, A. Shen, R. Isaacs, S. Mohan, G. Plesa, S. F. Lacey, J. M. Navenot, Z. Zheng, B. L. Levine, H. Okada, C. H. June, J. L. Brogdon and M. V. Maus: A single dose of peripherally infused EGFRvIII-directed CAR T cells mediates antigen loss and induces adaptive resistance in patients with recurrent glioblastoma;
Sci Transl Med, 2017; 399, 9.

K. J. Oestreich, K. A. Read, S. E. Gilbertson, K. P. Hough, P. W. McDonald, V. Krishnamoorthy and A. S. Weinmann: Bcl-6 directly represses the gene program of the glycolysis pathway;
Nat Immunol, 2014; 10, 15, 957-64.

S. Ohsawa, T. Watanabe, T. Katada, H. Nishina and M. Miura: Novel antibody to human BASP1 labels apoptotic cells post-caspase activation;
Biochem Biophys Res Commun, 2008; 4, 371, 639-43.

K. Pakos-Zebrucka, I. Koryga, K. Mnich, M. Ljujic, A. Samali and A. M. Gorman: The integrated stress response;
EMBO Rep, 2016; 10, 17, 1374-1395.

J. Park, H. Li, M. Zhang, Y. Lu, B. Hong, Y. Zheng, J. He, J. Yang, J. Qian and Q. Yi: Murine Th9 cells promote the survival of myeloid dendritic cells in cancer immunotherapy;
Cancer Immunol Immunother, 2014; 8, 63, 835-45.

K. E. Pauken and E. J. Wherry: Overcoming T cell exhaustion in infection and cancer;
Trends Immunol, 2015; 4, 36, 265-76.

E. L. Pearce, M. C. Walsh, P. J. Cejas, G. M. Harms, H. Shen, L. S. Wang, R. G. Jones and Y. Choi: Enhancing CD8 T-cell memory by modulating fatty acid metabolism;
Nature, 2009; 7251, 460, 103-7.

D. L. Porter, W. T. Hwang, N. V. Frey, S. F. Lacey, P. A. Shaw, A. W. Loren, A. Bagg, K. T. Marcucci, A. Shen, V. Gonzalez, D. Ambrose, S. A. Grupp, A. Chew, Z. Zheng, M. C. Milone, B. L. Levine, J. J. Melenhorst and C. H. June: Chimeric antigen receptor T cells persist and induce sustained remissions in relapsed refractory chronic lymphocytic leukemia;
Sci Transl Med, 2015; 303, 7, 303ra139.

G. Pulle, M. Vidric and T. H. Watts: IL-15-dependent induction of 4-1BB promotes antigen-independent CD8 memory T cell survival;
J Immunol, 2006; 5, 176, 2739-48.

R. Purwar, C. Schlapbach, S. Xiao, H. S. Kang, W. Elyaman, X. Jiang, A. M. Jetten, S. J. Khoury, R. C. Fuhlbrigge, V. K. Kuchroo, R. A. Clark and T. S. Kupper: Robust tumor immunity to melanoma mediated by interleukin-9-producing T cells;
Nat Med, 2012; 8, 18, 1248-53.

M. Quigley, J. Martinez, X. Huang and Y. Yang: A critical role for direct TLR2-MyD88 signaling in CD8 T-cell clonal expansion and memory formation following vaccinia viral infection;
Blood, 2009; 10, 113, 2256-64.

R Core Team: R: A language and environment for statistical computing;
R Foundation for Statistical Computing, 2021; Version 4.1.1 (2021-08-10), available from https://www.R-project.org/ [accessed 24 Jul 2021].

G. O. Rangel Rivera, H. M. Knochelmann, C. J. Dwyer, A. S. Smith, M. M. Wyatt, A. M. Rivera-Reyes, J. E. Thaxton and C. M. Paulos: Fundamentals of T Cell Metabolism and Strategies to Enhance Cancer Immunotherapy;
Frontiers in Immunology, 2021; 12.

N. J. Rowbotham, A. L. Hager-Theodorides, M. Cebecauer, D. K. Shah, E. Drakopoulou, J. Dyson, S. V. Outram and T. Crompton: Activation of the Hedgehog signaling pathway in T-lineage cells inhibits TCR repertoire selection in the thymus and peripheral T-cell activation;
Blood, 2007; 9, 109, 3757-66.

M. K. Ruhland and E. Alspach: Senescence and Immunoregulation in the Tumor Microenvironment;
Frontiers in Cell and Developmental Biology, 2021; 9.

D. T. Rutkowski, S. M. Arnold, C. N. Miller, J. Wu, J. Li, K. M. Gunnison, K. Mori, A. A. Sadighi Akha, D. Raden and R. J. Kaufman: Adaptation to ER stress is mediated by differential stabilities of pro-survival and pro-apoptotic mRNAs and proteins;
PLoS Biol, 2006; 11, 4, e374.

M. Sabatino, J. Hu, M. Sommariva, S. Gautam, V. Fellowes, J. D. Hocker, S. Dougherty, H. Qin, C. A. Klebanoff, T. J. Fry, R. E. Gress, J. N. Kochenderfer, D. F. Stroncek, Y. Ji and L. Gattinoni: Generation of clinical-grade CD19-specific CAR-modified CD8+ memory stem cells for the treatment of human B-cell malignancies;
Blood, 2016; 4, 128, 519-28.

Y. Salazar, X. Zheng, D. Brunn, H. Raifer, F. Picard, Y. Zhang, H. Winter, S. Guenther, A. Weigert, B. Weigmann, L. Dumoutier, J. C. Renauld, A. Waisman, A. Schmall, A. Tufman, L. Fink, B. Brüne, T. Bopp, F. Grimminger, W. Seeger, S. S. Pullamsetti, M. Huber and R. Savai: Microenvironmental Th9 and Th17 lymphocytes induce metastatic spreading in lung cancer;
J Clin Invest, 2020; 7, 130, 3560-3575.

N. E. Scharping, A. V. Menk, R. S. Moreci, R. D. Whetstone, R. E. Dadey, S. C. Watkins, R. L. Ferris and G. M. Delgoffe: The Tumor Microenvironment Represses T Cell Mitochondrial Biogenesis to Drive Intratumoral T Cell Metabolic Insufficiency and Dysfunction;
Immunity, 2016; 2, 45, 374-88.

S. J. Schuster, M. R. Bishop, C. S. Tam, E. K. Waller, P. Borchmann, J. P. McGuirk, U. Jäger, S. Jaglowski, C. Andreadis, J. R. Westin, I. Fleury, V. Bachanova, S. R. Foley, P. J. Ho, S. Mielke, J. M. Magenau, H. Holte, S. Pantano, L. B. Pacaud, R. Awasthi, J. Chu, Ö. Anak, G. Salles and R. T. Maziarz: Tisagenlecleucel in Adult Relapsed or Refractory Diffuse Large B-Cell Lymphoma;
N Engl J Med, 2019; 1, 380, 45-56.

S. Sehra, W. Yao, E. T. Nguyen, N. L. Glosson-Byers, N. Akhtar, B. Zhou and M. H. Kaplan: TH9 cells are required for tissue mast cell accumulation during allergic inflammation;
J Allergy Clin Immunol, 2015; 2, 136, 433-40.e1.

H. Seo, E. González-Avalos, W. Zhang, P. Ramchandani, C. Yang, C. J. Lio, A. Rao and P. G. Hogan: BATF and IRF4 cooperate to counter exhaustion in tumor-infiltrating CAR T cells;
Nat Immunol, 2021; 8, 22, 983-995.

E. L. Servais, C. Colovos, L. Rodriguez, A. J. Bograd, J. Nitadori, C. Sima, V. W. Rusch, M. Sadelain and P. S. Adusumilli: Mesothelin overexpression promotes mesothelioma cell invasion and MMP-9 secretion in an orthotopic mouse model and in epithelioid pleural mesothelioma patients;
Clin Cancer Res, 2012; 9, 18, 2478-89.

B. D. Shah, A. Ghobadi, O. O. Oluwole, A. C. Logan, N. Boissel, R. D. Cassaday, T. Leguay, M. R. Bishop, M. S. Topp, D. Tzachanis, K. M. O'Dwyer, M. L. Arellano, Y. Lin, M. R. Baer, G. J. Schiller, J. H. Park, M. Subklewe, M. Abedi, M. C. Minnema, W. G. Wierda, D. J. DeAngelo, P. Stiff, D. Jeyakumar, C. Feng, J. Dong, T. Shen, F. Milletti, J. M. Rossi, R. Vezan, B. K. Masouleh and R. Houot: KTE-X19 for relapsed or refractory adult B-cell acute lymphoblastic leukaemia: phase 2 results of the single-arm, open-label, multicentre ZUMA-3 study;
Lancet, 2021; 10299, 398, 491-502.

A. Sheih, V. Voillet, L. A. Hanafi, H. A. DeBerg, M. Yajima, R. Hawkins, V. Gersuk, S. R. Riddell, D. G. Maloney, M. E. Wohlfahrt, D. Pande, M. R. Enstrom, H. P. Kiem, J. E. Adair, R. Gottardo, P. S. Linsley and C. J. Turtle: Clonal kinetics and single-cell transcriptional profiling of CAR-T cells in patients undergoing CD19 CAR-T immunotherapy;
Nat Commun, 2020; 1, 11, 219.

Y. Shen, Z. Song, X. Lu, Z. Ma, C. Lu, B. Zhang, Y. Chen, M. Duan, L. Apetoh, X. Li, J. Guo, Y. Miao, G. Zhang, D. Yang, Z. Cai and J. Wang: Fas signaling-mediated T(H)9 cell differentiation favors bowel inflammation and antitumor functions;
Nat Commun, 2019; 1, 10, 2924.

T. R. Simpson, S. A. Quezada and J. P. Allison: Regulation of CD4 T cell activation and effector function by inducible costimulator (ICOS);
Curr Opin Immunol, 2010; 3, 22, 326-32.

L. Simula, M. Fumagalli, L. Vimeux, I. Rajnpreht, P. Icard, G. Birsen, D. An, F. Pendino, A. Rouault, N. Bercovici, D. Damotte, A. Lupo-Mansuet, M. Alifano, M.-C. Alves-Guerra and E. Donnadieu: Mitochondrial metabolism sustains CD8+ T cell migration for an efficient infiltration into solid tumors;
Nature Communications, 2024; 1, 15, 2203.

N. Singh, N. V. Frey, B. Engels, D. M. Barrett, O. Shestova, P. Ravikumar, K. D. Cummins, Y. G. Lee, R. Pajarillo, I. Chun, A. Shyu, S. L. Highfill, A. Price, L. Zhao, L. Peng, B. Granda, M. Ramones, X. M. Lu, D. A. Christian, J. Perazzelli, S. F. Lacey, N. H. Roy, J. K. Burkhardt, F. Colomb, M. Damra, M. Abdel-Mohsen, T. Liu, D. Liu, D. M. Standley, R. M. Young, J. L. Brogdon, S. A. Grupp, C. H. June, S. L. Maude, S. Gill and M. Ruella: Antigen-independent activation enhances the efficacy of 4-1BB-costimulated CD22 CAR T cells;
Nat Med, 2021; 5, 27, 842-850.

P. J. Siska, K. E. Beckermann, F. M. Mason, G. Andrejeva, A. R. Greenplate, A. B. Sendor, Y. J. Chiang, A. L. Corona, L. F. Gemta, B. G. Vincent, R. C. Wang, B. Kim, J. Hong, C. L. Chen, T. N. Bullock, J. M. Irish, W. K. Rathmell and J. C. Rathmell: Mitochondrial dysregulation and glycolytic insufficiency functionally impair CD8 T cells infiltrating human renal cell carcinoma;
JCI Insight, 2017; 12, 2.

L. Skalniak, D. Mizgalska, A. Zarebski, P. Wyrzykowska, A. Koj and J. Jura: Regulatory feedback loop between NF-kappaB and MCP-1-induced protein 1 RNase;
Febs j, 2009; 20, 276, 5892-905.

K. Slowikowski: ggrepel: Automatically Position Non-Overlapping Text Labels with 'ggplot2';
2021; R package version 0.9.1, available from https://CRAN.R-project.org/package=ggrepel [accessed 20 Aug 2021].

D. Sommermeyer, M. Hudecek, P. L. Kosasih, T. Gogishvili, D. G. Maloney, C. J. Turtle and S. R. Riddell: Chimeric antigen receptor-modified T cells derived from defined CD8+ and CD4+ subsets confer superior antitumor reactivity in vivo;
Leukemia, 2016; 2, 30, 492-500.

V. Staudt, E. Bothur, M. Klein, K. Lingnau, S. Reuter, N. Grebe, B. Gerlitzki, M. Hoffmann, A. Ulges, C. Taube, N. Dehzad, M. Becker, M. Stassen, A. Steinborn, M. Lohoff, H. Schild, E. Schmitt and T. Bopp: Interferon-regulatory factor 4 is essential for the developmental program of T helper 9 cells;
Immunity, 2010; 2, 33, 192-202.

S. Stoiber, B. L. Cadilha, M. R. Benmebarek, S. Lesch, S. Endres and S. Kobold: Limitations in the Design of Chimeric Antigen Receptors for Cancer Therapy;
Cells, 2019; 5, 8.

M. J. Strouch, E. C. Cheon, M. R. Salabat, S. B. Krantz, E. Gounaris, L. G. Melstrom, S. Dangi-Garimella, E. Wang, H. G. Munshi, K. Khazaie and D. J. Bentrem: Crosstalk between mast cells and pancreatic cancer cells contributes to pancreatic tumor progression;
Clin Cancer Res, 2010; 8, 16, 2257-65.

A. Subramanian, P. Tamayo, V. K. Mootha, S. Mukherjee, B. L. Ebert, M. A. Gillette, A. Paulovich, S. L. Pomeroy, T. R. Golub, E. S. Lander and J. P. Mesirov: Gene set enrichment analysis: a knowledge-based approach for interpreting genome-wide expression profiles;
Proc Natl Acad Sci U S A, 2005; 43, 102, 15545-50.

M. Sukumar, J. Liu, Y. Ji, M. Subramanian, J. G. Crompton, Z. Yu, R. Roychoudhuri, D. C. Palmer, P. Muranski, E. D. Karoly, R. P. Mohney, C. A. Klebanoff, A. Lal, T. Finkel, N. P. Restifo and L. Gattinoni: Inhibiting glycolytic metabolism enhances CD8+ T cell memory and antitumor function;
J Clin Invest, 2013; 10, 123, 4479-88.

C. Sun, P. Shou, H. Du, K. Hirabayashi, Y. Chen, L. E. Herring, S. Ahn, Y. Xu, K. Suzuki, G. Li, O. Tsahouridis, L. Su, B. Savoldo and G. Dotti: THEMIS-SHP1 Recruitment by 4-1BB Tunes LCK-Mediated Priming of Chimeric Antigen Receptor-Redirected T Cells;
Cancer Cell, 2020; 2, 37, 216-225.e6.

H. Sung, J. Ferlay, R. L. Siegel, M. Laversanne, I. Soerjomataram, A. Jemal and F. Bray: Global Cancer Statistics 2020: GLOBOCAN Estimates of Incidence and Mortality Worldwide for 36 Cancers in 185 Countries;
CA: A Cancer Journal for Clinicians, 2021; 3, 71, 209-249.

T. Tamiya, K. Ichiyama, H. Kotani, T. Fukaya, T. Sekiya, T. Shichita, K. Honma, K. Yui, T. Matsuyama, T. Nakao, S. Fukuyama, H. Inoue, M. Nomura and A. Yoshimura: Smad2/3 and IRF4 play a cooperative role in IL-9-producing T cell induction;
J Immunol, 2013; 5, 191, 2360-71.

C. Tan, M. K. Aziz, J. D. Lovaas, B. P. Vistica, G. Shi, E. F. Wawrousek and I. Gery: Antigen-specific Th9 cells exhibit uniqueness in their kinetics of cytokine production and short retention at the inflammatory site;
J Immunol, 2010; 11, 185, 6795-801.

C. Tan, L. Wei, B. P. Vistica, G. Shi, E. F. Wawrousek and I. Gery: Phenotypes of Th lineages generated by the commonly used activation with anti-CD3/CD28 antibodies differ from those generated by the physiological activation with the specific antigen;
Cell Mol Immunol, 2014; 3, 11, 305-13.

H. Tan, S. Wang and L. Zhao: A tumour-promoting role of Th9 cells in hepatocellular carcinoma through CCL20 and STAT3 pathways;
Clin Exp Pharmacol Physiol, 2017; 2, 44, 213-221.

A. Teijeira, S. Labiano, S. Garasa, I. Etxeberria, E. Santamaría, A. Rouzaut, M. Enamorado, A. Azpilikueta, S. Inoges, E. Bolaños, M. A. Aznar, A. R. Sánchez-Paulete, D. Sancho and I. Melero: Mitochondrial Morphological and Functional Reprogramming Following CD137 (4-1BB) Costimulation;
Cancer Immunol Res, 2018; 7, 6, 798-811.

The Gene Ontology Consortium, S. A. Aleksander, J. Balhoff, S. Carbon, J. M. Cherry, H. J. Drabkin, D. Ebert, M. Feuermann, P. Gaudet, N. L. Harris, D. P. Hill, R. Lee, H. Mi, S. Moxon, C. J. Mungall, A. Muruganugan, T. Mushayahama, P. W. Sternberg, P. D. Thomas, K. Van Auken, J. Ramsey, D. A. Siegele, R. L. Chisholm, P. Fey, M. C. Aspromonte, M. V. Nugnes, F. Quaglia, S. Tosatto, M. Giglio, S. Nadendla, G. Antonazzo, H. Attrill, G. dos Santos, S. Marygold, V. Strelets, C. J. Tabone, J. Thurmond, P. Zhou, S. H. Ahmed, P. Asanitthong, D. Luna Buitrago, M. N. Erdol, M. C. Gage, M. Ali Kadhum, K. Y. C. Li, M. Long, A. Michalak, A. Pesala, A. Pritazahra, S. C. C. Saverimuttu, R. Su, K. E. Thurlow, R. C. Lovering, C. Logie, S. Oliferenko, J. Blake, K. Christie, L. Corbani, M. E. Dolan, H. J. Drabkin, D. P. Hill, L. Ni, D. Sitnikov, C. Smith, A. Cuzick, J. Seager, L. Cooper, J. Elser, P. Jaiswal, P. Gupta, P. Jaiswal, S. Naithani, M. Lera-Ramirez, K. Rutherford, V. Wood, J. L. De Pons, M. R. Dwinell, G. T. Hayman, M. L. Kaldunski, A. E. Kwitek, S. J. F. Laulederkind, M. A. Tutaj, M. Vedi, S.-J. Wang, P. D'Eustachio, L. Aimo, K. Axelsen, A. Bridge, N. Hyka-Nouspikel, A. Morgat, S. A. Aleksander, J. M. Cherry, S. R. Engel, K. Karra, S. R. Miyasato, R. S. Nash, M. S. Skrzypek, S. Weng, E. D. Wong, E. Bakker, T. Z. Berardini, L. Reiser, A. Auchincloss, K. Axelsen, G. Argoud-Puy, M.-C. Blatter, E. Boutet, L. Breuza, A. Bridge, C. Casals-Casas, E. Coudert, A. Estreicher, M. Livia Famiglietti, M. Feuermann, A. Gos, N. Gruaz-Gumowski, C. Hulo, N. Hyka-Nouspikel, F. Jungo, P. Le Mercier, D. Lieberherr, P. Masson, A. Morgat, I. Pedruzzi, L. Pourcel, S. Poux, C. Rivoire, S. Sundaram, A. Bateman, E. Bowler-Barnett, H. Bye-A-Jee, P. Denny, A. Ignatchenko, R. Ishtiaq, A. Lock, Y. Lussi, M. Magrane, M. J. Martin, S. Orchard, P. Raposo, E. Speretta, N. Tyagi, K. Warner, R. Zaru, A. D. Diehl, R. Lee, J. Chan, S. Diamantakis, D. Raciti, M. Zarowiecki, M. Fisher, C. James-Zorn, V. Ponferrada, A. Zorn, S. Ramachandran, L. Ruzicka and M. Westerfield: The Gene Ontology knowledgebase in 2023;
Genetics, 2023; 1, 224.

G. Tozbikian, E. Brogi, K. Kadota, J. Catalano, M. Akram, S. Patil, A. Y. Ho, J. S. Reis-Filho, B. Weigelt, L. Norton, P. S. Adusumilli and H. Y. Wen: Mesothelin expression in triple negative breast carcinomas correlates significantly with basal-like phenotype, distant metastases and decreased survival;
PLoS One, 2014; 12, 9, e114900.

B. O. Tschumi, N. Dumauthioz, B. Marti, L. Zhang, E. Lanitis, M. Irving, P. Schneider, J. P. Mach, G. Coukos, P. Romero and A. Donda: CART cells are prone to Fas- and DR5-mediated cell death;
J Immunother Cancer, 2018; 1, 6, 71.

S. Uematsu and S. Akira: Toll-like Receptors and Type I Interferons *;
Journal of Biological Chemistry, 2007; 21, 282, 15319-15323.

J. A. C. van Bruggen, A. W. J. Martens, J. A. Fraietta, T. Hofland, S. H. Tonino, E. Eldering, M. D. Levin, P. J. Siska, S. Endstra, J. C. Rathmell, C. H. June, D. L. Porter, J. J. Melenhorst, A. P. Kater and G. J. W. van der Windt: Chronic lymphocytic leukemia cells impair mitochondrial fitness in CD8(+) T cells and impede CAR T-cell efficacy;
Blood, 2019; 1, 134, 44-58.

S. J. van der Stegen, M. Hamieh and M. Sadelain: The pharmacology of second-generation chimeric antigen receptors;
Nat Rev Drug Discov, 2015; 7, 14, 499-509.

G. J. van der Windt, B. Everts, C. H. Chang, J. D. Curtis, T. C. Freitas, E. Amiel, E. J. Pearce and E. L. Pearce: Mitochondrial respiratory capacity is a critical regulator of CD8+ T cell memory development;
Immunity, 2012; 1, 36, 68-78.

F. Végran, H. Berger, R. Boidot, G. Mignot, M. Bruchard, M. Dosset, F. Chalmin, C. Rébé, V. Dérangère, B. Ryffel, M. Kato, A. Prévost-Blondel, F. Ghiringhelli and L. Apetoh: The transcription factor IRF1 dictates the IL-21-dependent anticancer functions of TH9 cells;
Nat Immunol, 2014; 8, 15, 758-66.

M. Veldhoen, C. Uyttenhove, J. van Snick, H. Helmby, A. Westendorf, J. Buer, B. Martin, C. Wilhelm and B. Stockinger: Transforming growth factor-beta 'reprograms' the differentiation of T helper 2 cells and promotes an interleukin 9-producing subset;
Nat Immunol, 2008; 12, 9, 1341-6.

N. A. Vitanza, A. J. Johnson, A. L. Wilson, C. Brown, J. K. Yokoyama, A. Künkele, C. A. Chang, S. Rawlings-Rhea, W. Huang, K. Seidel, C. M. Albert, N. Pinto, J. Gust, L. S. Finn, J. G. Ojemann, J. Wright, R. J. Orentas, M. Baldwin, R. A. Gardner, M. C. Jensen and J. R. Park: Locoregional infusion of HER2-specific CAR T cells in children and young adults with recurrent or refractory CNS tumors: an interim analysis;
Nat Med, 2021; 9, 27, 1544-1552.

A. Wang, D. Pan, Y. H. Lee, G. J. Martinez, X. H. Feng and C. Dong: Cutting edge: Smad2 and Smad4 regulate TGF-β-mediated Il9 gene expression via EZH2 displacement;
J Immunol, 2013; 10, 191, 4908-12.

C. Wang, A. J. McPherson, R. B. Jones, K. S. Kawamura, G. H. Lin, P. A. Lang, T. Ambagala, M. Pellegrini, T. Calzascia, N. Aidarus, A. R. Elford, F. Y. Yue, E. Kremmer, C. M. Kovacs, E. Benko, C. Tremblay, J. P. Routy, N. F. Bernard, M. A. Ostrowski, P. S. Ohashi and T. H. Watts: Loss of the signaling adaptor TRAF1 causes CD8+ T cell dysregulation during human and murine chronic infection;
J Exp Med, 2012; 1, 209, 77-91.

C. Wang, Y. Lu, L. Chen, T. Gao, Q. Yang, C. Zhu and Y. Chen: Th9 cells are subjected to PD-1/PD-L1-mediated inhibition and are capable of promoting CD8 T cell expansion through IL-9R in colorectal cancer;
Int Immunopharmacol, 2020; 78, 106019.

D. Wang, B. Aguilar, R. Starr, D. Alizadeh, A. Brito, A. Sarkissian, J. R. Ostberg, S. J. Forman and C. E. Brown: Glioblastoma-targeted CD4+ CAR T cells mediate superior antitumor activity;
JCI Insight, 2018; 10, 3.

D. Wang, R. Starr, D. Alizadeh, X. Yang, S. J. Forman and C. E. Brown: In Vitro Tumor Cell Rechallenge For Predictive Evaluation of Chimeric Antigen Receptor T Cell Antitumor Function;
J Vis Exp, 2019; 144.

M. Wang, J. Munoz, A. Goy, F. L. Locke, C. A. Jacobson, B. T. Hill, J. M. Timmerman, H. Holmes, S. Jaglowski, I. W. Flinn, P. A. McSweeney, D. B. Miklos, J. M. Pagel, M. J. Kersten, N. Milpied, H. Fung, M. S. Topp, R. Houot, A. Beitinjaneh, W. Peng, L. Zheng, J. M. Rossi, R. K. Jain, A. V. Rao and P. M. Reagan: KTE-X19 CAR T-Cell Therapy in Relapsed or Refractory Mantle-Cell Lymphoma;
N Engl J Med, 2020; 14, 382, 1331-1342.

M. Wang, T. Siddiqi, L. I. Gordon, M. Kamdar, M. Lunning, A. V. Hirayama, J. S. Abramson, J. Arnason, N. Ghosh, A. Mehta, C. Andreadis, S. R. Solomon, A. Kostic, C. Dehner, R. Espinola, L. Peng, K. Ogasawara, A. Chattin, L. Eliason and M. L. Palomba: Lisocabtagene Maraleucel in Relapsed/Refractory Mantle Cell Lymphoma: Primary Analysis of the Mantle Cell Lymphoma Cohort From TRANSCEND NHL 001, a Phase I Multicenter Seamless Design Study;
J Clin Oncol, 2024; 10, 42, 1146-1157.

A. Weber, P. Wasiliew and M. Kracht: Interleukin-1 (IL-1) Pathway;
Science Signaling, 2010; 105, 3, cm1-cm1.

E. W. Weber, M. V. Maus and C. L. Mackall: The Emerging Landscape of Immune Cell Therapies;
Cell, 2020; 1, 181, 46-62.

E. W. Weber, K. R. Parker, E. Sotillo, R. C. Lynn, H. Anbunathan, J. Lattin, Z. Good, J. A. Belk, B. Daniel, D. Klysz, M. Malipatlolla, P. Xu, M. Bashti, S. Heitzeneder, L. Labanieh, P. Vandris, R. G. Majzner, Y. Qi, K. Sandor, L. C. Chen, S. Prabhu, A. J. Gentles, T. J. Wandless, A. T. Satpathy, H. Y. Chang and C. L. Mackall: Transient rest restores functionality in exhausted CAR-T cells through epigenetic remodeling;
Science, 2021; 6537, 372.

T. J. Welsh, R. H. Green, D. Richardson, D. A. Waller, K. J. O'Byrne and P. Bradding: Macrophage and mast-cell invasion of tumor cell islets confers a marked survival advantage in non-small-cell lung cancer;
J Clin Oncol, 2005; 35, 23, 8959-67.

E. J. Wherry, S. J. Ha, S. M. Kaech, W. N. Haining, S. Sarkar, V. Kalia, S. Subramaniam, J. N. Blattman, D. L. Barber and R. Ahmed: Molecular signature of CD8+ T cell exhaustion during chronic viral infection;
Immunity, 2007; 4, 27, 670-84.

E. J. Wherry and M. Kurachi: Molecular and cellular insights into T cell exhaustion;
Nat Rev Immunol, 2015; 8, 15, 486-99.

H. Wickham: ggplot2: Elegant Graphics for Data Analysis;
Springer-Verlag New York, 2016; R package version 3.4.0, available from https://ggplot2.tidyverse.org [accessed 13 Nov 2022].

C. O. Wilke: cowplot: Streamlined Plot Theme and Plot Annotations for 'ggplot2';
2020; R package version 1.1.1, available from https://CRAN.R-project.org/package=cowplot [accessed 20 Aug 2021].

T. Willinger, T. Freeman, H. Hasegawa, A. J. McMichael and M. F. Callan: Molecular signatures distinguish human central memory from effector memory CD8 T cell subsets;
J Immunol, 2005; 9, 175, 5895-903.

H. Wu, X. Zhao, S. M. Hochrein, M. Eckstein, G. F. Gubert, K. Knöpper, A. M. Mansilla, A. Öner, R. Doucet-Ladevèze, W. Schmitz, B. Ghesquière, S. Theurich, J. Dudek, G. Gasteiger, A. Zernecke, S. Kobold, W. Kastenmüller and M. Vaeth: Mitochondrial dysfunction promotes the transition of precursor to terminally exhausted T cells through HIF-1α-mediated glycolytic reprogramming;
Nature Communications, 2023; 1, 14, 6858.

G. Xue, G. Jin, J. Fang and Y. Lu: IL-4 together with IL-1β induces antitumor Th9 cell differentiation in the absence of TGF-β signaling;
Nature Communications, 2019; 1, 10, 1376.

G. Xue, N. Zheng, J. Fang, G. Jin, X. Li, G. Dotti, Q. Yi and Y. Lu: Adoptive cell therapy with tumor-specific Th9 cells induces viral mimicry to eliminate antigen-loss-variant tumor cells;
Cancer Cell, 2021; 12, 39, 1610-1622.e9.

Y. Yang, M. E. Kohler, C. D. Chien, C. T. Sauter, E. Jacoby, C. Yan, Y. Hu, K. Wanhainen, H. Qin and T. J. Fry: TCR engagement negatively affects CD8 but not CD4 CAR T cell expansion and leukemic clearance;
Sci Transl Med, 2017; 417, 9.

J. Ye, M. Kumanova, L. S. Hart, K. Sloane, H. Zhang, D. N. De Panis, E. Bobrovnikova-Marjon, J. A. Diehl, D. Ron and C. Koumenis: The GCN2-ATF4 pathway is critical for tumour cell survival and proliferation in response to nutrient deprivation;
Embo j, 2010; 12, 29, 2082-96.

J. Ye, C. Ma, E. C. Hsueh, J. Dou, W. Mo, S. Liu, B. Han, Y. Huang, Y. Zhang, M. A. Varvares, D. F. Hoft and G. Peng: TLR8 signaling enhances tumor immunity by preventing tumor-induced T-cell senescence;
EMBO Mol Med, 2014; 10, 6, 1294-311.

J. Ye and G. Peng: Controlling T cell senescence in the tumor microenvironment for tumor immunotherapy;
Oncoimmunology, 2015; 3, 4, e994398.

F. P. You, J. Zhang, T. Cui, R. Zhu, C. Q. Lv, H. T. Tang and D. W. Sun: Th9 cells promote antitumor immunity via IL-9 and IL-21 and demonstrate atypical cytokine expression in breast cancer;
Int Immunopharmacol, 2017; 52, 163-167.

T. Yu, J. L. Robotham and Y. Yoon: Increased production of reactive oxygen species in hyperglycemic conditions requires dynamic change of mitochondrial morphology;
Proc Natl Acad Sci U S A, 2006; 8, 103, 2653-8.

Y.-R. Yu, H. Imrichova, H. Wang, T. Chao, Z. Xiao, M. Gao, M. Rincon-Restrepo, F. Franco, R. Genolet, W.-C. Cheng, C. Jandus, G. Coukos, Y.-F. Jiang, J. W. Locasale, A. Zippelius, P.-S. Liu, L. Tang, C. Bock, N. Vannini and P.-C. Ho: Disturbed mitochondrial dynamics in CD8+ TILs reinforce T cell exhaustion;
Nature Immunology, 2020; 12, 21, 1540-1551.

R. Zander, D. Schauder, G. Xin, C. Nguyen, X. Wu, A. Zajac and W. Cui: CD4(+) T Cell Help Is Required for the Formation of a Cytolytic CD8(+) T Cell Subset that Protects against Chronic Infection and Cancer;
Immunity, 2019; 6, 51, 1028-1042.e4.

X. Zhang, C. Zhang, M. Qiao, C. Cheng, N. Tang, S. Lu, W. Sun, B. Xu, Y. Cao, X. Wei, Y. Wang, W. Han and H. Wang: Depletion of BATF in CAR-T cells enhances antitumor activity by inducing resistance against exhaustion and formation of central memory cells;
Cancer Cell, 2022; 11, 40, 1407-1422.e7.

Y. Zhao, X. Chu, J. Chen, Y. Wang, S. Gao, Y. Jiang, X. Zhu, G. Tan, W. Zhao, H. Yi, H. Xu, X. Ma, Y. Lu, Q. Yi and S. Wang: Dectin-1-activated dendritic cells trigger potent antitumour immunity through the induction of Th9 cells;
Nat Commun, 2016; 7, 12368.

Z. Zhao, M. Condomines, S. J. C. van der Stegen, F. Perna, C. C. Kloss, G. Gunset, J. Plotkin and M. Sadelain: Structural Design of Engineered Costimulation Determines Tumor Rejection Kinetics and Persistence of CAR T Cells;
Cancer Cell, 2015; 4, 28, 415-428.

X. S. Zhong, M. Matsushita, J. Plotkin, I. Riviere and M. Sadelain: Chimeric antigen receptors combining 4-1BB and CD28 signaling domains augment PI3kinase/AKT/Bcl-XL activation and CD8+ T cell-mediated tumor eradication;
Mol Ther, 2010; 2, 18, 413-20.

L. Zhou, M. M. Chong and D. R. Littman: Plasticity of CD4+ T cell lineage differentiation;
Immunity, 2009; 5, 30, 646-55.

A. Zhu, J. G. Ibrahim and M. I. Love: Heavy-tailed prior distributions for sequence count data: removing the noise and preserving large differences;
Bioinformatics, 2018; 12, 35, 2084-2092.

Acknowledgments

First and foremost, I would like to thank my supervisor Prof. Dr. med. Sebastian Kobold for giving me the opportunity to work on my thesis in such a stimulating environment. I am grateful for the support and guidance in planning and discussing experiments and in writing this thesis.

I would also like to thank Prof. Dr. med. Stefan Endres for his advice and input throughout this thesis and for giving me the chance to do research in such state-of-the-art facilities.

I would also like to thank Prof. Dr. med. Sebastian Theurich for his valuable support as part of my thesis advisory committee.

I am grateful to Dr. Mohamed-Reda Benmebarek for teaching me valuable laboratory skills and for always being there for me as a source of advice and guidance in conceiving experiments, helping in the lab whenever needed, and discussing results and future directions. I would also like to thank Dr. med. Sophia Stock for taking on a role as a second advisor, for her assistance in the lab and for teaching me valuable skills for drafting publications. I am thankful for the support of fellow doctoral students and colleagues at the Abteilung für Klinische Pharmakologie.

I would further like to thank the members of Prof. Dr. Roland Rad's lab at the Technical University Munich, especially Rupert Öllinger and Thomas Engleitner, for their help in performing and analyzing the RNA sequencing experiments.

I am grateful for the financial and non-material support provided by the FöFoLe Stipendium of the Ludwig-Maximilians-Universität München.

And to my family – I cannot thank you enough for your constant support and encouragement. You have always been my rock, and I could not have done it without you.

Eidesstattliche Versicherung

Klüver, Anna-Kristina

Name, Vorname

Ich erkläre hiermit an Eides statt, dass ich die vorliegende Dissertation mit dem Titel

Interleukin-1-Beta-Differentiated Th9 CD4+ T Cells as a Novel Effector Cell Subset for Chimeric Antigen Receptor T Cell Therapy

selbständig verfasst, mich außer der angegebenen keiner weiteren Hilfsmittel bedient und alle Erkenntnisse, die aus dem Schrifttum ganz oder annähernd übernommen sind, als solche kenntlich gemacht und nach ihrer Herkunft unter Bezeichnung der Fundstelle einzeln nachgewiesen habe.

Ich erkläre des Weiteren, dass die hier vorgelegte Dissertation nicht in gleicher oder in ähnlicher Form bei einer anderen Stelle zur Erlangung eines akademischen Grades eingereicht wurde.

München, 30.07.2025

Ort, Datum

Anna-Kristina Klüver

Unterschrift Anna-Kristina Klüver

LMU LUDWIG-MAXIMILIANS-UNIVERSITÄT MÜNCHEN

Dekanat Medizinische Fakultät
Promotionsbüro

Erklärung zur Übereinstimmung der gebundenen Ausgabe der Dissertation mit der elektronischen Fassung

Klüver, Anna-Kristina

Name, Vorname

Hiermit erkläre ich, dass die elektronische Version der eingereichten Dissertation mit dem Titel:

Interleukin-1-Beta-Differentiated Th9 CD4+ T Cells as a Novel Effector Cell Subset for Chimeric Antigen Receptor T Cell Therapy

in Inhalt und Formatierung mit den gedruckten und gebundenen Exemplaren übereinstimmt.

München, 30.07.2025

Ort, Datum

Anna-Kristina Klüver

Unterschrift Anna-Kristina Klüver

List of publications

Publications

A. K. Kluever and E. Deindl: Extracellular Nucleic Acids in Health and Disease;
Curr Pharm Biotechnol, 2018; 15, 19, 1180-1181.

A. K. Kluever and E. Deindl: Extracellular RNA, a Potential Drug Target for Alleviating Atherosclerosis, Ischemia/Reperfusion Injury and Organ Transplantation;
Curr Pharm Biotechnol, 2018; 15, 19, 1189-1195.

S. Vedantham, **A. K. Kluever** and E. Deindl: Is there a Chance to Promote Arteriogenesis by DPP4 Inhibitors Even in Type 2 Diabetes? A Critical Review;
Cells, 2018; 10, 7.

A. K. Kluever, A. Braumandl, S. Fischer, K. T. Preissner and E. Deindl: The Extraordinary Role of Extracellular RNA in Arteriogenesis, the Growth of Collateral Arteries;
Int J Mol Sci, 2019; 24, 20.

K. Kumaraswami, N. Salei, S. Beck, S. Rambichler, **A. K. Kluever**, M. Lasch, L. Richter, B. U. Schraml and E. Deindl: A Simple and Effective Flow Cytometry-Based Method for Identification and Quantification of Tissue Infiltrated Leukocyte Subpopulations in a Mouse Model of Peripheral Arterial Disease;
Int J Mol Sci, 2020; 10, 21.

S. Stock, M. R. Benmebarek, **A. K. Kluever**, D. Darowski, C. Jost, K. G. Stubenrauch, J. Benz, A. Freimoser-Grundschober, E. Moessner, P. Umana, M. Subklewe, S. Endres, C. Klein and S. Kobold: Chimeric antigen receptor T cells engineered to recognize the P329G-mutated Fc part of effector-silenced tumor antigen-targeting human IgG1 antibodies enable modular targeting of solid tumors;
J Immunother Cancer, 2022; 7, 10.

S. Stock, **A. K. Kluever**, S. Endres and S. Kobold: Enhanced Chimeric Antigen Receptor T Cell Therapy through Co-Application of Synergistic Combination Partners;
Biomedicines, 2022; 2, 10.

F. Märkl, M. R. Benmebarek, J. Keyl, B. L. Cadilha, M. Geiger, C. Karches, H. Obeck, M. Schwerdtfeger, S. Michaelides, D. Briukhovetska, S. Stock, J. Jobst, P. J. Müller, L. Majed, M. Seifert, **A. K. Klüver**, T. Lorenzini, R. Grünmeier, M. Thomas, A. Gottschlich, R. Klaus, C. Marr, M. von Bergwelt-Baildon, S. Rothenfusser, M. P. Levesque, M. V. Heppt, S. Endres, C. Klein and S. Kobold: Bispecific antibodies redirect synthetic agonistic receptor modified T cells against melanoma;
J Immunother Cancer, 2023; 5, 11.

S. Stock, **A. K. Klüver**, L. Fertig, V. D. Menkhoff, M. Subklewe, S. Endres and S. Kobold: Mechanisms and strategies for safe chimeric antigen receptor T-cell activity control;
Int J Cancer, 2023; 10, 153, 1706-1725.

Conferences

D. Darowski, M. R. Benmebarek, S. Stock, **A. K. Kluever**, C. Jost, K. G. Stubenrauch, U. Wessels, J. Benz, A. Freimoser-Grundschober, E. Moessner, R. Myburgh, S. Endres, P. Umana, S. Kobold and C. Klein: P329G-CAR®-T: A novel adaptor CAR-T cell platform recognizing the P329G mutation in therapeutic IgG1 antibodies for adoptive T cell therapy applications [Poster];
ICLE Congress, 31 Mar – 2 Apr, 2022, Munich, Germany.

D. Darowski, M. R. Benmebarek, S. Stock, **A. K. Kluever**, C. Jost, K. G. Stubenrauch, U. Wessels, J. Benz, A. Freimoser-Grundschober, E. Moessner, R. Myburgh, S. Endres, P. Umana, S. Kobold and C. Klein: Developing a novel adaptor P329G-CAR®-T cell platform based on the recognition of the P329G Fc mutation in therapeutic IgG1 antibodies for adoptive T cell therapy [Poster];
AACR Annual Meeting 8-13 Apr 2022, New Orleans, USA.

S. Stock, M. R. Benmebarek, **A. K. Kluever**, D. Darowski, C. Jost, K. G. Stubenrauch, J. Benz, A. Freimoser-Grundschober, E. Moessner, P. Umana, M. Subklewe, S. Endres, C. Klein and S. Kobold: P329G-CAR T cells engineered to recognize the P329G-Fc part of effector-silenced tumor antigen-targeting human IgG1 antibodies enable modular targeting of solid tumors [Poster];
Scientific Symposium, Department of Medicine III, LMU Klinikum, 29 - 30 April 2022, Hohenkammer, Germany.

S. Stock, M. R. Benmebarek, **A. K. Kluever**, D. Darowski, C. Jost, K. G. Stubenrauch, J. Benz, A. Freimoser-Grundschober, E. Moessner, P. Umana, M. Subklewe, S. Endres, C. Klein and S. Kobold: P329G-CAR T cells engineered to recognize the P329G-Fc part of effector-silenced tumor antigen-targeting human IgG1 antibodies enable modular targeting of solid tumors [Talk and poster];
CIMT Annual Meeting, 10 – 12 May 2022, Mainz, Germany.

S. Stock, M. R. Benmebarek, **A. K. Kluever**, D. Darowski, C. Jost, K. G. Stubenrauch, J. Benz, A. Freimoser-Grundschober, E. Moessner, P. Umana, M. Subklewe, S. Endres, C. Klein and S. Kobold: Modular P329G-binding CAR T cells engineered to recognize human effector-silenced antibodies carrying a P329G Fc-mutation for targeting of solid tumor antigens [Poster];
9th Immunotherapy of Cancer Conference, 22 – 24 Sept 2022, Munich, Germany.

S. Stock, M. R. Benmebarek, **A. K. Kluever**, D. Darowski, C. Jost, K. G. Stubenrauch, J. Benz, A. Freimoser-Grundschober, E. Moessner, P. Umana, M. Subklewe, S. Endres, C. Klein and S. Kobold: P329G-targeting CAR T cells engineered to recognize effector-silenced tumor antigen-targeting human IgG1 antibodies carrying the P329G mutation in the Fc part for modular targeting of solid tumors [Talk];
DGHO Annual Meeting, 7 – 10 Oct 2022, Vienna, Austria.

S. Stock, M. R. Benmebarek, **A. K. Kluever**, T. Strzalkowski, V. D. Menkhoff, D. Darowski, M. Surowka, L. Rohrbacher, M. von Bergwelt-Baildon, S. Endres, M. Subklewe, C. Klein and S. Kobold: Adaptor CAR T cells targeting the P329G mutation in the Fc part of effector-silenced tumor antigen-targeting human PGLALA-mutated-IgG1 antibodies for modular targeting of hematological diseases and solid tumors [Poster];
10th Munich Cancer Retreat, 12 - 13 July 2023, Hohenkammer, Germany.